REPORT NO.
UCB/EERC-83/24
NOVEMBER 1983

EARTHQUAKE ENGINEERING RESEARCH CENTER

# DESIGN CONSIDERATIONS FOR SHEAR LINKS IN ECCENTRICALLY BRACED FRAMES

by

JAMES O. MALLEY
EGOR P. POPOV

Report to the National Science Foundation

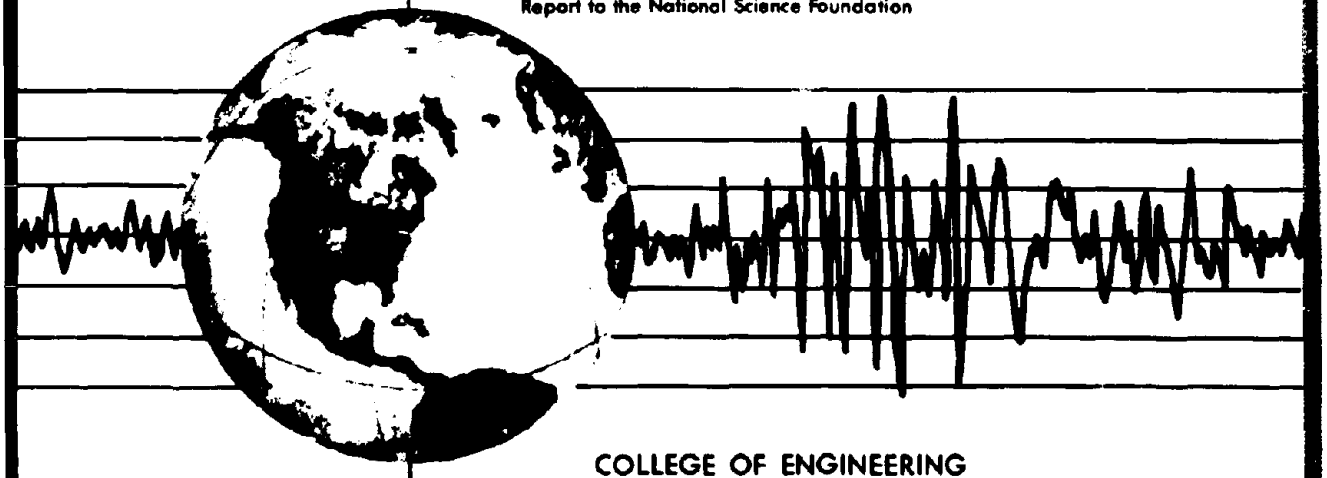

COLLEGE OF ENGINEERING

UNIVERSITY OF CALIFORNIA · Berkeley, California

For sale by the National Technical Information Service, U.S. Department of Commerce, Springfield, Virginia 22161.

See back of report for up to date listing of EERC reports.

272-101

| REPORT DOCUMENTATION PAGE | 1. REPORT NO. NSF/CEE - 83037 | 2. | 3. Recipient's Accession No. PB84 192186 |
|---|---|---|---|
| 4. Title and Subtitle: Design Considerations for Shear Links in Eccentrically Braced Frames | | | 5. Report Date: November 1983 |
| | | | 6. |
| 7. Author(s): James O. Malley and Egor P. Popov | | | 8. Performing Organization Rept. No. UCB/EERC - 83/24 |
| 9. Performing Organization Name and Address: Earthquake Engineering Research Center, University of California, 1301 South 46th Street, Richmond, CA 94804 | | | 10. Project/Task/Work Unit No. |
| | | | 11. Contract(C) or Grant(G) No. (C) (G) CEE81-07217 |
| 12. Sponsoring Organization Name and Address: National Science Foundation, 1800 "G" Street NW, Washington, DC 20550 | | | 13. Type of Report & Period Covered |
| | | | 14. |

15. Supplementary Notes

16. Abstract (Limit: 200 words)

The performance of an eccentrically braced frame depends to a great extent on the behavior of short beam segments called active links which, through bending and shear, transfer the axial forces in the diagonal braces to other braces or to columns. The sensitivity of link behavior to the imposed loading history, the link-column connection detail, and the web stiffener design and details are discussed in this report. The results of twelve full size shear link specimens are presented. Each of the specimens was designed to investigate specific shear link response characteristics. Four specimens were tested with stiffener details which differed significantly from those of previous experiments and early design applications. Another set of four specimens were designed and tested with widely varying loading histories. A set of four specimens which employed conventional moment resisting connection details were also tested. Test conclusions and design recommendations generated by the test results are presented. A practical method for web stiffener design is developed. A design procedure for eccentrically braced frames which employ shear links is outlined.

17. Document Analysis a. Descriptors

b. Identifiers/Open-Ended Terms

c. COSATI Field/Group

| 18. Availability Statement: Release Unlimited | 19. Security Class (This Report) | 21. No. of Pages 137 |
|---|---|---|
| | 20. Security Class (This Page) | 22. Price |

(See ANSI-Z39.18) See Instructions on Reverse OPTIONAL FORM 272 (4-77) (Formerly NTIS-35) Department of Commerce

# DESIGN CONSIDERATIONS FOR SHEAR LINKS IN ECCENTRICALLY BRACED FRAMES

by

James O. Malley
Research Assistant
University of California, Berkeley

and

Egor P. Popov
Professor Emeritus of Civil Engineering
University of California, Berkeley

Report to
National Science Foundation

Report No. UCB/EERC - 83/24
Earthquake Engineering Research Center
University of California
Berkeley, California

November 1983

## ABSTRACT

Eccentrically braced framing has been gaining acceptance in seismic applications because this system can provide both high elastic stiffness and large energy dissipation capacity. The performance of an eccentrically braced frame depends to a great extent on the behavior of short beam segments called active links. Through bending and shear, active links transfer the axial forces in the diagonal braces to other braces or to columns. These short beam members provide the primary energy dissipation mechanism for properly designed eccentrically braced frames.

The results of previous experimental and analytical research has provided a good deal of information on the cyclic behavior of active links. This work has demonstrated that short active links which yield in shear (shear links) can dissipate more energy than longer active links which yield primarily in bending (bending links). However, some aspects critical to the economical design of an eccentrically braced frame which employs shear links have yet to be addressed, including the sensitivity of link behavior to the imposed loading history, the link-column connection detail, and the web stiffener design and details. These three important considerations of shear link behavior are discussed in this report.

The results of twelve full size shear link specimens are presented. Each of the specimens was designed to investigate specific shear link response characteristics. Four specimens were tested with stiffener details which differed significantly from those of previous experiments and early design applications. Another set of four specimens were designed and tested with widely varying loading histories. A set of four specimens which employed conventional moment resisting connection details were also tested.

The qualitative and quantitative results of these experiments were compared and analyzed using energy dissipation capacity as a major parameter. Test conclusions and design recommendations generated by the test results are then presented.

A practical method for web stiffener design is developed. This method considers both the axial force and bending rigidity requirements which shear link web stiffeners must satisfy. An example of this stiffener design method is given in an Appendix.

A design procedure for eccentrically braced frames which employ shear links is outlined. Based on the results of this and previous investigations, and the common practices of seismic design, this procedure attempts to summarize the major considerations of shear link design. This procedure includes recommendations on the determination of structural configuration, member sizes, link-connection details, and web stiffener sizes and details. The suggested connection and stiffener details are illustrated.

## ACKNOWLEDGEMENTS

The authors gratefully acknowledge the support of the National Science Foundation, Grant No. CEE 81-07217, which provided the funds for this research. The opinions expressed in this report are those of the authors and do not necessarily reflect the views of the National Science Foundation.

Many people made significant contributions to the completion of this project and the preparation of this report. Gail Feazell prepared the figures presented in this report. Wes Neighbour provided the technical expertise necessary to perform the experiments reported herein. The suggestions and comments provided throughout the project by Keith D. Hjelmstad helped to form many of the conclusions and recommendations presented in this report. The authors greatly appreciate the contributions made by these individuals.

The authors also acknowledge the suggestions concerning web stiffener design provided by the Sacramento branch of the California Office of the State Architect and one of the author's (J.O.M.) colleagues at H.J. Degenkolb Associates.

Figures A.1 through A.4 were reproduced with the permission of the Royal Aeronautical Society. Their cooperation is appreciated.

# Table of Contents

## LIST OF FIGURES

## LIST OF TABLES

# CHAPTER 1 - INTRODUCTION

## 1.1 Principles of Earthquake Resistant Design

Structures located in seismic regions must be designed to resist inertial forces caused by earthquake induced support excitations. The nature of earthquake ground motions causes the support excitations to be unique for every seismic event. Also, during a seismic event the support motions of different structures vary widely due to local soil conditions. Furthermore, the specific composition of each structure determines the magnitude, location, and duration of the inertial forces. As a result of all these factors, the possible future inertial forces caused by earthquake ground motions cannot be determined with accuracy.

Due to the uncertainty involved in determining seismically induced inertial forces, the structural engineer must rely on satisfying the basic requirements of earthquake resistant design. Three limit states comprise the fundamental philosophy of seismic design.

First, serviceability requirements dictate that the structure should resist relatively frequent minor earthquakes without damage. Generally, structural damage is avoided by providing the structure with enough strength to remain elastic throughout the minor events. Sufficient elastic stiffness must be provided to prevent excessive deflections and thereby preclude the occurrence of non-structural damage.

The second requirement of earthquake resistant design considers the structural response during the less frequent moderate earthquake. During the moderate event, the structure should not undergo any structural damage. But, a limited amount of non-structural damage is allowed. To meet these requirements, the structure can undergo minor inelastic activity in critical regions. The resulting deflections can become large enough to cause some non-structural damage, since in this intermediate limit state the costs incurred to provide structural stiffness

sufficient to restrain deflections below the limit of non-structural damage may be much greater than the expenditure required to repair the resulting damage.

The final requirement of earthquake resistant design is that the structure should not collapse during the most severe earthquake. Both structural and non-structural damage may occur during this rare event. Inelastic structural behavior is allowed, since for the vast majority of structures the costs necessary to resist major earthquakes elastically becomes prohibitive. The underlying motivation for this requirement is to prevent structural collapse and minimize the possibility for loss of life. To meet this requirement, the structure must be able to dissipate large amounts of energy through inelastic deformations. In general, structural systems which exhibit stable hysteretic loops perform well under the large inelastic cyclic loadings of major earthquakes.

### 1.2 Typical Structural Steel Framing Systems

By proper application of these three requirements, the appropriate structural system can be devised. Because of its excellent strength and ductility properties, structural steel has been used for many applications, especially those involving high and medium rise buildings. In the past, structural engineers have utilized two types of structural steel framing for these applications: moment resisting fames and concentrically braced frames.

Moment resisting frames, depicted in Fig. 1.1, are by far the most widely used structural steel framing system. From an architectural standpoint this system is advantageous since there are no obstructions between columns. The capacity of this system to dissipate energy during a major earthquake is provided by inelastic action at beam-column joint locations. Use of the strong column-weak beam approach causes the formation of plastic hinges in the beams near the column connection. Tests on moment resisting beam-column subassemblages demonstrated the stable non-deteriorating hysteretic loops desirable for energy dissipation purposes [16]. With proper detailing, the moment resisting frame can be expected to provide sufficient ductility and energy dissipation capacity in the event of a major earthquake. This confidence in

the desirable inelastic behavior of the moment resisting system has led to reduced code lateral force requirements for these frames [31].

Moment resisting frames also have disadvantages. First, the elastic stiffness required to limit deflections and thereby prevent non-structural damage during minor earthquakes results in member sizes larger than those necessary for other framing systems. This can result in increased material costs and story heights. Second, the large beam end moments inherent with this system often result in substantial shearing deformations in the column panel zones. These panel deformations can contribute significant amounts to the story drift, resulting in increased P-$\Delta$ effects. Often these panel deformations are reduced by the addition of costly web doubler plates.

The second widely used framing system is the concentrically braced frame, as shown in Fig. 1.2. In this system, a set of diagonal braces are provided to increase the lateral stiffness of the frame. The braces are located so that member centerlines intersect at the joints, effectively forming a vertical truss. The intrinsic stiffness of braced frames often makes them economically advantageous for the shorter plan dimension. Architecturally, such frames are less desirable than moment resisting frames because of the obstructions produced by the braces.

The seismic resistance characteristics of concentrically braces frames differ significantly from those exhibited by moment resisting frames. The braces cause the system to resist lateral forces primarily through axial forces in the members. This results in smaller beam bending moments and therefore smaller member sizes. Consequently, some savings in material costs may be realized. Also, panel zone shearing deformations are insignificant due to the small bending moments at the beam ends. The excellent elastic stiffness properties of such systems makes the concentrically braced system quite efficient for resisting minor seismic events.

In contrast, the inelastic behavior of such systems is suspect, even though the damage caused by the 1976 Managua earthquake demonstrated that stiff buildings with sufficient ductility can exhibit desirable performance. Caution should be exercised in adopting such a system because repeated buckling of the diagonal braces causes a rapid decrease in the brace capacity

[4]. This causes pinched hysteretic loops for such systems during inelastic load reversals [17]. The severity of the pinching depends on the slenderness ratio of the brace, with lower $Kl/r$ values exhibiting better hysteretic behavior. The slenderness ratio of diagonal braces is typically quite high, so rapid deterioration of the systems' energy dissipation capacity can be expected. Building code provisions recognize this undesirable behavior by requiring a larger lateral force coefficient than that of moment resisting frames. Also, in highly seismic regions the Uniform Building Code requires a moment resisting system capable of resisting 25 percent of the lateral forces for all structures taller than 160 feet [31].

Thus, neither of the traditional structural steel framing systems efficiently meets all of three of the principal requirements of earthquake resistant design In the past structural engineers have often employed both systems to meet all three requirements. As an alternative to providing a combination of the traditional systems, a hybrid system which can satisfy both the elastic stiffness and energy dissipation criteria has been gaining acceptance. This system is the eccentrically braced frame.

### 1.3 The Eccentrically Braced System

In eccentrically braced frames, the axial forces in the diagonal braces are transferred to columns or to other braces by bending and shear in a portion of the beam called the active link, as shown in Fig. 1.3. By offsetting the braces in this fashion the maximum force that can be imparted to the brace depends on the shear capacity of the beam. With this limitation on brace forces, the braces can be designed to avoid the deleterious effects of cyclic buckling. The active links provide the primary energy dissipation mechanism for the system. The length of these links determines the dominant mode of inelastic behavior. Shorter links generally dissipate energy through inelastic web shear strains, while longer links dissipate energy in a manner similar to moment resisting frames, through inelastic flange normal strains. In addition, the elastic stiffness of the system approaches that of the concentrically braced frame for low to moderate eccentricities [11]. Properly designed eccentrically braces frames can therefore meet both the

elastic stiffness and ultimate ductility requirements of earthquake resistant design.

**1.3.1 The Development of the Eccentrically Braced System as a Framing Alternative-** As early as 1930 the eccentric bracing system was proposed as a method to resist wind loads [27]. The interest in this system for seismic applications has developed recently. Early Japanese research demonstrated that eccentrically braced K frames, such as that depicted in Fig. 1.4a, can dissipate large amounts of energy without excessive lateral deflection [8]. Other studies in Japan effectively made use of inverted Y braces such as that shown in Fig. 1.4b [10].

The initial research of Roeder and Popov [24] demonstrated the excellent stiffness and dissipative capacities of systems braced similar to that depicted in Fig. 1.5(a). This research also showed that the excellent cyclic shear yielding properties of short active links require proper restraint to control web buckling. Further, this investigation presented the first set of recommendations for the overall design of an eccentrically braced frame. The encouraging results of this early research led to further study and the earliest design applications.

Manheim extended the work of Roeder and Popov to the split K eccentrically braced system of Fig. 1.5(c) [18]. This work also developed an analysis and design procedure from limit analysis techniques, and presented a method for analyzing overall frame stability and the effects of beam lateral torsional buckling.

In addition to developing a program for the preliminary design of eccentrically braced frames, Kasai [15] studied the response of V-type bracing, such as that shown in Fig. 1.5(d).

The critical importance of active link behavior to the energy dissipation capacity of the entire system motivated further study of link properties. In this research Hjelmstad isolated the link element to investigate local response characteristics [12]. This research included a series of fifteen tests designed to investigate both links which yield primarily in shear and those which yield in bending. The major conclusions obtained from this study included the following: 1.) Shear links achieve greater ductilities and dissipate more energy than bending links. 2.) Strain hardening in shear links can increase the ultimate shear capacity well above the yield value. Bending links do not benefit as significantly from strain hardening. 3.) Web buckling greatly

deteriorates the energy dissipation capacity of active links. 4.) To delay and restrain web buckling, stiffeners should be provided. Equal spacing of shear link stiffeners was found to be optimum. The minimum stiffener spacing for shear links should be on the order of 20 to 30 $t_w$, where $t_w$ is the link web thickness. 5.) The post-buckling behavior of shear links depends on the stiffener spacing. The post-buckling life decreases with increased web stiffening.

### 1.4 Scope and Objectives of this Investigation

A good deal of information has been developed from the four investigations cited previously. From this research, the elastic, inelastic, and energy dissipation characteristics of both entire eccentrically braced frames and the critical active links is now better understood. But, some of the considerations critical to the economical design of eccentrically braced frames have yet to be investigated. Many of the details required for shear link design have not been studied explicitly. In an effort to investigate the critical response parameters, earlier studies employed overly conservative design details in many cases. In this investigation a deliberate effort was made to find more efficient detailing procedures that might provide significant cost economies without seriously inhibiting shear link behavior. The possible cost economies, the importance of providing adequate seismic connection details, and the critical significance of shear link behavior combined to motivate this investigation.

The specific design considerations investigated included the following:

1 *What impacts do varied loading histories have on the performance of the links?*

2. *What are the most efficient stiffener details considering both economy and structural performance?*

3. *How do the typical connection details affect the performance of shear links?*

4. *What types and magnitudes of loads do the web stiffeners resist? How should the stiffeners be designed to resist these loads?*

5. *What are the performance characteristics of shear links connected to the web of a column?*

A series of twelve specimens were designed, tested and analyzed to investigate the design considerations listed above. From the results of these tests, recommendations are given for shear link design. A method for stiffener design is developed such that a complete shear link design method can be presented.

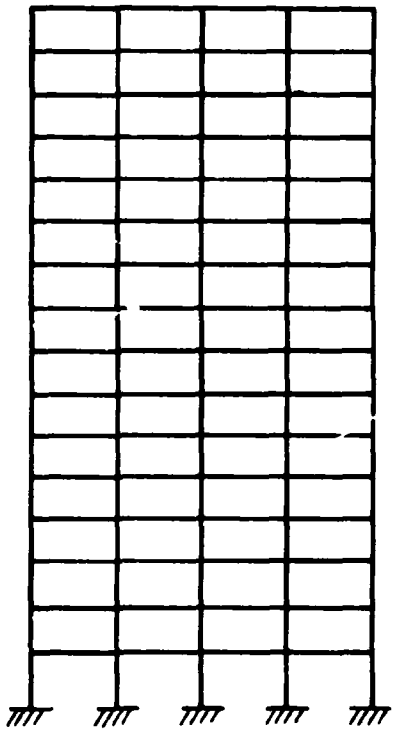

MOMENT RESISTING FRAMING SYSTEM

Fig. 1.1 Moment Resisting Framing for a 16 Story Frame.

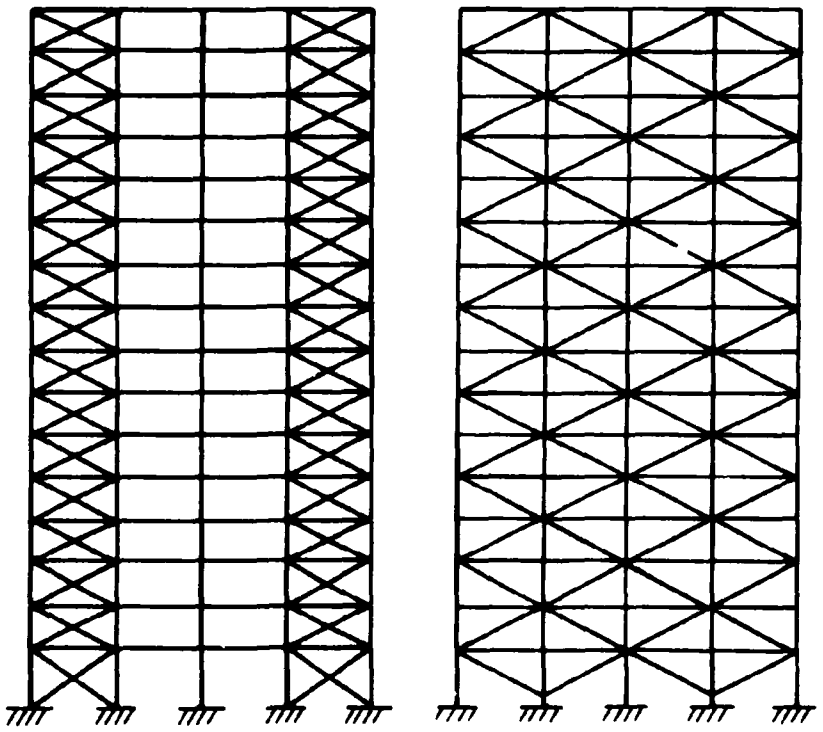

CONCENTRICALLY BRACED FRAMING SYSTEMS

Fig. 1.2 Two Possible Configurations for a 16 Story Concentrically Braced Frame.

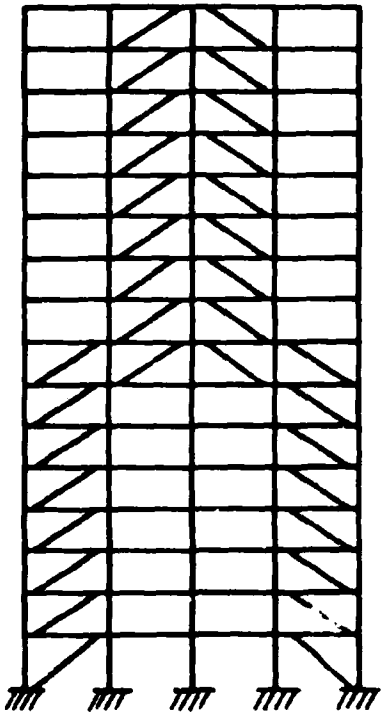

Fig. 1.3 One Possible Configuration for a 16 Story Eccentrically Braced Steel Frame.

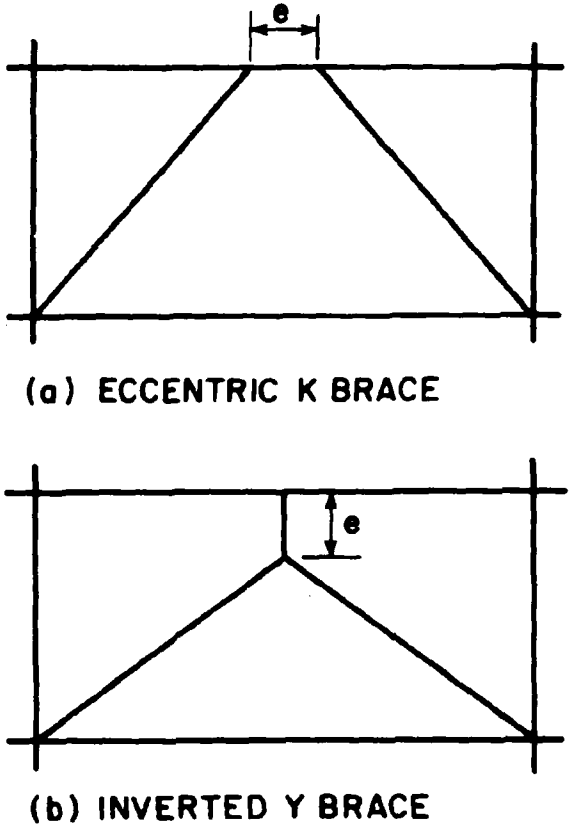


Fig. 1.4 Two Arrangements of Eccentrically Braced Framing Studied in Early Japanese Research [8, 10].

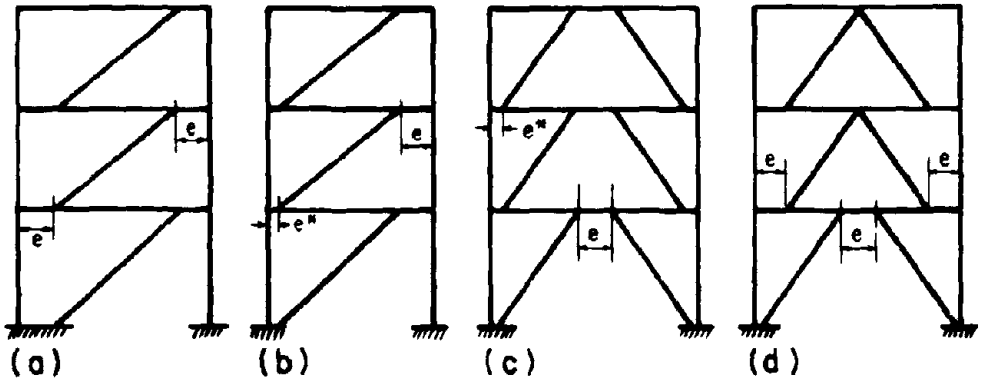


Fig. 1.5 Four Alternative Arrangements of Eccentrically Braced Framing [11].

# CHAPTER 2 - THE EXPERIMENTAL SYSTEM

Research into structural engineering topics generally takes one of two forms. The first method, the analytical approach, utilizes a mathematical formulation of the structural problem. But, in some cases structural problems are so complex that the cost of obtaining meaningful results solely through analytical techniques becomes prohibitive. In these instances it becomes necessary to use experimental techniques.

The goal of any type of structural research is to accurately model the real system. In experimental research this entails developing an experimental system that captures as many of the important features of the actual system as possible. Past research on eccentrically braced frames [18,24] concentrated on the global properties of the entire framed system. A recent investigation [12,13] focused on the local response of the critical component of the system, the active links. The experimental model used in this investigation was extracted from the two possible prototype configurations shown in Fig. 2.1.

## 2.1 The Modeling Assumptions of the System

Designing an experimental system involves making some simplifying assumptions. Rational justification of these assumptions is essential if the tests are to provide results that closely correlate with the performance of an actual structure.

The assumptions employed in the experimental system developed for this investigation were as follows [12,13]:

1. *The ends of the link were fixed against warping.* A two inch thick steel plate at each end connected the specimens to the testing apparatus and provided fixity against warping. This condition is present in the actual system, since the link is either contiguous to a region of low shear, or directly connected to a column.

2. *A moment connection was provided at both ends of the link.* In all cases, full penetration or fillet welds connected the beam flanges to the end plates to provide the required moment continuity.

3. *Yielding was constrained to the link region.* This assumption was necessary in order to test the link separately from the rest of the frame. Previous experimental research on frame subassemblages [18,24] demonstrated that the amount of inelastic behavior in regions adjacent to the links is negligible when compared to that within the links.

4. *The links were loaded with a constant shear force.* Since during seismic activity the load from the eccentric brace is likely to be much greater than the distributed floor load, the link in the prototype structure has a nearly constant shear force along its length.

5. *The links were subjected to reverse curvature with equal end moments.* This condition is not actually present in the prototype structure until it has undergone several inelastic cycles [13]. It is believed that the inelastic behavior causes redistribution of stresses through plastification, leading to the assumed condition. A current investigation is studying the validity of this assumption.

6. *The test links were not loaded with any axial forces.* The development of large axial forces in the active links can significantly reduce their energy dissipation capacity. Therefore, it is advantageous to locate the active links such that they are not required to axially transfer large seismic forces to the braces. This can be accomplished through judicious location of the braces, or through the use of parallel gathering beams. An investigation presently in progress is studying the effects of axial forces on link response.

To provide stability and to impose the condition of zero end rotation, small axial forces were imposed on the system. This created slightly unequal end moments in the links. But, the axial force was generally small enough that its effect on the performance of the specimens was negligible.

## 2.2 The Test Set-up

The testing apparatus, depicted in Fig. 2.2, was designed to provide the system with the modeling assumptions listed above. All the specimens in this series of tests were 36 in. long, 18 in. deep wide flange sections. As noted earlier, the links were welded to large end plates. Each end plate was in turn attached to a stiff steel assemblage by sixteen 1 1/4 in. diameter A490 bolts. The "fixed" end of the testing apparatus was connected to a large concrete reaction block by means of twelve 2 in. diameter prestressed steel rods. The "free" end of the specimen was attached to a rigid system of steel plates. A 350 kip loading ram transmitted the shear force, while a sidearm with a 125 kip transducer provided the axial load required for system stability and zero free end rotation. The loads were applied to the specimen in the plane of the web centerline. The eccentricity of the axial sidearm was 55 in. from the center of the specimen, while the loading ram was positioned at the center of the test link. Support for the massive loading arm was provided by two Teflon lined support pedestals. The frictional resistance of the supporting system was insignificant.

## 2.3 Instrumentation

All of the test data was monitored by a Neff high speed data acquisition system. The information was recorded on magnetic tape so that subsequent data analysis could be performed with a CDC 6400 computer. The instrumentation used to record the test data included load cells, linear potentiometers, linear variable differential transformers (LVDT), and strain gages.

The shear and axial forces imparted to the specimens were measured by transducers, located as shown in Fig. 2.2. The accuracy of the data obtained from the 350 kip and the 125 kip transducers were $\pm 1.0$ kip and $\pm 0.5$ kips respectively.

Linear potentiometers, located as shown in Fig. 2.3, measured many of the important specimen displacements. Four potentiometers measured the lateral displacement of the free end of the specimen. Axial displacements and free end rotations of the specimens were recorded by another set of four potentiometers. In the first four tests these instruments were also used to

measure out of plane web displacements. The resolution of the potentiometers was ±0.001 in.

Previous tests using this test set-up revealed elastic link stiffnesses on the order of one-half of that expected from Timoshenko shear beam theory [13]. This was in part due to lack of complete end fixity. In the first four tests, a system of six LVDTs were used to measure the displacements of the fixed end, as shown in Fig. 2.3. Two LVDTs measured lateral displacements while the other four determined the fixed end rotation. The resolution of these instruments was ±0.0001 in.

Axial flange strains were measured by means of uniaxial SR-4 post yield strain gages, located as shown in Fig. 2.4. In the first four specimens, three gages were provided in each corner. Single gages located 3.5 in. from each corner were employed in the other tests. Strain rosettes, composed of three uniaxial gages, recorded the web shear strains. In the first four tests, each panel contained a centrally located rosette on both sides of the web. Only one panel shear strain was measured in this manner during subsequent tests. Gages were also centrally located on both sides of the web stiffeners to measure their axial skin strains. The gage adhesive limited the maximum strain measurement to approximately eight per cent. Since temperature effects were neglected, strains were assumed to be accurate to fifty microstrain.

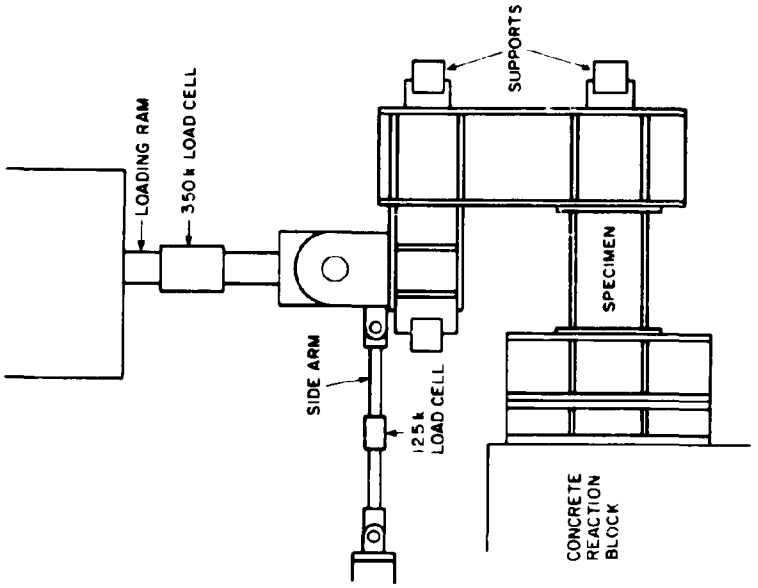


Fig. 2.2 The Experimental Setup [12].

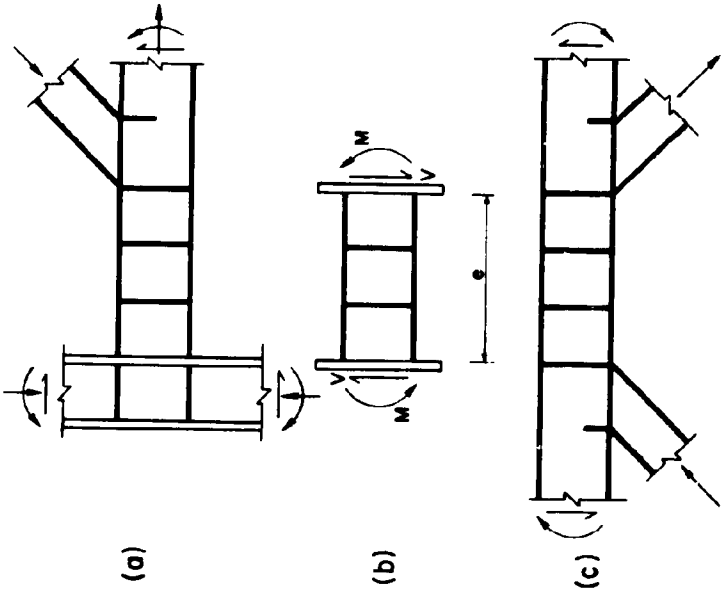


Fig. 2.1 The Active Link Model Extracted from Two Possible Prototype Configurations [12].

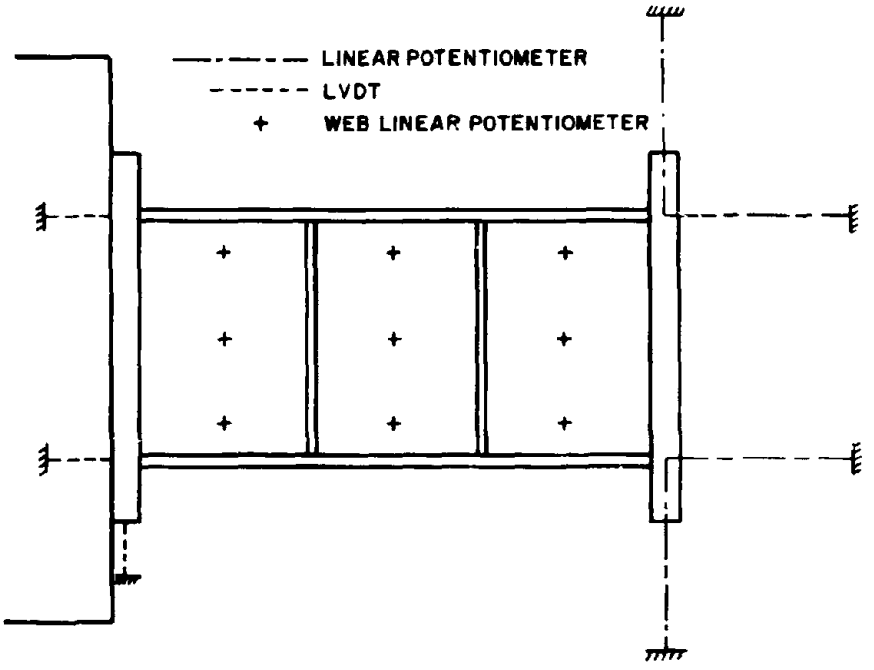


Fig. 2.3 Location of Linear Potentiometers and LVDTs Used in the Instrumentation of the Specimens.

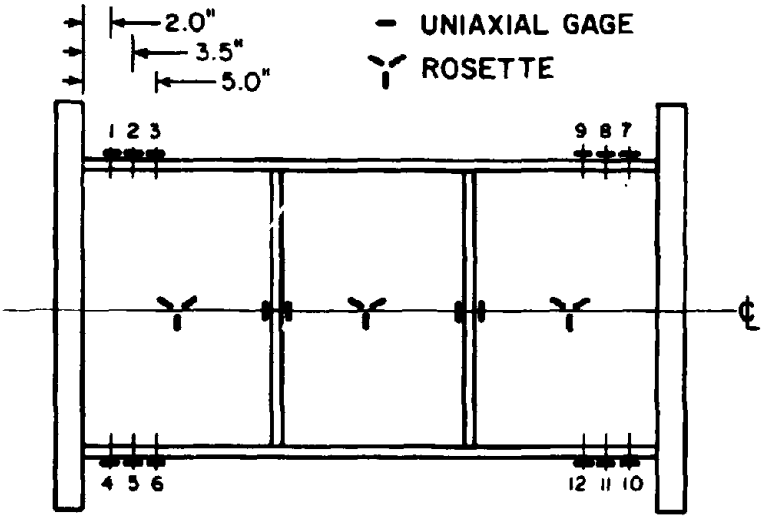


Fig. 2.4 Location of the Strain Gages Used in the Instrumentation of the Specimens.

# CHAPTER 3 - DESIGN OF TEST SPECIMENS

Due to the encouraging results of the earlier investigations on eccentrically braced frame subassemblages, the use of this framing system is being repeatedly adopted in practice, even though investigation concerning many of the important considerations of shear link design are not yet complete. Since the performance of shear links is vital to the satisfactory performance of the entire system, a series of further tests were designed to determine the effects of loading history, stiffener details, and connection details on link response.

## 3.1 Common Features of the Tests

Before discussing the design of specific specimens, the common features of all the specimens should be noted. The design of the specimens followed the AISC Specifications [1] for such details as weld size, bolt size and number, bolt hole size, spacing, edge distance, etc. Each of the specimens was an 18 in. deep, 36 in. long rolled wide flange section. The basic end plate connection detail employed all-around fillet welds. Some tests were designed to investigate typical end connection details used in practice. In all cases, the stiffeners were positioned on only side of the web. The stiffeners were connected to the link by full length fillet welds. Fig. 3.1 shows a specimen with typical details.

## 3.2 Material Properties

The large inelastic strain demand which can be imposed on shear links during an extreme seismic event requires a highly ductile material, such as mild carbon steel. Therefore, A36 steel was chosen for these tests. The relevant properties of the steel are listed in Table 3.1. This data were obtained from manufacturer's mill sheets. Coupon tests were not considered necessary, since comparisons were made from normalized values of the test results.

The sections chosen for the tests included two different sections, W18x40 and W18x60. The reasons for choosing these sections was twofold. These sections are typical beam sizes for multi-story braced frame construction, and when made 36 in. long to fit into the available apparatus they exhibit the desired shear link behavior. The basic properties for these sections are listed in Table 3.2. Since deviation of the actual dimensions from those given in the AISC Manual [1] were negligible, the nominal values were used throughout this investigation.

### 3.3 Stiffener Detail Tests

The large displacements demanded of shear links in eccentrically braced frames can cause web buckling problems. Web buckling should be prevented, since it severely reduces the energy dissipation capacity of a link. The addition of web stiffeners delays the initiation of web buckling and improves the postbuckling behavior of shear links. In all the previous research [12,13], the web stiffeners were placed on both sides of the web, and fillet welded to both flanges as well as the web. While sufficient to meet the stiffener structural requirements, this detail is not the most economical. A series of four tests were therefore designed to investigate the effects of less expensive stiffener details on the performance of shear links.

The effect of providing one-sided web stiffening was investigated in Specimen 17. In this specimen, the 1/2 in. one-sided stiffeners were welded to both flanges as well as to the web, as shown in Fig. 3.2. In previous tests, the two-sided stiffeners were 3/8 in. thick [12,13]. Because of the excellent performance of this specimen, all of the succeeding tests had webs stiffened on only one side.

The cost of providing web stiffeners can be further reduced by relaxing the requirement of welding the stiffeners to both beam flanges as well as to the web. Specimen 21 employed a simplified detail which required the two 1/2 in. thick stiffeners to be connected to the web and one flange only, as shown in Fig. 3.3. The stiffeners on one side terminated a distance k from the outer edge of the flange, (See AISC [1] Manual). Both stiffeners were welded to the same flange. It may be more advantageous to alternate the attachment of stiffeners to flanges, but

this could cause fabrication problems. Moreover, buckling of the top flange is generally restrained by the concrete deck.

The webs of two specimens, 26 and 27, were reinforced with stiffeners which were not attached to either of the link flanges. In Specimen 26, depicted, in Fig. 3.4, the three stiffeners reduced the effective panel width to less than 9 in. The four stiffeners employed in Specimen 27 reduced the panel width even further, as shown in Fig. 3.5. In these two tests the stiffeners were 3/8 in. thick.

### 3.4 Loading Program Tests

All of the tests in previous research [12,13] employed a loading history of cyclic displacements increasing incrementally until failure. The loading history used as the "control" program for these tests was quite similar to that used previously. First, a few linear cycles were performed to check the instrumentation. After the linear cycles, the control program included a cycle near the expected yield displacement. The next cycle began the incremental portion of the loading history. Two cycles were performed at displacement levels of $\pm 0.5$ in., $\pm 1.0$ in., $\pm 1.5$ in., etc. until failure of the specimen. This loading history is shown in Fig. 3.6.

Since in the inelastic range structural response is dependent on prior load and displacement history, it was considered necessary to investigate the effects of varying the loading histories. Of the twelve tests, a total of four had loading histories which varied significantly from the control program.

Specimens 16 and 18 were W18x60 sections with no web stiffening, as shown in Fig 3.7. In the loading for Specimen 16, the initial cycles were two large displacement pulses in the same direction. After these large pulses, the typical incremental cyclic program was followed until failure. This loading history is shown in Fig. 3.8. Nine complete cycles with $\pm 1$ in. displacements were employed at the beginning of the loading program for Specimen 18, as shown in Fig 3.9. These nine cycles dissipated the same amount of energy as an identical previous specimen (Specimen 8 [12,13]) which employed the incremental loading history. After these

cycles, two linear cycles were followed by two cycles at ±2.5 in. displacements. The final cycle had a 4 in. displacement.

All of the remaining specimens were W18x40 sections. The loading history of Specimen 20, with two 1/2 in. thick stiffeners, shown in Fig. 3.2, is shown in Fig. 3.10. To investigate the detrimental effects of imposing two cycles at each displacement level, this specimen underwent only one cycle at each level after the first six cycles. In an effort to demonstrate the displacement capacity of shear links, Specimen 24 was tested under monotonically applied loading. This specimen was displaced 7.2 in. to the limit of the test set-up, and then unloaded and loaded in the reverse direction to generate a large hysteretic loop.

### 3.5 End Connection Detail Tests

The performance of different end connection details under large cyclic loads has been studied previously [21]. These tests indicated that all welded connections generally perform better than hybrid connections with welded flanges and bolted webs. The repetitive nature of the hysteretic loops demonstrated the excellent energy dissipation capacity of these connections in typical moment resisting frames.

In some eccentrically braced systems, one end of the shear link region is a connection to a column. In some respects, the deformation characteristics of shear links under cyclic loads differ from those of beams in moment resisting frames. The shear links dissipate energy primarily through shear yielding of the web. This mode of energy dissipation varies considerably from that of beams in moment resisting frames, which mainly dissipate energy through flexural yielding of the flanges. Moreover, the web buckling phenomenon typical of shear links is not generally encountered. These unique aspects of shear link behavior, coupled with the importance of beam-column connection integrity, led to the investigation of different column-link details.

Four specimens were designed to investigate typical beam-column connection details. A connection detail with flanges connected by full penetration field welds, and the web bolted to a

shop welded shear tab is the predominant detail for steel construction in California due to its cost economy. Specimens 22 and 28 employed this detail. In specimen 22, depicted in Fig. 3.11, four 1 in. diameter A325 bolts provided the connection between a 1/2 in. thick shear tab and the web of the link. Fillet welds on both sides attached the shear tab to the end plate. Two 1/2 in. web stiffeners provided the web restraint. The stiffeners were spaced equally from the bolt line. Specimen 28 was identical to Specimen 22, except that three stiffeners were welded to the web only. This specimen is shown in Fig. 3.12.

Another typical construction detail is the all field welded connection in which the web is fillet welded to a shear tab which was shop welded to the column flange. While being slightly less cost effective than the bolted web connection, this detail provides a stiffer mode of shear transfer. As shown in Fig. 3.13, Specimen 23 was of this type, with a welded web connection to a 1/2 in. shear tab. The stiffener details were identical to those of Specimen 22, with two fully welded stiffeners spaced from the bolt line. Two 3/4 in. diameter erection bolts were added to simulate the actual construction detail more accurately.

In the grid floor systems generally encountered in high rise building construction, one also encounters beam-to-column web connections. Tests at Berkeley and at Lehigh University [20,6] indicated that the commonly used connections of this type do not perform in a sufficiently ductile manner. Flange weld failures caused by stress concentrations were also observed in these investigations. To investigate the behavior of this type of link connection, a specimen (Specimen 25) was fabricated and tested. In this specimen, shown in Fig. 3.14, 1/2 in. stiffener plates were welded to a W14x193 section in the plane of the link flanges and web. Full penetration welds connected these plates to the link. Two fully welded stiffeners were spaced equally from the edge of the column flanges.

Table 3.3 is presented to summarize some of important properties of the specimens. The stiffener details and end connections identified in this table are referenced from Figs. 3.15 and 3.16.

| Section | $\sigma_y$ (ksi) | $\sigma_u$ (ksi) | $\epsilon_u$ (in./in.) |
|---|---|---|---|
| 18x60 | 44 | 67 | 0.24 |
| 18x40 | 48 | 64 | 0.26 |

Table 3.1 Properties of the Steel Used in This Investigation.

| Section | $A$ ( $in.^2$ ) | $d$ ( $in.$ ) | $t_w$ ( $in.$ ) | $b_f$ ( $in.$ ) | $t_f$ ( $in.$ ) |
|---|---|---|---|---|---|
| W18x60 | 17.60 | 18.24 | 0.415 | 7.555 | 0.695 |
| W18x40 | 11.80 | 17.90 | 0.315 | 6.015 | 0.525 |

Table 3.2 Section Properties of the Specimens Used in This Investigation.

| Test Feature | Specimen Number | Section | No. of Panels | Loading History | Stiffener Detail | Connection Detail |
|---|---|---|---|---|---|---|
| Loading History | 16 | W 18x60 | 1 | Large Initial Displ. | - | 3.16(a) |
| | 18 | W 18x60 | 1 | Nine 1 in. (25 mm) Cycles | - | 3.16(a) |
| | 20 | W 18x40 | 3 | One Cycle at Each Level | 3.15(a) | 3.16(a) |
| | 24 | W 18x40 | 3 | Monotonic | 3.15(a) | 3.16(a) |
| Stiffener Details | 17 | W 18x40 | 3 | Two Cycles at Each Displ. Level, Increasing in 1/2 in. (13 mm) Increments | 3.15(a) | 3.16(a) |
| | 21 | W 18x40 | 3 | | 3.15(b) | 3.16(a) |
| | 26 | W 18x40 | 4 | | 3.15(c) | 3.16(b) |
| | 27 | W 18x40 | 4 | | 3.15(c) | 3.16(b) |
| Connection Details | 22 | W 18x40 | 3 | Two Cycles at Each Displ. Level, Increasing in. (13 mm) 1/2 in. Increments | 3.15(a) | 3.16(c) |
| | 23 | W 18x40 | 3 | | 3.15(a) | 3.16(b) |
| | 25 | W 18x40 | 3 | | 3.15(a) | 3.16(d) |
| | 28 | W 18x40 | 4 | | 3.15(c) | 3.16(c) |

Table 3.3 Summary of Test Specimen Details

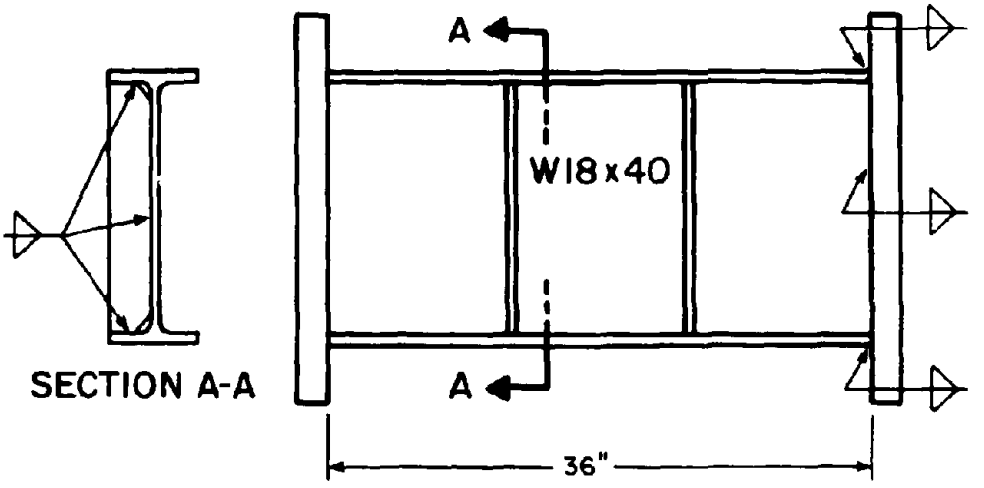


Fig. 3.1 Typical Section and Connection Details of the Specimens.

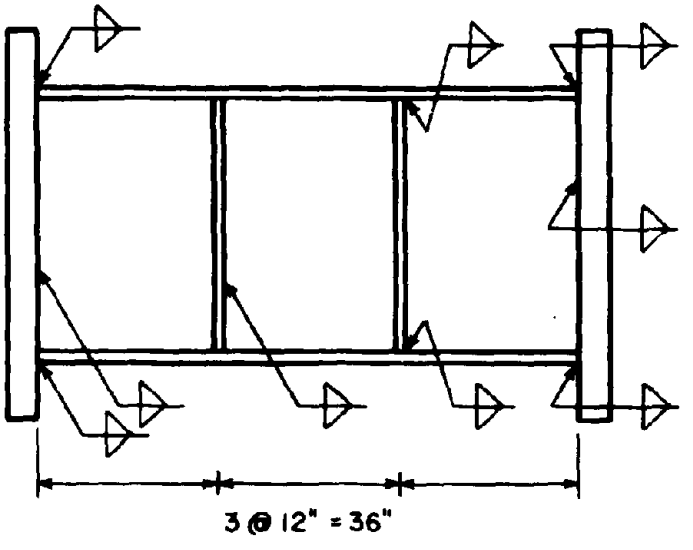


Fig. 3.2 Connection Details of Specimen 17.

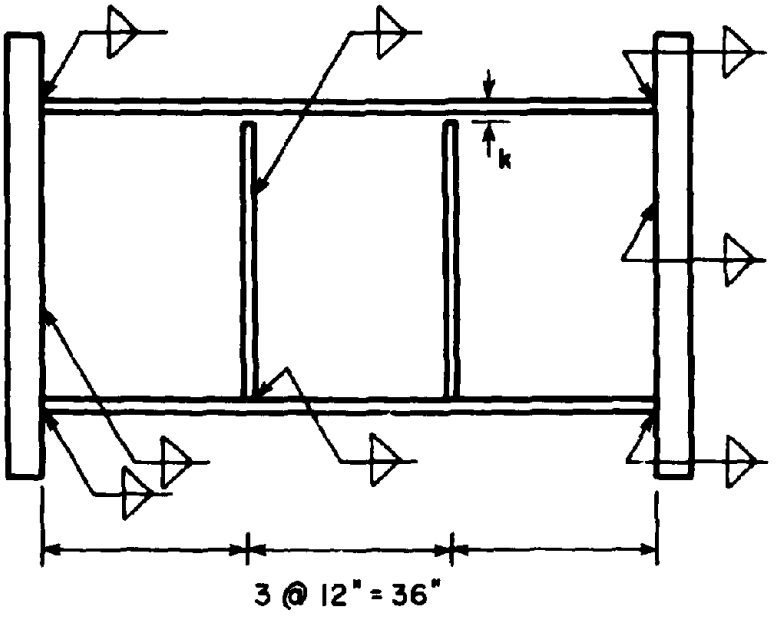


Fig. 3.3 Connection Details of Specimen 21.

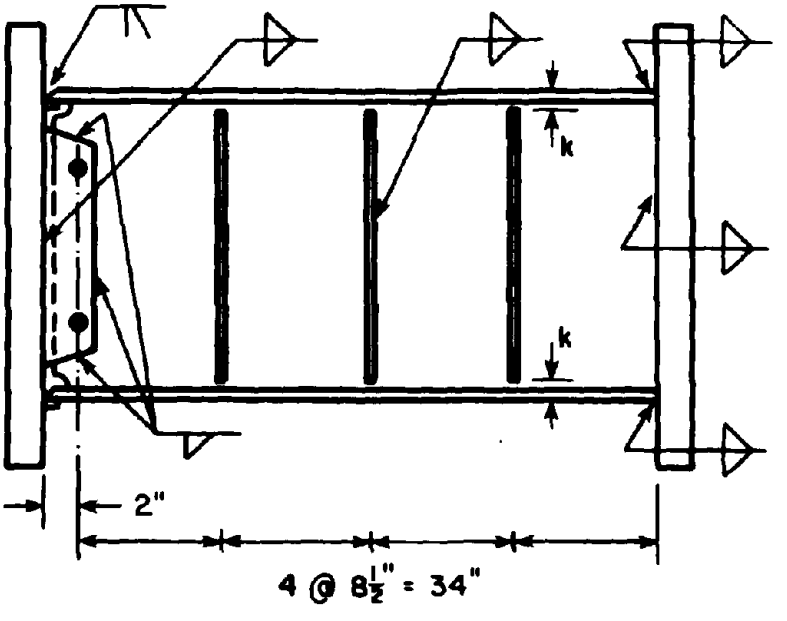


Fig. 3.4 Connection Details of Specimen 26.

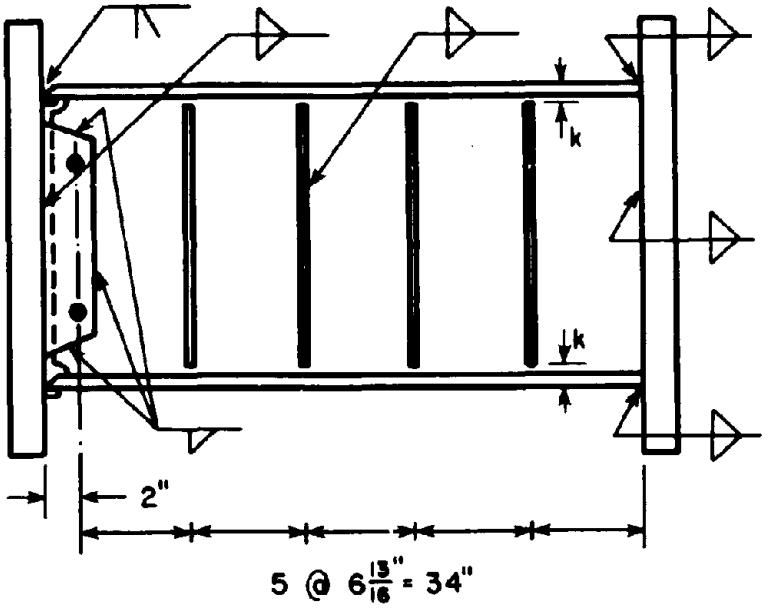


Fig. 3.5 Connection Details of Specimen 27.

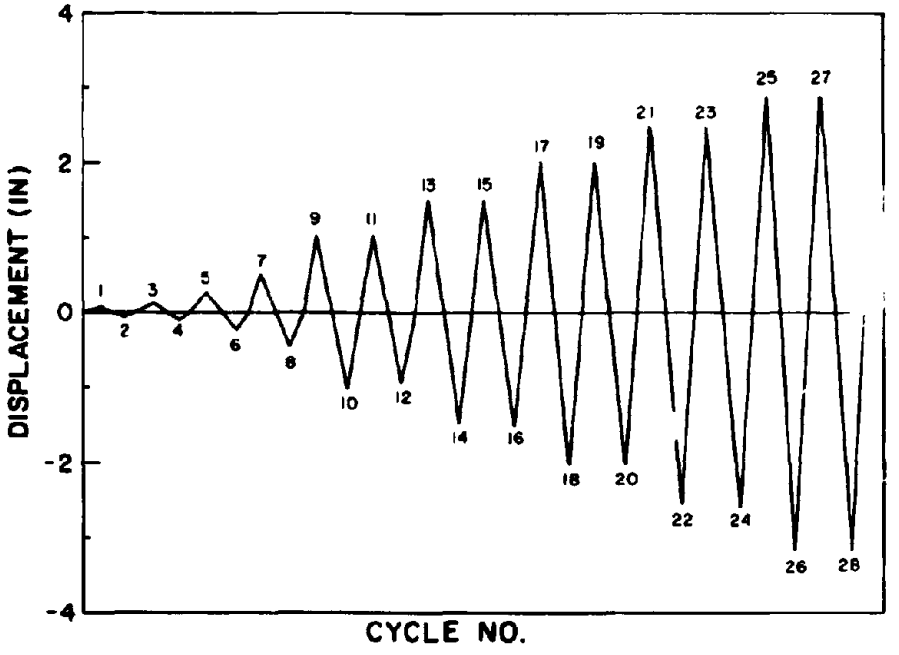


Fig. 3.6 "Control" Program of Incrementally Increasing Displacements Used Throughout the Experimental Investigation.

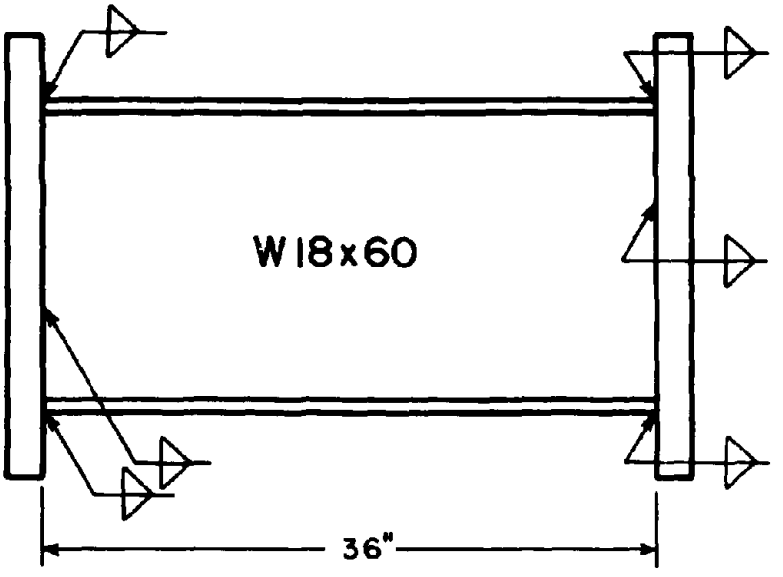


Fig. 3.7 Section and Connection Details of Specimens 16 and 18.

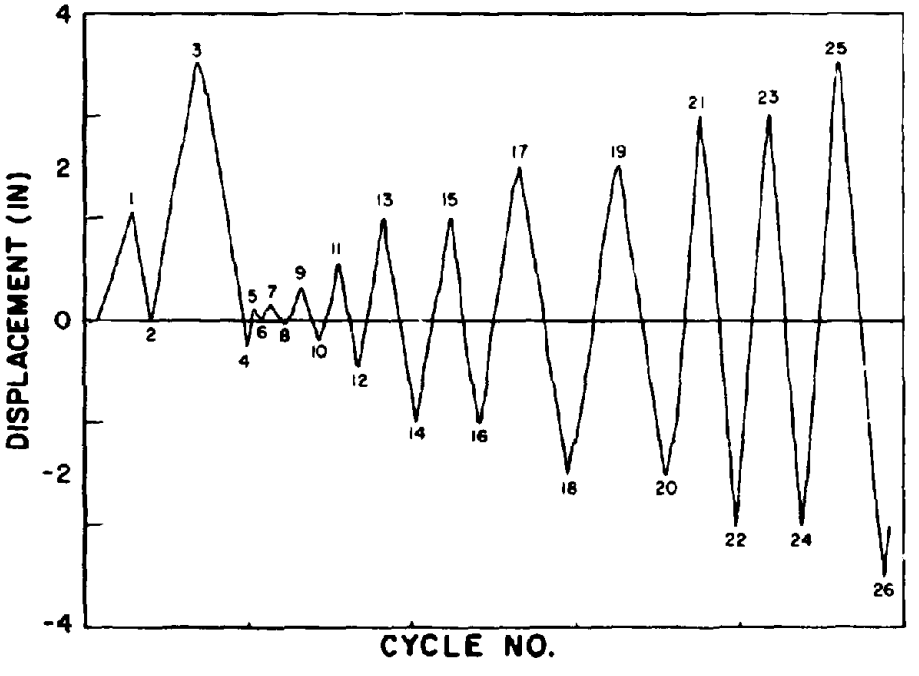


Fig. 3.8 Loading History Employed in Experiment 16.

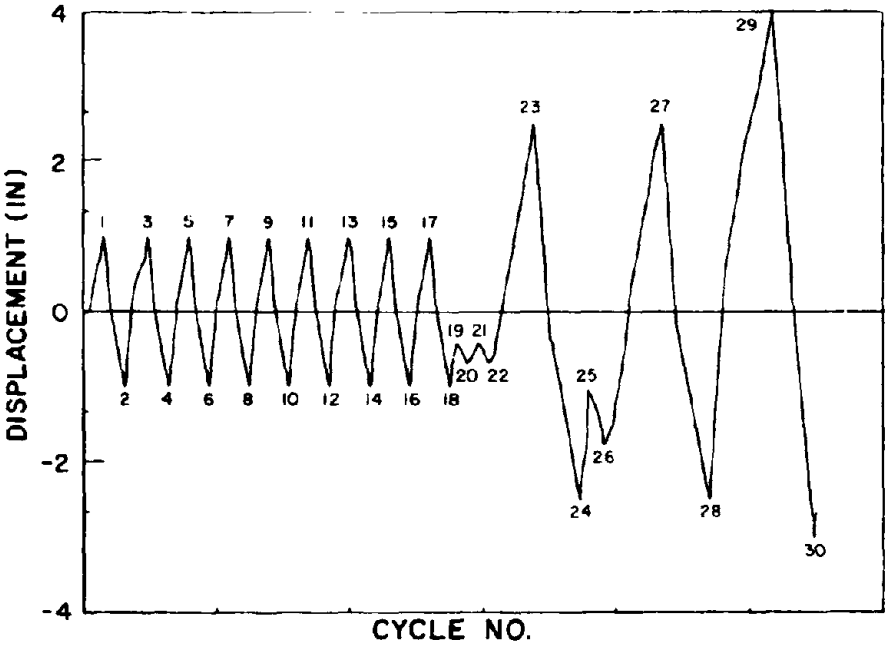


Fig. 3.9 Loading History Employed in Experiment 18.

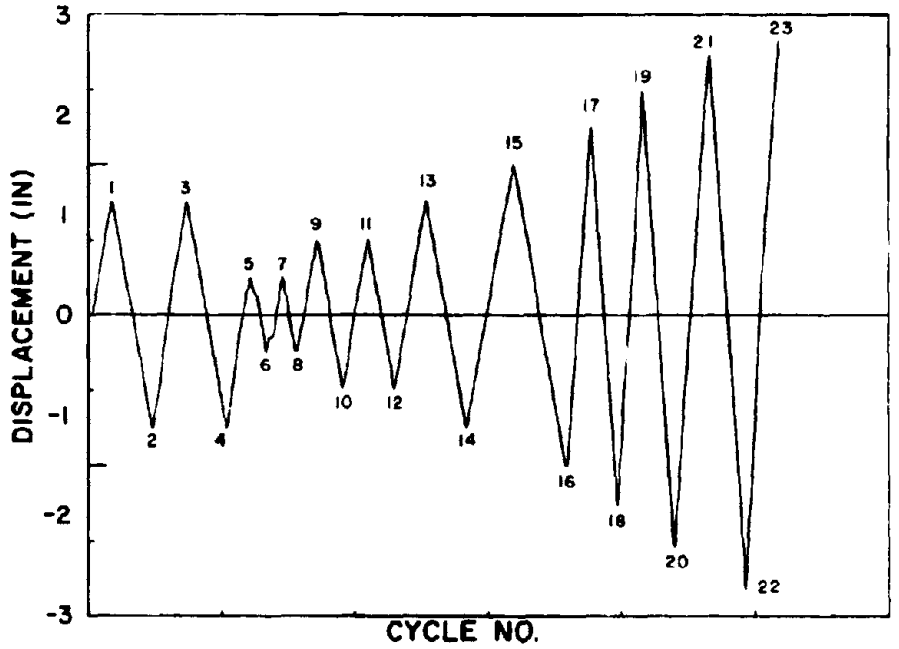


Fig. 3.10 Loading History Employed in Experiment 20.

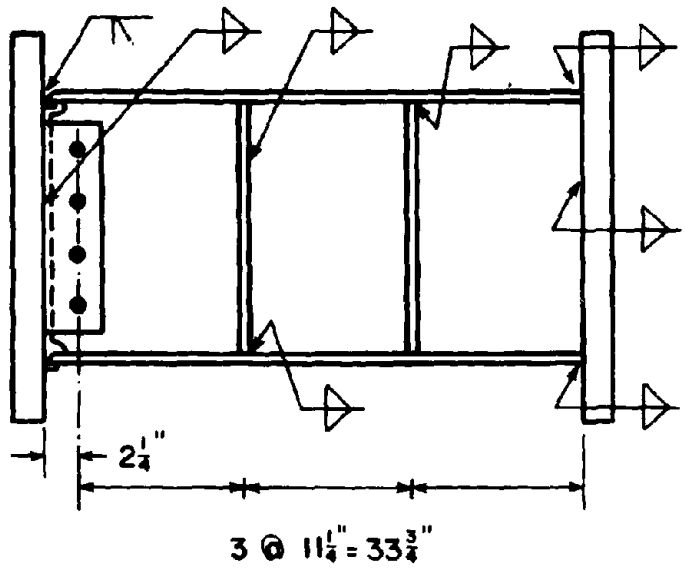


Fig. 3.11 Connection Details of Specimen 22.

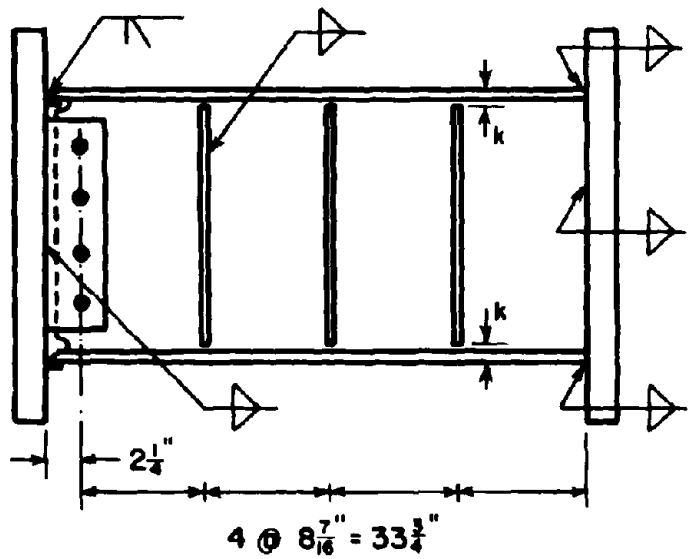


Fig. 3.12 Connection Details of Specimen 28.

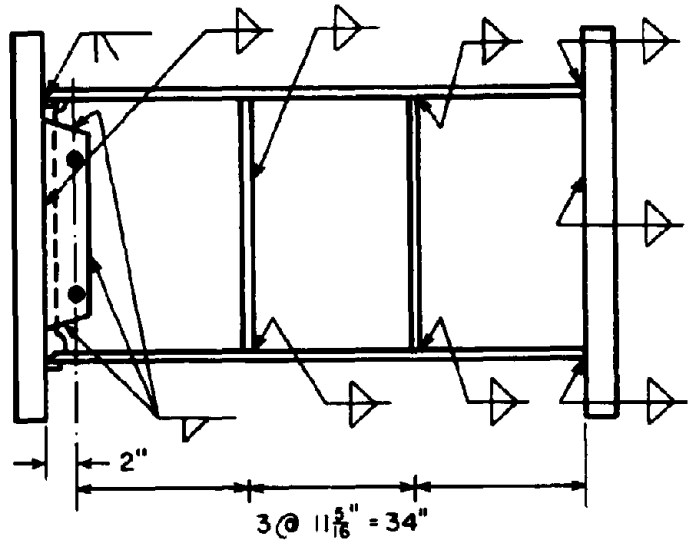


Fig. 3.13 Connection Details of Specimen 23.

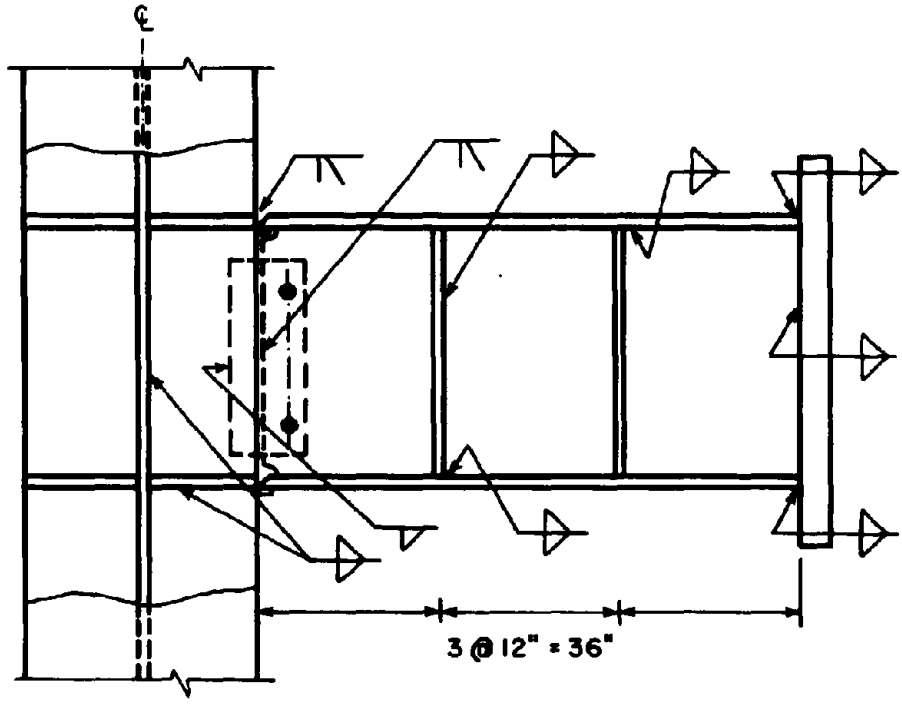


Fig. 3.14 Connection Details of Specimen 25.

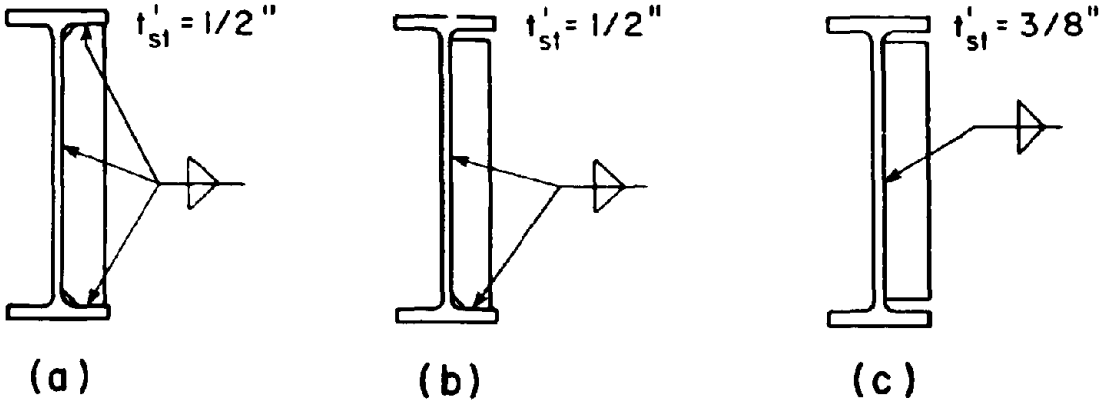


Fig. 3.15 Stiffener Details Employed in the Experiments.

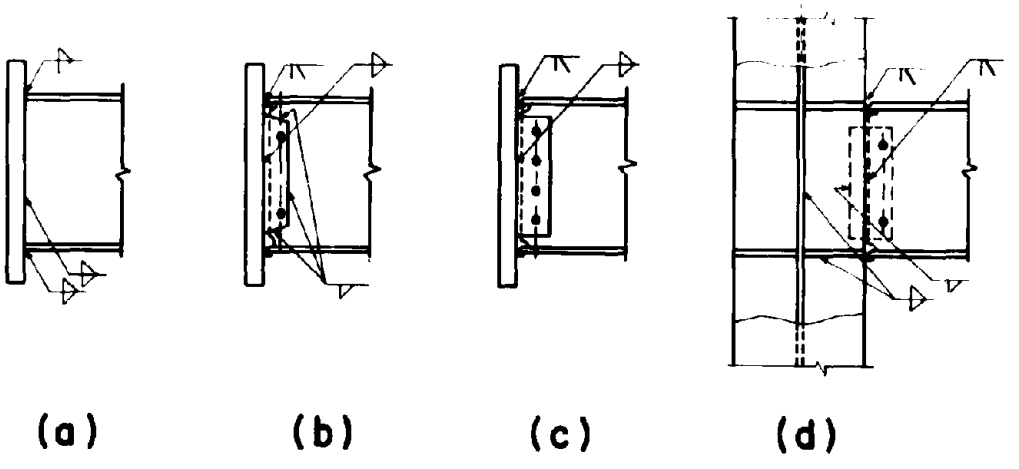


Fig. 3.16 Connection Details Utilized in the Experiments.

# CHAPTER 4 - DISCUSSION OF TEST RESULTS

The specimens fabricated to meet the design requirements discussed in the previous chapter were tested in the experimental apparatus described in Chapter 2. Since the response of all the links follow a similar pattern, a general discussion of link behavior will be presented. Special features of each test will then be commented upon. The force-displacement hysteretic loops and a photograph of each failed specimen are included to aid in understanding the results of the experiments. It should be noted that the initial excursion to any specified displacement is defined to be the positive direction for all the force-displacement curves. This chapter is intended to give a qualitative discussion of the test results. Quantitative analyses of the tests will be discussed in subsequent chapters.

## 4.1 General Discussion of Specimen Behavior

The basic features of shear link response to large overloads are common to all active links. A typical displacement curve, shown in Fig. 4.1 (from Specimen 26), will be used as an aid in describing these basic features. The initial elastic region, is shown by the line between points A and B of this figure. This region exhibited the expected linear response with a stiffness near that predicted by Timoshenko beam theory. First yield occurred at a displacement of approximately 0.20 in. at a shear near the theoretical yield shear of $V_y = \sigma_y dt_w/\sqrt{3}$ (Pt. C). Because of the cyclic loading program, the specimens did not exhibit the yield plateau and subsequent strain hardening characteristics of tension tests on mild carbon steel. Unloading followed a path essentially parallel to the elastic stiffness, as shown by the region between points D and E. During this loading process the specimens dissipated a considerable amount of energy. Reversed loading continued elastically until the onset of yielding in the opposite direction. The Bauschinger effect was clearly present as the loads approached the new maximum displacement

(Pt. F). This effect became more pronounced as the tests progressed. The cyclic nature of the loading history, coupled with increasing displacements, produced significant strain hardening in the specimens. The specimens commonly reached loading peaks (Pt. G) 50 percent higher than the initial yield load. The specimens exhibited essentially kinematic strain hardening, with elastic rebounds of approximately twice the yield shear before the onset of the Bauschinger effect. Before web buckling occurred, successive load peaks to the same displacement level increased slightly (Pts. H and I).

After the web buckled, the behavior of the links changed considerably. Web buckling of shear links generally followed a cyclical symmetrical mode, depicted in Fig. 4.2 [13]. To meet compatibility requirements, this type of buckled configuration caused pinching flange displacements. Stress concentrations induced by the one-sided stiffener welds caused buckling to take place toward the stiffened side of the web. In general, only one panel zone exhibited significant buckling, although in some cases multiple panel buckling did occur.

Along with large web displacements, web buckling caused substantial axial shortening of the links. Peak out-of-plane displacements were 3.25 in. for unstiffened webs and 2.5 in. for webs with two stiffeners. Peak axial shortening values were on the order of 1.0 in.

The onset of web buckling initiated the deterioration of link performance. As shown by points J and K in Fig. 4.1, successive peaks to the same displacement decreased after buckling. Also, the load-displacement curves showed a significant drop in strength before regaining capacity, as shown by point L. This phenomenon is illustrated more specifically in Figs. 4.3 and 4.4. Figure 4.4(a) shows the initially buckled configuration. Reversal of the load caused an unaligned buckled shape similar to that of Fig. 4.4(b). At this point the load carrying capacity reached its minimum point, point b in Fig. 4.3. When the load reversal was completed, the buckle had formed in the complementary direction, as shown in Fig. 4.4(c). Once the new buckled shape had formed, tension field action similar to that of a Pratt truss made possible the capacity increase shown by point c in Fig. 4.3.

Continued large displacement cycling finally caused material tearing in the links. This material tearing was considered the failure point of the specimens. For the unstiffened specimens, tearing took place near the center of the web region due to material fatigue from severe web curvature reversals. In the stiffened specimens, the tearing took place around the perimeter of the buckled panel. Certain specimens, though, failed due to connection failure rather than web web tearing. This type of failure occurred in a sudden manner, while material tearing took place gradually.

### 4.2 Special Features of the Different Tests

Virtually all the basic features mentioned above were exhibited by the different specimens throughout the testing sequence, but, the degree varied considerably. These variations make it possible to compare the effectiveness of shear links with different details or loading histories. In this section, qualitative comparisons will be discussed. Later chapters will explicate the quantitative comparisons. From these comparisons, conclusions and design recommendations can be determined.

#### 4.2.1 Stiffener Detail Tests-

*4.2.1.1 Specimen 17-* The effectiveness of one-sided stiffeners was first investigated in Specimen 17. Remarkably, the hysteretic loops for this specimen, depicted in Fig. 4.5, are virtually identical to those of an earlier specimen which had two-sided stiffeners, shown in Fig. 4.7 [13]. Even the post buckling behavior of the two specimens proved to be amazingly similar, as comparison of the two figures indicates. The only real difference between the two curves is that the yield strength of Specimen 17 was approximately 20 percent higher than that of the earlier specimen. The fact that these two specimens behaved almost identically led to the conclusion that sufficient one-sided stiffening is structurally equivalent to that of stiffening on both sides of the web. The failed specimen, in which buckling initiated during the second 2 in. cycle, is shown in Fig. 4.6.

*4.2.1.2 Specimen 21-* Specimen 21, a W 18x40 section with two stiffeners, was designed to investigate the performance of shear links with the one-sided stiffeners welded to only one flange. The response of this specimen is shown in Fig. 4.8. Prior to buckling, the behavior of this specimen was almost identical to that of Specimen 17. Once buckling occurred during the second 2 in. cycle, the capacity reduction of this specimen was more rapid than that of Specimen 17. The curves also show that there is a smaller increase in load due to realignment of the buckled field for the specimen with stiffeners welded to only one flange. But, Specimen 21 was able to undergo two full cycles more than Specimen 17, due mainly to the fact that web buckling in two panels placed less severe local strain requirements on this specimen. As shown in Fig. 4.9, Specimen 21 failed by tearing near a panel corner in which the stiffener was not welded to the flange.

*4.2.1.3 Specimen 26-* The favorable performance of Specimen 21 led to the decision to try stiffeners cut away from both flanges. As Fig. 4.10 shows, the W18x40 section with three stiffeners used in Specimen 26 performed quite well. The closely spaced stiffeners delayed buckling until the second 2.5 in. cycle. Delaying web buckling allowed the web to continue to strain harden, permitting this specimen to reach a load of 213 kips, 80 kips above the expected yield, and 25 kips above the peaks of previous specimens with two stiffeners. This large amount of strain hardening also caused yielding in the 1/2 in. shear tab. This specimen resisted only one and one-half cycles after web buckling, indicating that an increased number of web stiffeners tends to reduce the postbuckling life of shear links. With the onset of buckling, the end of one of the stiffeners pulled away from the web fillet weld. This loss of weld integrity led to buckling across this stiffener during the failure cycle. The large displacements of this stiffener may be seen in Fig. 4.11. Welding the stiffener to the flange would have eliminated the possibility of the initial weld pull-out which led to this failure mode.

*4.2.1.4 Specimen 27-* This W18x40 specimen was identical to Specimen 26, except that another stiffener was added to reduce the panel size. Significant buckling never took place during this test, as Fig. 4.12 demonstrates by the lack of pinching in the hysteresis loops. The

added stiffener permitted this specimen to strain harden more than Specimen 26. The maximum load resisted was 238 kips, which is almost twice the yield shear. A sudden fracture of one of the full penetration flange welds caused failure of the specimen at the end of the second 2.5 in. cycle. Inspection of the fractured weld showed that weld defects in the heat affected zone caused the failure. A photograph of the weld is shown in Fig. 4.14. One can note that web and flange strain hardening enabled the end moments to exceed the theoretical plastic moment capacity of the section. The sudden failure exhibited by this specimen indicated that too close a stiffener spacing may contribute to this undesirable failure mode. After the weld failed, the specimen was loaded in the opposite direction to a displacement of 5 in. Even after the loss of one flange connection, the link continued to resist tremendous loads. Figure 4.13 shows the residual displacement. Note the apparent lack of web buckling of this specimen.

**4.2.2 Loading Program Tests-**

*4.2.2.1 Specimen 16-* The loading program for the unstiffened W18x60 section used in Specimen 16 was designed to cause web buckling during the initial cycle. As Fig. 4.15 shows, the initial cycle exhibited a yield plateau similar to that characteristic of monotonic tension tests on ductile steels. The peak load occurred during this initial cycle. The large shear forces generated moments which caused some crushing and spalling of the concrete reaction block. The effect of this crushing on link displacements will be discussed in the next chapter. Significant load capacity reduction due to web buckling caused pinching of the hysteretic loops. Despite this pinching effect, this specimen dissipated a great deal of energy after the initiation of buckling. This appears to be characteristic of links with thick unstiffened panels. The failed specimen is shown in Fig. 4.16.

*4.2.2.2 Specimen 18-* The unstiffened W18x60 section for this test was subjected to nine successive one inch cycles, generating the load displacement curve shown in Fig. 4.17. The initial excursion exhibited a yield plateau similar to that of Specimen 16. In the first load reversal and the four complete cycles which preceded buckling, the hysteresis loops were virtually

identical. The characteristic dip in the postbuckled curve during load reversal did not occur during the 1 in. cycles due to the comparatively small maximum displacements. At the conclusion of the ninth cycle, a linear cycle to approximately one-half of the yield load was performed to measure the residual elastic stiffness. The small amount of hysteresis exhibited by this specimen showed that it retained its elastic stiffness even after severe inelastic deformations. A similar subsequent cycle to three-quarters of the yield shear demonstrated the increasing Bauschinger effects at large deformations. Figure 4.18 depicts the material tearing which caused the specimen failure after a 4 in. positive displacement. This figure also points out the comparatively small amount of flange distress that occurred at large displacements of this unstiffened, thick web shear link. Succeeding photographs of stiffened specimens with thinner webs display large local flange displacements in the region of the buckled panel.

*4.2.2.3 Specimen 20-* The initial cycle to 1.5 in. did not buckle this stiffened W18x40 section. As Fig. 4.19 shows, the second cycle caused a slight amount of web buckling, though this did not significantly deteriorate the link capacity during later cycles. The web stiffening restrained the postbuckled pinching of the hysteresis loops exhibited by the unstiffened specimens. Cycling once at each displacement level allowed this specimen to retain good capacity to a displacement of 3.5 in. Buckling occurred in all three panels, though the buckling in the center panel predominated. Application of only a single cycle at each displacement level and multiple panel buckling combined to allow this specimen to dissipate a tremendous amount of energy. The material tearing in a corner of the center panel is shown in Fig. 4.20.

*4.2.2.4 Specimen 24-* In Specimen 24, a monotonic loading history was imposed on a W18x40 section with two fully welded stiffeners. As depicted in Fig. 4.21, this specimen exhibited a yield plateau. First buckling of the specimen occurred just beyond a displacement of 3.5 in. The maximum load of 189 kips was only slightly above that of the peaks for cyclically loaded specimens with identical details. This peak load occurred just after buckling, at a displacement near 3.25 in. The specimen resistance dropped only slightly as the displacement increased beyond this point. At a displacement of 6 in. the test was delayed because of a

constraint in the apparatus, causing a drop in the load due to stress relaxation. On removing the mechanical interference in the apparatus, the applied displacement was continued to 7.2 in., reaching the limit of the loading ram. At the maximum displacement the specimen still resisted a load of 172 kips. Upon load reversal, the specimen did not resist as large a force as that in the positive direction, though the 160 kips peak was still well above the yield shear. This specimen also was subjected an additional 6 in. cycle, which is not shown in Fig. 4.21. During this cycle no yield plateau was observed, with the load increasing monotonically to 162 kips. The load was then reversed, achieving a maximum shear of 148 kips, before conclusion of the test. The failed specimen, as shown in Fig. 4.22, had severe buckling in the two exterior panels and minor buckling in the center. Also, this figure shows the extremely severe flange buckling which allowed the specimen to achieve the large displacements.

### 4.2.3 End Connection Tests-

*4.2.3.1 Specimen 22-* The bolted web, welded flange connection utilized in Specimen 22 has become a common connection detail in California. This W18x40 specimen had two one-sided stiffeners. The hysteretic response of this type of connection includes bolt slip at large cyclic loads. The first slip in this specimen occurred long after the initial yielding, during the second one inch cycle. Thereafter, bolt slippage took place near the initial yield load. As Fig. 4.23 shows, the prebuckled response of this specimen was quite similar to that of previous tests. After the specimen buckled during the second 2 in. cycle the load carrying capacity deteriorated significantly. Buckling occurred in the panel containing the bolted connection. The bolt holes were severely distorted by the slippage of the bolts, although the bolts themselves were not severely damaged. Figure 4.25 displays the distorted holes. The bolt slippage transferred a large portion of the shear to the specimen flanges. These flange shear forces initiated tearing at the web-flange junction near the flange weld. The final failure of the specimen resulted from a flange shear failure, as shown in Fig. 4.24. The mode of failure exhibited by this specimen was identical to those of bolted connections tested previously [21].

*4.2.3.2 Specimen 23-* Another common beam-to-column flange connection is the connection with a shear tab fillet welded to the beam web. This detail was investigated in Specimen 23, a W18x40 section with two one-sided stiffeners. The load-displacement curve for this specimen is shown in Fig. 4.26. Before the initiation of buckling the response of this specimen was very close to that of Specimen 22. But, the more efficient shear transfer mechanism allowed Specimen 23 to regain more load following buckle realignment than Specimen 22. It is interesting to note that this specimen buckled in the center panel, away from the column-link connection. In the all-welded case the shear was transferred at the fillet weld, effectively reducing the web end panel width. In the bolted web case, the shear is transferred at the bolt line, which results in a larger effective end panel width than that of the fillet welded web connection. In general, buckling is preferred in interior panels, since end panel buckling may lead to sudden connection failures. Specimen 23 failed by web tearing in an interior panel, as Fig. 4.27 shows.

*4.2.3 3 Specimen 25-* Since connection to the column flange is not always possible, Specimen 25, a W18x40 section with two one-sided stiffeners, tested the connection of a shear link to a column web. Initially, this specimen performed quite well, as Fig. 4.28 indicates. The lack of ability to regain previous loads during postbuckling behavior can be noted. The shear link property of energy dissipation through inelastic web strains rather than flange yielding appears to have prevented any problems with the flange connection. The column stiffener plates provided to transfer the flange forces to to the column showed no signs of distress, while the web plate was slightly bent about 2 in. from the full penetration web weld. The specimen buckled in all three panels, as Fig. 4.29 shows. This fact made possible the large displacements which this specimen resisted. While one test cannot be considered conclusive, the nature of the shear link energy dissipation mechanism and the results of this test implies that connections to column webs do not appear to seriously impair shear link behavior.

*4.2.3.4 Specimen 28-* The bolted web connection of Specimen 28, a W18x40 section, included three web stiffeners. The added web stiffening delayed the initiation of buckling and allowed for increased strain hardening. Slippage of the bolts initiated during the one inch

cycles. The short flat regions near one inch displacements in Fig. 4.30 depicts the bolt slippage. Bolt slippage continued to occur until a small tear initiated at the web-flange junction near the full penetration flange weld. After the bolt slip occurred on the next cycle, the specimen failed suddenly. It appears that the bolt slip transferred large shear forces to the flanges, causing the 1/2 in. thick flange to shear off just outside the heat affected zone of the weld. This specimen showed no web buckling, and reached cyclic displacements of only 1.5 in. before failure. The failed specimen is depicted in Fig. 4.31. The small displacement capacity and the abrupt failure exhibited by the bolted web connection of this specimen demonstrated the possible deficiencies of this detail for links with large ductility demands.

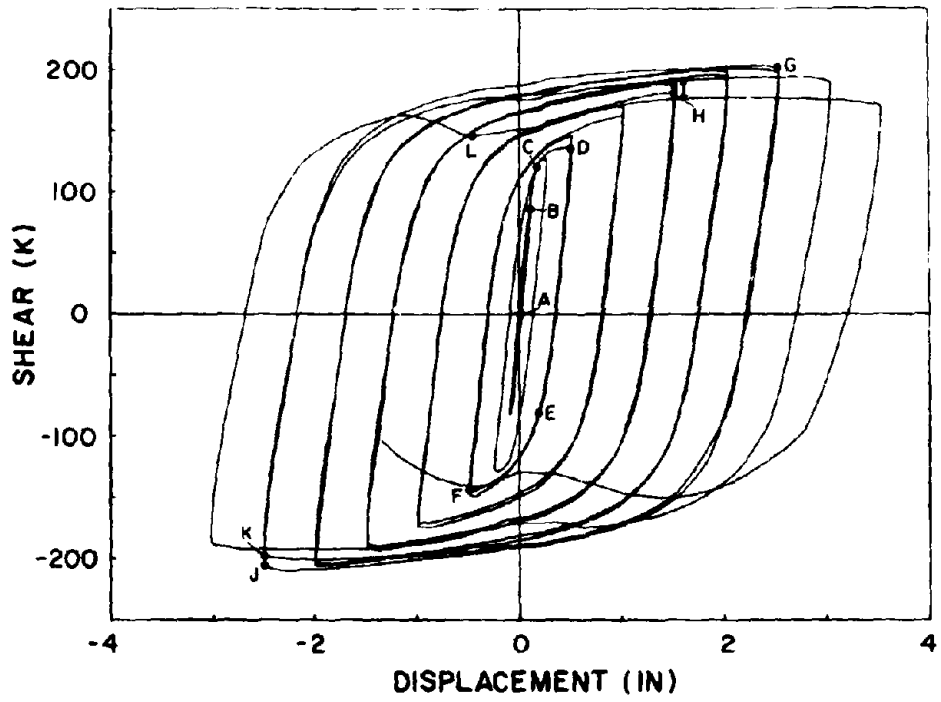


Fig. 4.1 Typical Load vs. Displacement Curve for a Well Stiffened Shear Link.

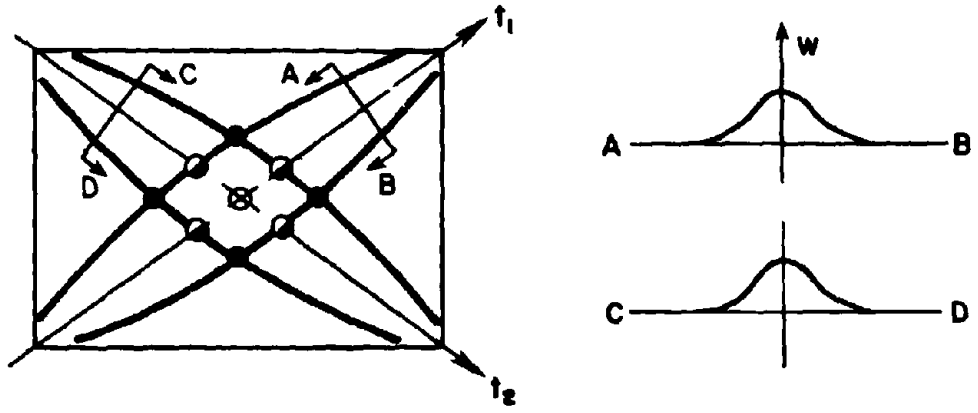


Fig. 4.2 Symmetrical Buckling Mode of Shear Link Webs [13].

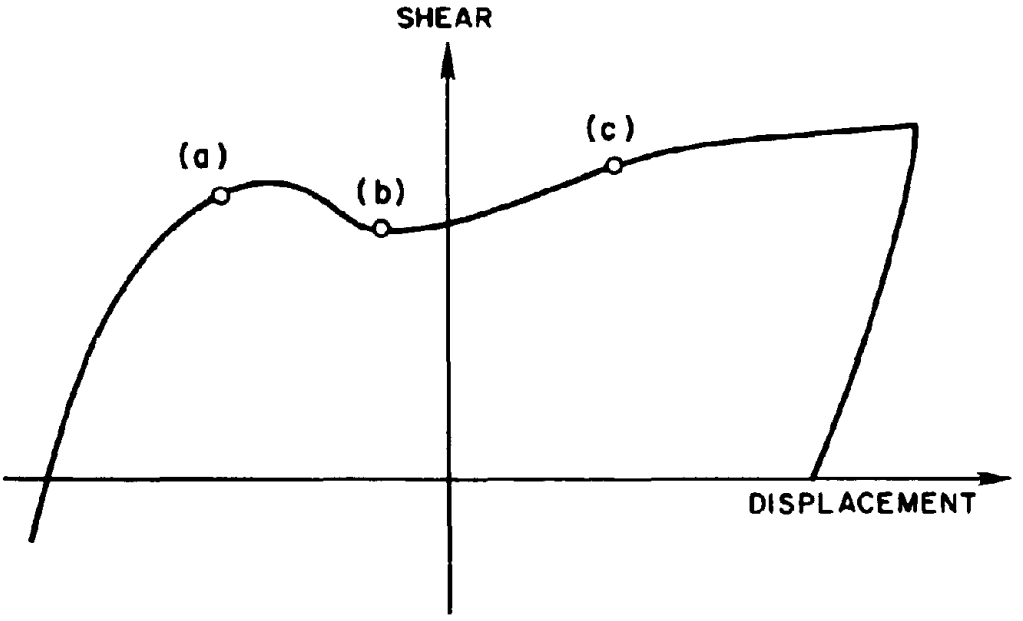


Fig. 4.3 Typical Half Cycle for a Shear Link During Postbuckled Response.

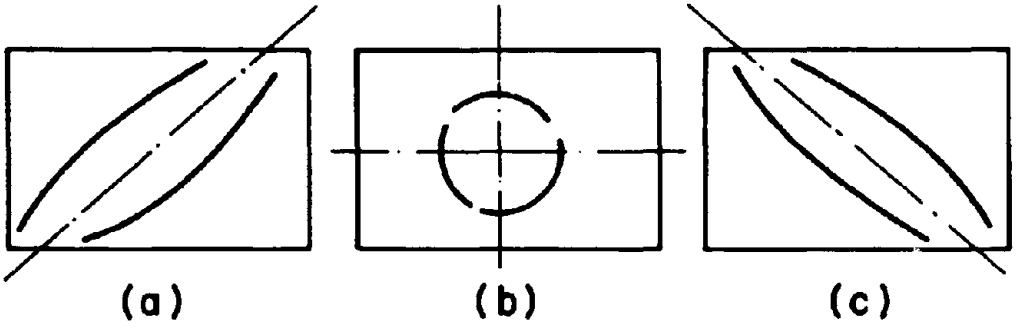


Fig. 4.4 Orientation of Web Buckling at Different Stages of Half Cycle.

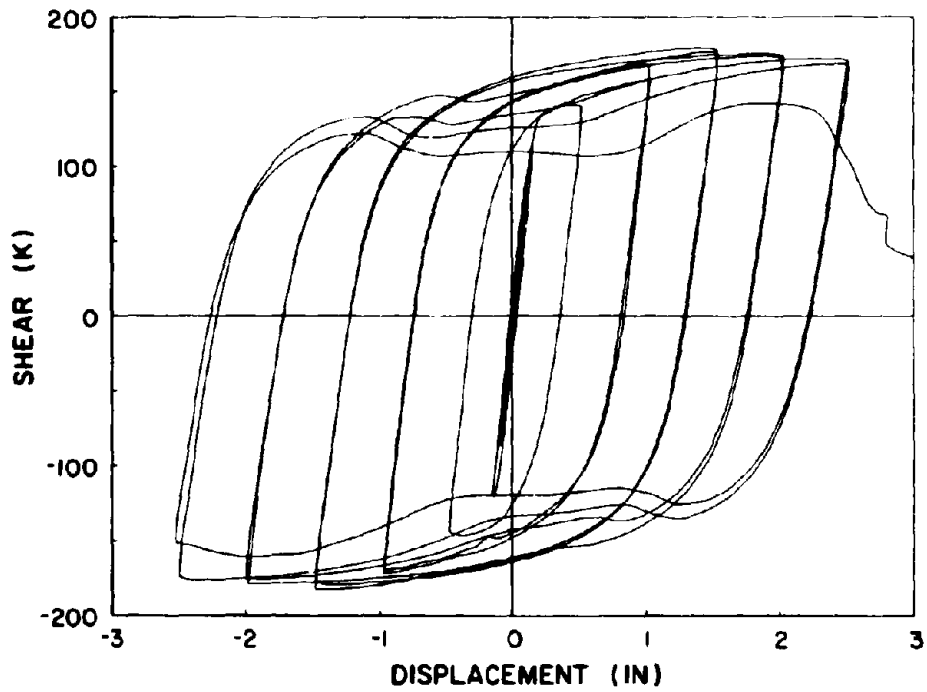


Fig. 4.5 Force-Displacement Hysteretic Loops of Specimen 17.

Fig. 4.6 Photo of Specimen 17, a W18x40 Section with Two 1/2 in. Thick Stiffeners, at the End of Testing.

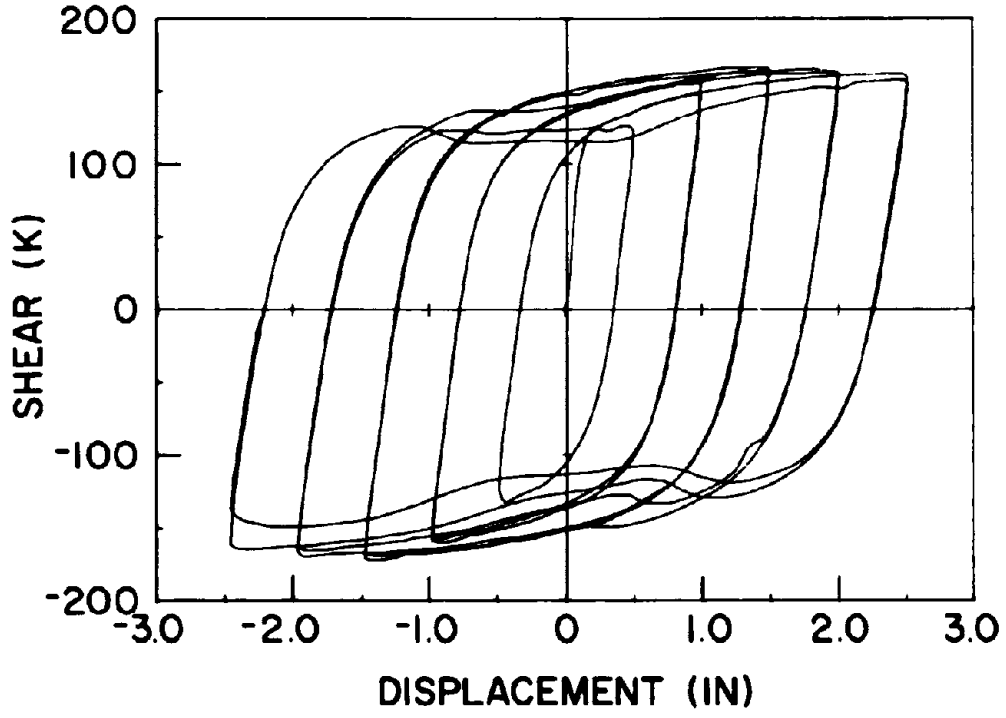


Fig. 4.7 Force-Displacement Hysteretic Loops of a Similar Specimen (Specimen 9 [13]) with Two-Sided Stiffeners.

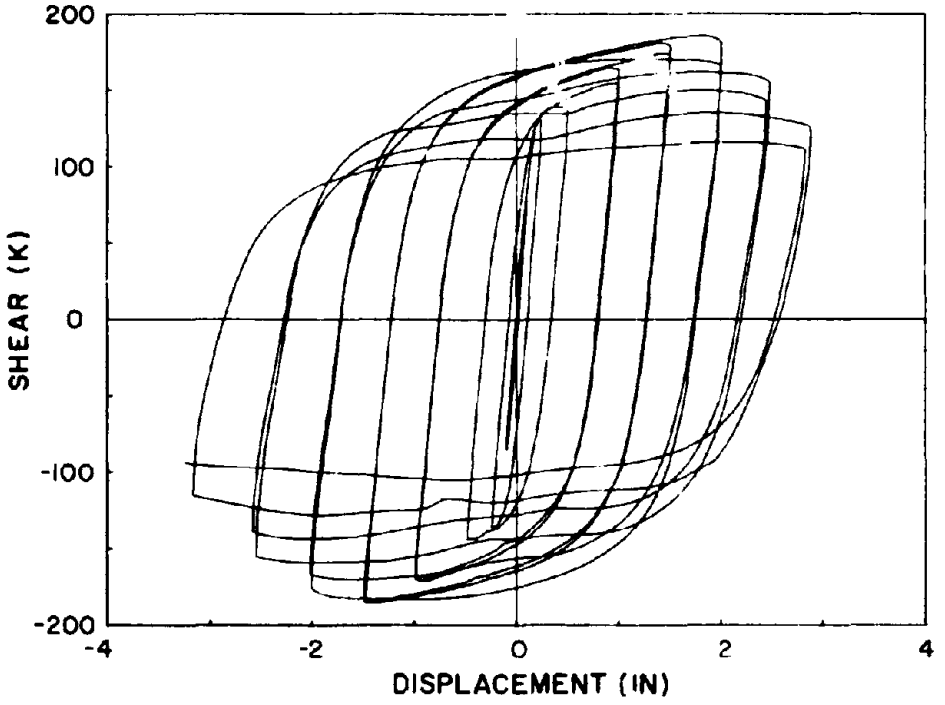


Fig. 4.8 Force-Displacement Hysteretic Loops of Specimen 21.

Fig. 4.9 Photo of Specimen 21, a W18x40 Section with Two 1/2 in. Thick Stiffeners, at the End of Testing.

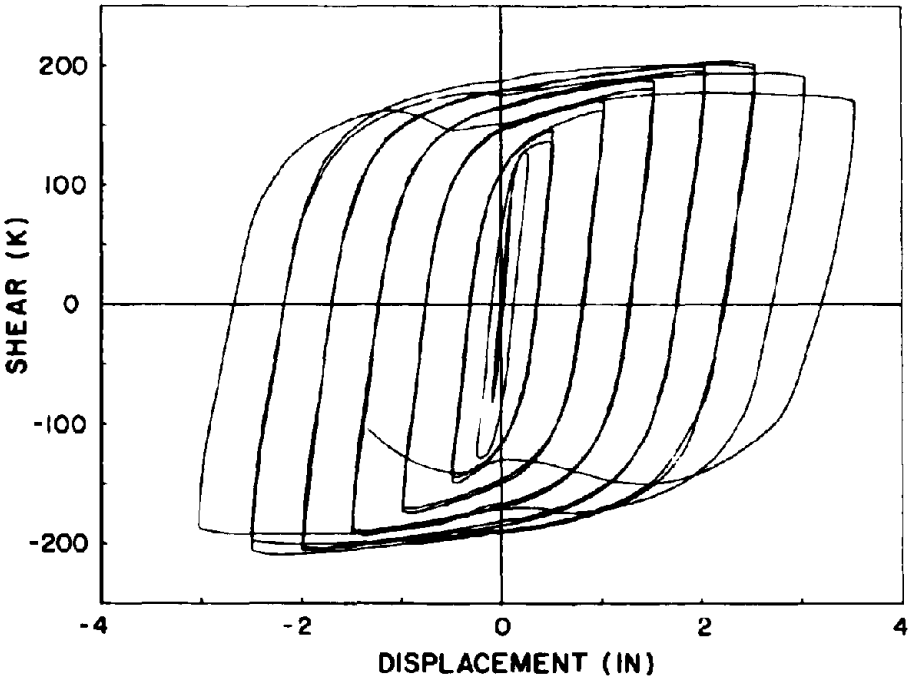


Fig. 4.10 Force-Displacement Hysteretic Loops of Specimen 26.

Fig. 4.11 Photo of Specimen 26, a W18x40 Section with Three 3/8 in. Thick Stiffeners, at the End of Testing.

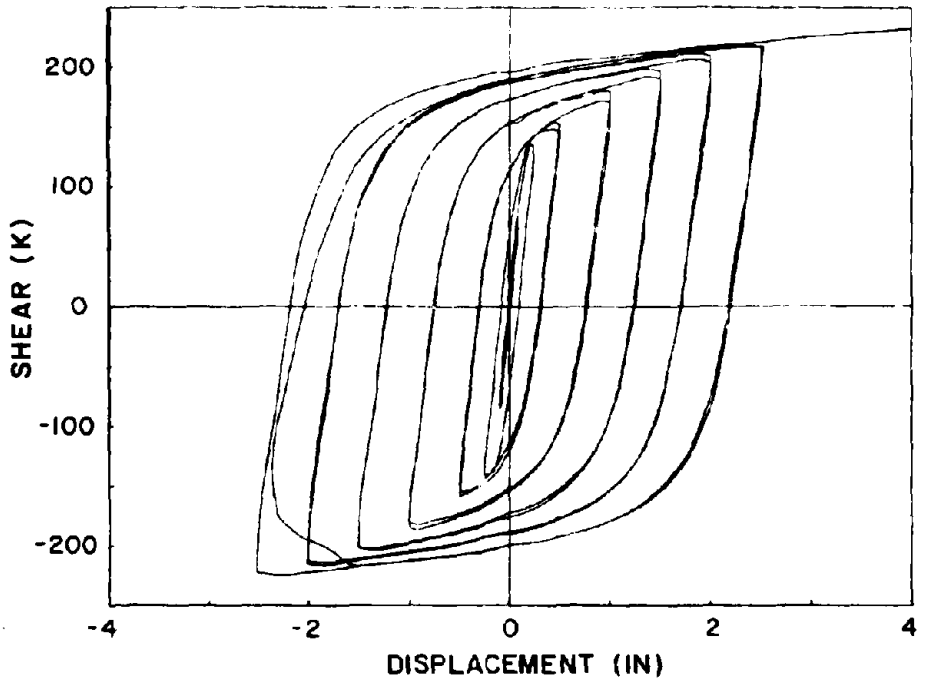


Fig. 4.12 Force-Displacement Hysteretic Loops of Specimen 27.

Fig. 4.13 Photo of Specimen 27, a W18x40 Section with Four 3/8 in. Thick Stiffeners, at the End of Testing.

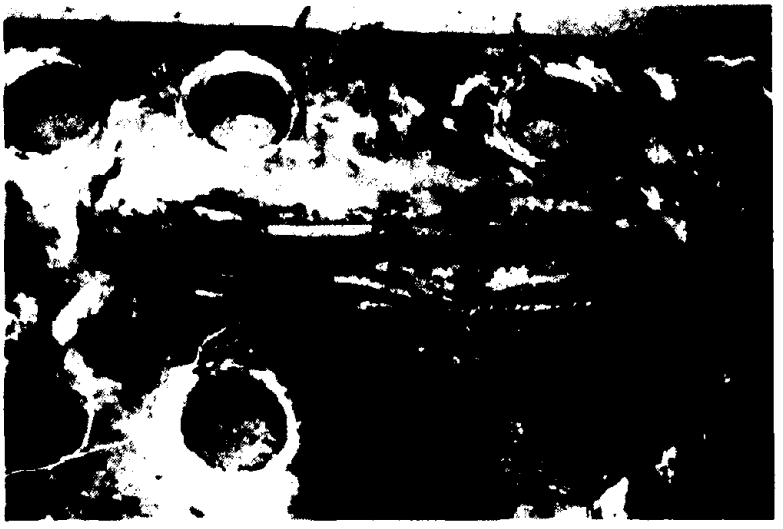

Fig. 4.14 Photo of the Failed Flange Weld of Specimen 27.

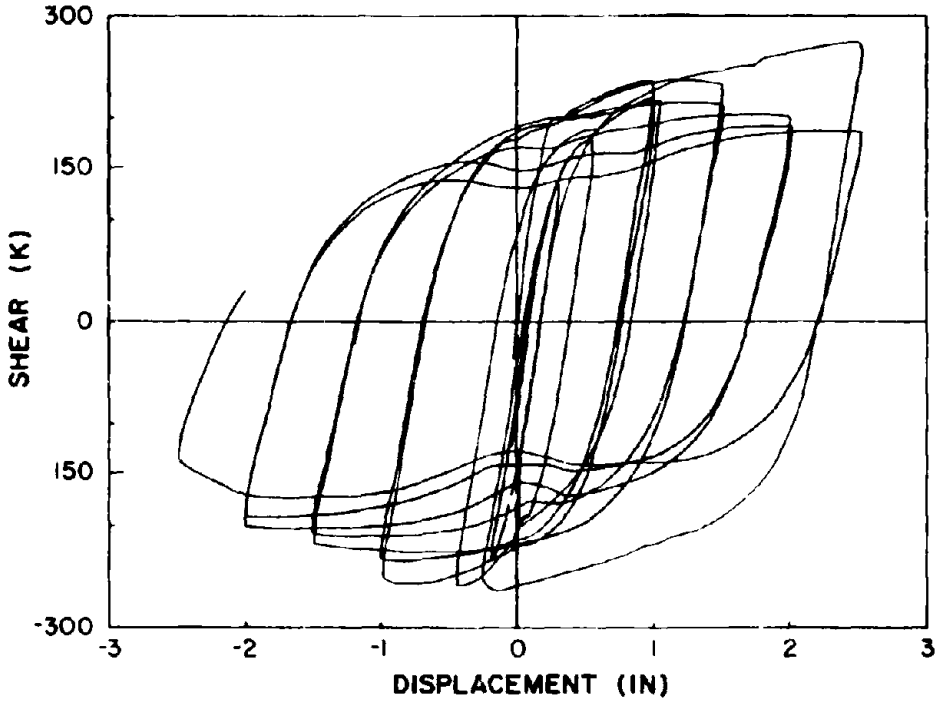


Fig. 4.15 Force-Displacement Hysteretic Loops of Specimen 16.

Fig. 4.16 Photo of Specimen 16, an Unstiffened W18x60 Section, at the End of Testing.

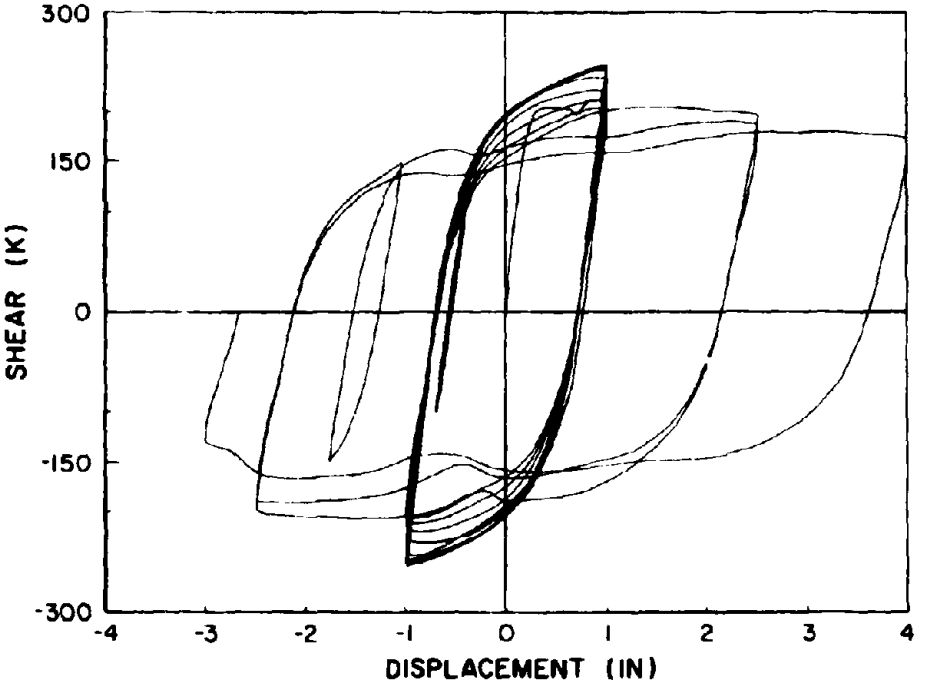


Fig. 4.17 Force-Displacement Hysteretic Loops of Specimen 18.

Fig. 4.18 Photo of Specimen 18, an Unstiffened W18x60 Section, at the End of Testing.

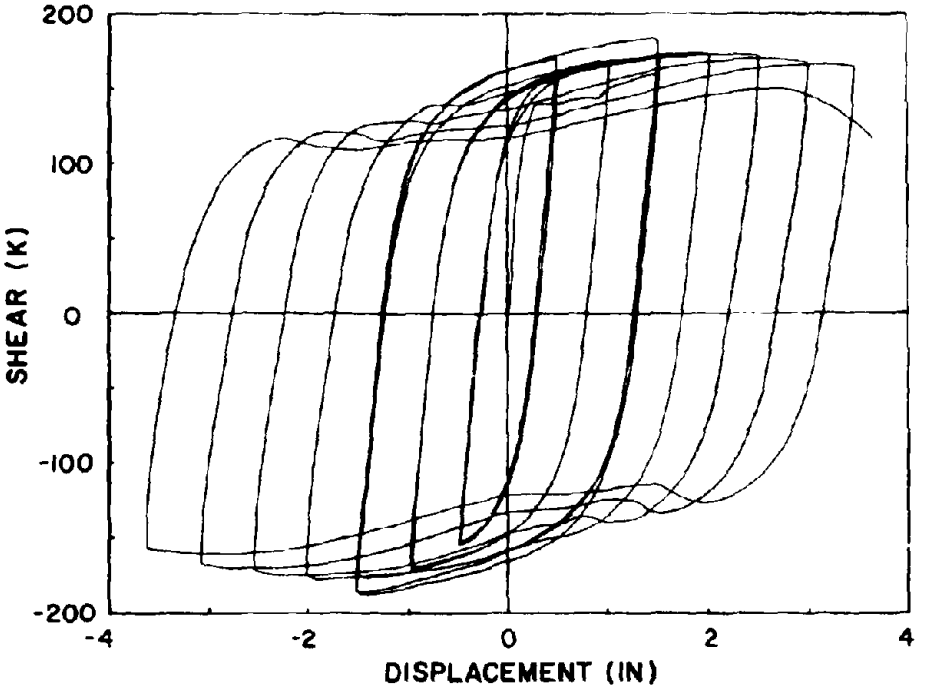


Fig. 4.19 Force-Displacement Hysteretic Loops of Specimen 20.

Fig. 4.20 Photo of Specimen 20, a W18x40 Section with Two 1/2 in. Thick Stiffeners, at the End of Testing.

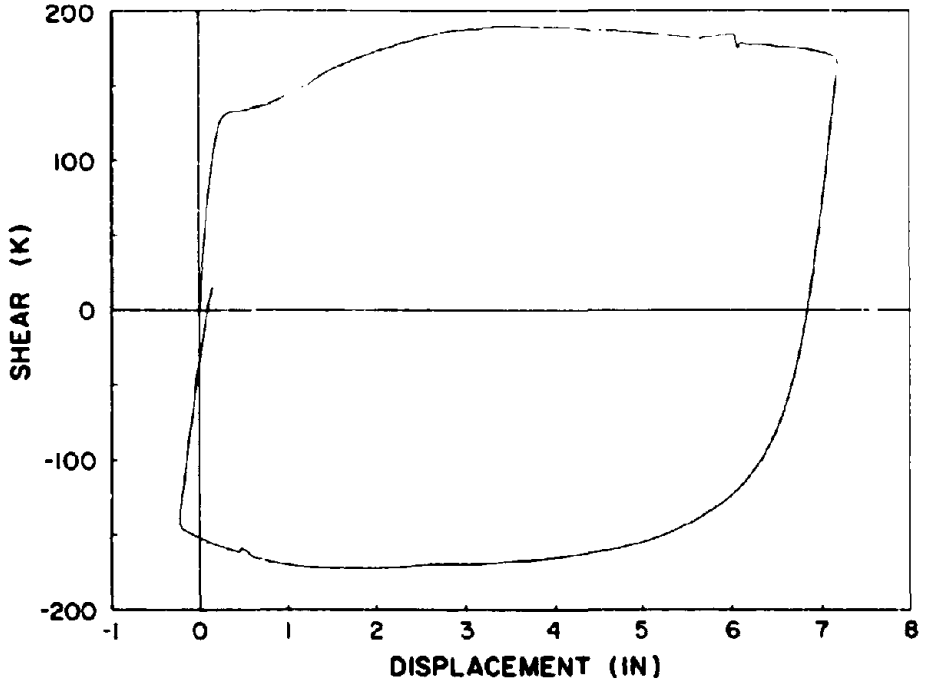


Fig. 4.21 Force-Displacement Hysteretic Loop of Specimen 24.

Fig. 4.22 Photo of Specimen 24, a W18x40 Section with Two 1/2 in. Thick Stiffeners, at the End of Testing.

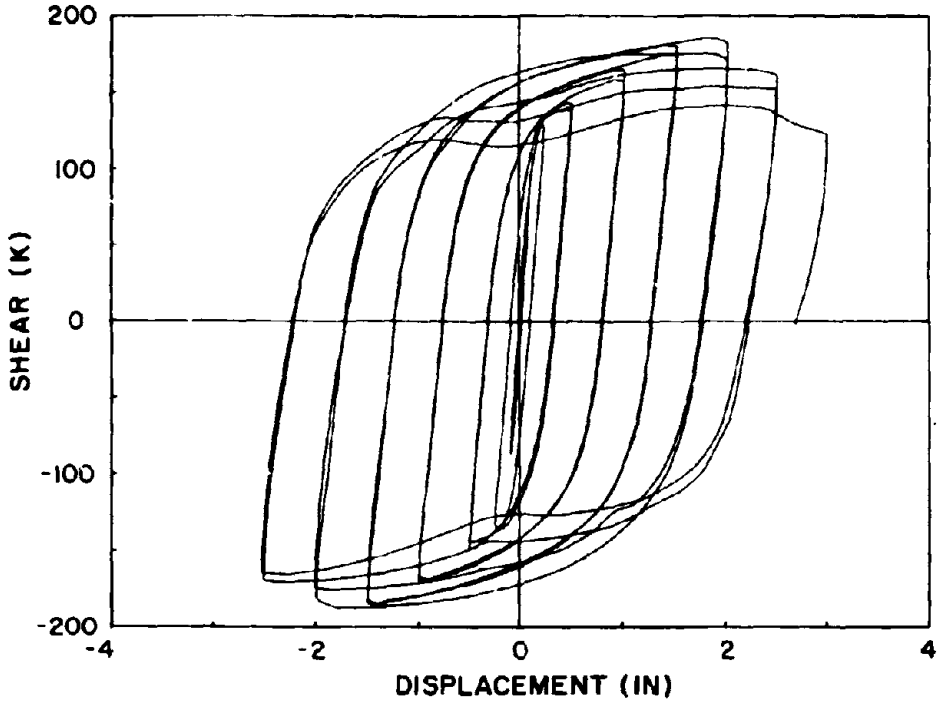


Fig. 4.23 Force-Displacement Hysteretic Loops of Specimen 22.

Fig. 4.24 Photo of Specimen 22, a W18x40 Section with Two 1/2 in. Thick Stiffeners, at the End of Testing.

Fig. 4.25 Photo of Distorted Bolt Holes of Specimen 22.

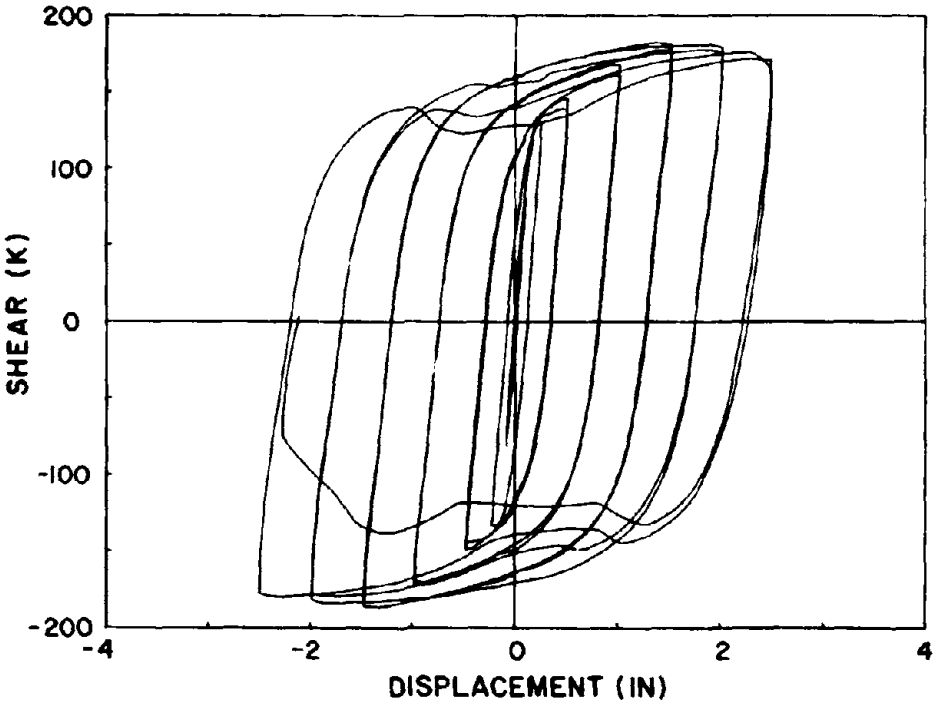


Fig. 4.26 Force-Displacement Hysteretic Loops of Specimen 23.

Fig. 4.27 Photo of Specimen 23, a W18x40 Section with Two 1/2 in. Thick Stiffeners, at the End of Testing.

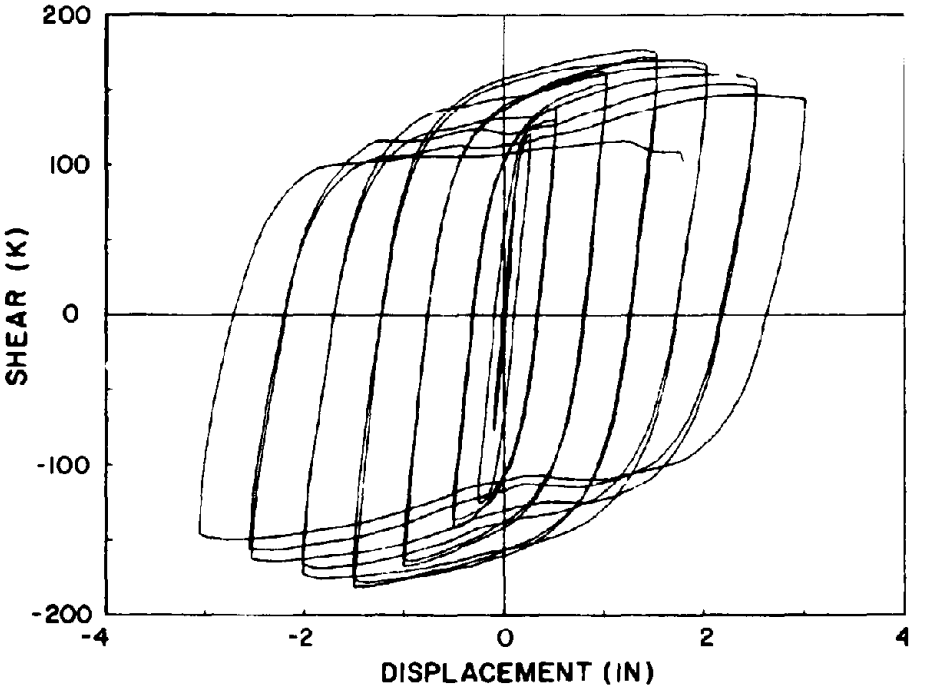


Fig. 4.28 Force-Displacement Hysteretic Loops of Specimen 25.

Fig. 4.29 Photo of Specimen 25, a W18x40 Section with Two 1/2 in. Thick Stiffeners, at the End of Testing.

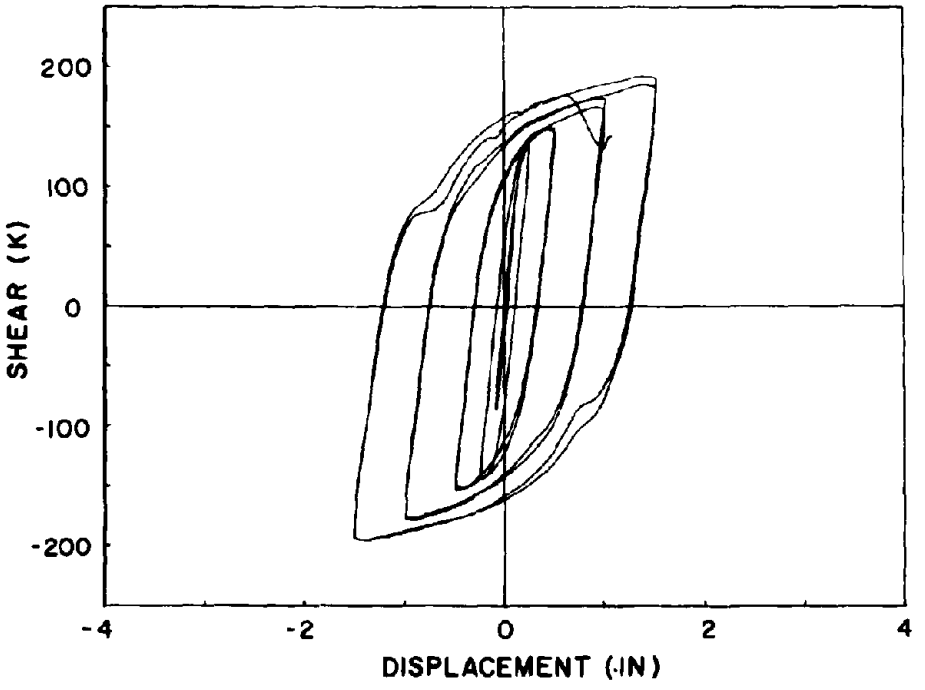


Fig. 4.30 Force-Displacement Hysteretic Loops of Specimen 28.

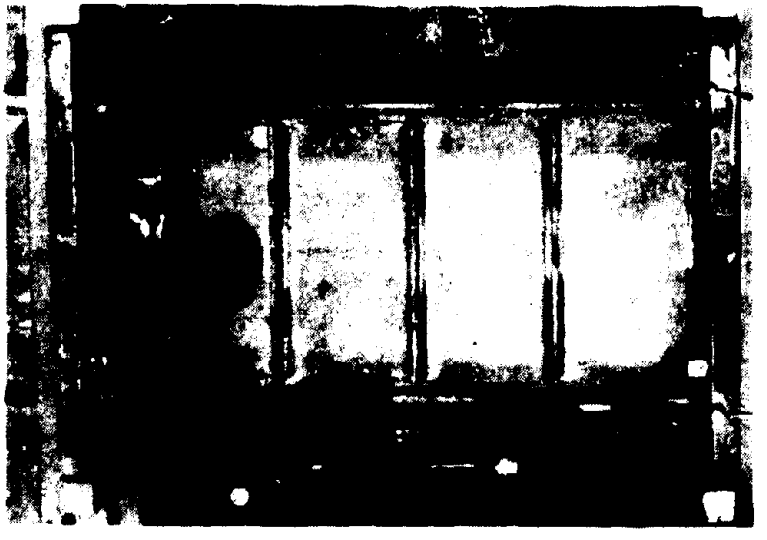

Fig. 4.31 Photo of Specimen 28, a W18x40 Section with Three 3/8 in. Thick Stiffeners, at the End of Testing.

# CHAPTER 5 - ANALYSIS OF EXPERIMENTAL RESULTS

Chapter 4 dealt with the results of the twelve tests in a qualitative manner. These results enabled the development of some basic conclusions regarding the behavior of shear links. The data collected by the instrumentation provided quantitative information regarding specific aspects of the tests. In this chapter, this test data are used to analyze the four stages of shear link response: elastic, inelastic pre-buckling, post-buckling, and failure. The next chapter will concentrate on energy dissipation characteristics as a measure of link performance. Evaluation of the qualitative observations and the quantitative analyses provides the basis for conclusions and recommendations for shear link design.

## 5.1 Elastic Behavior

The elastic response of a beam is usually analyzed using the Bernoulli-Euler-Navier hypothesis that initially normal and plane sections remain normal and plane after deformation. As the length of the beam decreases, shearing deformations become significant and the basic theory becomes less accurate. In Timoshenko beam theory, shearing deformations are accounted for by assuming that a constant average shear stress acts on an effective shear area, $A'$. For wide flange sections, the shear area is generally taken as the area of the web, $A'=A_w=dt_w$.

On the above basis, the elastic displacements of shear links due to shear can be taken as:

$$v=v_b(1+2\beta) \tag{5.1}$$

In this equation, $\beta$ introduces the contribution of shearing deformations to link displacements. The term $\beta$ is approximately:

$$\beta=\frac{6EI}{GA'L^2} \tag{5.2}$$

For the analytical model of these experiments corresponding to Fig. 5.1, the displacement due

$$v_b = \frac{VL^3}{12EI} \tag{5.3}$$

Assuming a value of $E/G=2.50$, the values of $\beta$ for the W18x60 and W18x40 sections used in this investigation are 1.51 and 1.26, respectively. For these $\beta$ values, the theoretical contributions of shear deformation as a fraction of the total, $2\beta/1+2\beta$, are 0.75 and 0.72, respectively.

Web shear deformations integrated over the specimen length determine the specimen displacement due to shear. Using the simple model depicted in Fig. 5.1, the shear displacement contribution during the linear cycles of each experiment are listed in Table 5.1. As this table shows, the shear contribution to the total deflection is on the order of 0.50 when the model shown in Fig. 5.1 is employed.

The actual end fixity of the specimens was not complete. Throughout the tests, the "fixed" end at the rigid concrete reaction block side slipped and rotated slightly. A refined model of the prevailing conditions at the fixed end is shown in Fig. 5.2. This diagram shows that a lateral displacement support stiffness, $K_\Delta$, and a rotational support stiffness, $K_\Theta$, can be introduced to obtain a more accurate formulation. From the test data shown in Figs. 5.3 and 5.4, the values of $K_\Delta$ and $K_\Theta$ are estimated to be 4400 k/in. and 8,200,000 k/rad, respectively. Therefore, the true stiffness of the system, $K^*$, can be defined as:

$$\frac{1}{K^*} = \frac{1}{K} + \frac{1}{K_\Delta} + \frac{L}{K_\Theta} \tag{5.4}$$

In this equation, the member stiffness, $K$, is given by:

$$K = 12\frac{EI}{L^3(1+2\beta)} \tag{5.5}$$

and the link displacement, $v$, for the refined link model becomes:

$$v=\frac{V}{K}=V\left[(1+2\beta)\frac{L^3}{12EI}+\frac{1}{K_A}+\frac{L}{K_G}\right] \tag{5.6}$$

From the values determined for these tests, it was calculated that the support displacements contributed approximately 23 per cent of the total displacement in the linear elastic range. Using the more refined model depicted in Fig. 5.2, the shear displacement contribution was again calculated. These values, listed in the right column of Table 5.1, are quite close to the 72 per cent contribution expected from Timoshenko beam theory. Therefore, it seems that the elastic stiffness of shear links in eccentrically braced frames can be analyzed quite accurately using Timoshenko beam theory.

### 5.2 Inelastic Pre Buckling Response

During an extreme seismic event, a properly designed eccentrically braced frame will cause the shear links to undergo extensive inelastic deformations. The inelastic pre-buckling stage is important to consider for two reasons. First, most of the energy dissipation occurs during this response phase. The amount of energy dissipated after web buckling is usually quite small for links with sufficient web stiffening. Second, the inelastic behavior of the link prior to web buckling is important, as this is tacitly assumed in plastic analysis methods. After, the occurrence of web buckling, the behavior of the link is unreliable and difficult to model analytically.

**5.2.1 Inelastic Displacement Contributions-** The primary yielding mechanism exhibited by a link forms the basis for the distinction between shear and bending links. Shear links yield primarily by inelastic shearing stresses in the web. In bending links, normal stresses in the flanges dominate the inelastic behavior. During inelastic response, therefore, shearing displacements predominate in shear links, and bending displacements predominate in bending links.

*5.2.1.1 Shear Displacement Contribution-* The global displacement for the specimens tested in this investigation can be expressed as:

$$v(x)=v_{sh}(x)+v_b(x)+v_{sp}(x) \tag{5.7}$$

In this equation, $v_{sh}(x)$ is the displacement due to shear strains,

$$v_{sh}(x)=\int_0^x \gamma(x)\,dx \tag{5.8}$$

The displacement due to flexural strains, $v_{(x)}$, is

$$v_{(x)}=\int_0^x \kappa(x)\,dx \tag{5.9}$$

The displacement due to support movements in Eqn. 5.7 is $v_{sp}(x)$.

The $v_{sh}$ term in Eqn 5.7 was evaluated numerically using the data collected from the web strain gages. Table 5.2, lists the average contribution of shear to displacement in the inelastic range prior to buckling. After buckling occurred, the gage readings did not accurately determine shear displacement. Since the webs of Specimens 16 and 18 buckled during the initial cycle, the results from these tests are not included in the table. This table clearly shows that the shear displacements contributed the major component to the link deflection in the inelastic range.

*5.2.1.2 Support Contributions in the Inelastic Range-* In the elastic range, the support stiffness contributed up to 23 percent of the total specimen displacement. The support stiffnesses were nearly linearly elastic as Figs. 5.3 and 5.4 demonstrate. The support displacement contribution therefore became negligible during the large inelastic displacement cycles. Figure 5.5 is a plot comparing the recorded specimen displacement with the actual displacement adjusted for support conditions. As this figure shows, except for the linear cycles at the start of the test, the difference between adjusted and recorded displacements was indiscernible.

The above result applied to all specimens except Specimen 16. This heavier section caused spalling of the concrete reaction block during this test. Figure 5.6 shows the effect of this spalling on the adjusted displacement. Although this effect was recognizable, it did not significantly affect the response of the specimen. This problem was eradicated, and further

spalling of the reaction block did not occur in any of the subsequent tests.

**5.2.2 Link Moments and Flange Strains-** Although shear deformations dominate the response of shear links, flexural actions also play an important role. As Fig. 5.1 shows, for the link model used here, the relationship between end moment and shear was $M_{max}=VL/2$. Due to large amounts of strain hardening, the specimens usually resisted moments above the nominal plastic moment, $M_p$. Table 5.3 lists the values of $M_p$ based on the plastic modulus values, Z, for the W18x60 and W18x40 sections ( 123 $in.^3$ and 78.4 $in.^3$ respectively), and the actual ( $\sigma_y = 48$ *ksi*) and nominal values ( $\sigma_y = 36$ *ksi* ) of yield stresses. Table 5.4 lists the values of measured maximum end moments resisted by the specimens. As can be seen from this table, in all cases the links resisted bending moments in excess of the nominal values of $M_p$. For well stiffened webs, these moments even exceeded the values of $M_p$ based on $\sigma_y = 48$ *ksi*. It should be noted, however, that the plastic moment must be reduced since the webs fully yield [13]. The corresponding values of $M_p' = \sigma_y bt_f(d-t_f)$ for $\sigma_y = 48$ *ksi* are also given in Table 5.3. Since the end moments given in Table 5.4 are above $M_p'$, some strain hardening must have occurred in the flanges as well as the webs. Analysis of the flange strain data verified this conclusion. The maximum flange strains at each gage location for Specimen 16 (See Fig. 2.4 for gage locations) are listed in Table 5.5. These values show that large inelastic strains developed near the ends of the links. (The yield strain was approximately 1700 *in./in.*) The flange strain distributions were quite similar to those found in an earlier investigation [13], showing an almost linear variation of flange normal strain from the maximum value at the ends of the specimens.

### 5.3 Control of Post Buckled Behavior

The development of web buckling makes large local strains gage readings erratic. Qualitative aspects of post-buckled behavior are nonetheless significant. The characteristics of post-buckled behavior depend directly on the link design details. Proper detailing of the link can therefore ensure the desired post-buckling behavior. In this section three aspects of web

buckling that can be controlled through proper design will be discussed: *1.) delaying buckling, 2.) controlling the location of buckling, and 3.) developing multiple panel buckling.*

**5.3.1 Delaying Buckling-** The first and foremost objective of stiffening the link web is to delay the onset of buckling, since the energy dissipative capacity of shear links is greatly reduced by buckling. The spacing of stiffeners is the crucial consideration in delaying buckling. Earlier research [12] presented a set of relationships between the stiffener spacing and the energy dissipation capacity before the initiation of buckling. These relationships demonstrate the significant increase in energy dissipation capacity which can be realized by employing closely spaced stiffeners. As Specimen 27 demonstrated, though, reducing stiffener spacing below certain limits tends to lead to abrupt failures, causing the specimen to lose its ability to withstand large deformations. Based on the completed work, the minimum spacing for stiffeners providing excellent energy dissipation capacity appears to be about $20t_w$.

**5.3.2 Controlling the Location of Buckling-** The most desirable location for the development of a web buckle is an interior panel of the shear link. Buckling in the web panel adjacent to the column should be avoided since it can lead to premature link-column connection failure. Protection of the connection panel zone is accomplished by proper location of the stiffeners. In the web connection detail shown in Fig. 5.7, the shear is transferred to the shear tab along the fillet weld. For this case the stiffeners can be spaced from the erection bolt line, as shown in this figure. Since the panel width is reduced by the shear tab, web buckling is likely to occur in an interior panel.

Slippage may occur along the bolt line of bolted web shear link-to-column connections due to large shear forces. To protect the panel zone adjacent to the column in this case, it is advisable to space the stiffeners from the column face rather than the bolt line, as Fig. 5.8 shows. The same approach can be adopted for the link-column connection with full penetration web welds.

**5.3.3 Developing Multiple Panel Buckling-** In general, the buckling phenomenon depends on plate topology (panel size, initial imperfections, etc.), material properties, and the

boundary conditions. Typically, buckling occurs in only one panel of shear links. Once one panel begins to buckle, the displacement capacity demanded of the other panels is reduced. But, significant buckling occurred in multiple panels of equal size in four of the twelve specimens detailed in this investigation. Therefore, to induce multiple panel buckling the stiffeners should be equally spaced center-to-center.

### 5.4 Failure Modes of Shear Links

Typically, the final failure of the specimens was caused by material tearing due to severe reversals of web plate curvature. In unstiffened webs this occurred near the center of the buckled region, while in stiffened webs, this tearing took place around the perimeter of the buckled panel zone. These types of failure did not produce catastrophic results. Significant buckling preceded the final material tearing, and the tearing took place gradually; large loads could still be resisted throughout the tearing process.

Reduced stiffener spacing delays buckling and permits large increases in load resistance due to strain hardening. The increased shear force required larger moment resistance of the test specimens. Specimen 27 demonstrated that without excellent weld integrity, a sudden weld failure can take place in an excessively stiffened specimen. To avoid this type of failure, the stiffener spacing should not be less than $20t_w$.

| Specimen | % $\Delta_{shear}$ (test results) | % $\Delta_{shear}$ (incl. end rots.) |
|---|---|---|
| 17 | 49 | 72 |
| 21 | 45 | 68 |
| 22 | 52 | 75 |
| 23 | 51 | 74 |
| 25 | 50 | 73 |
| 26 | 52 | 75 |
| 27 | 48 | 71 |
| 28 | 49 | 72 |

Table 5.1 Experimental Contribution of Shear Displacement During Linear Cycles.

| Specimen | %$\Delta_{shear}$ |
|---|---|
| 17 | 89 |
| 21 | 82 |
| 22 | 85 |
| 23 | 95 |
| 25 | 83 |
| 26 | 92 |
| 27 | 97 |
| 28 | 93 |

Table 5.2 Experimental Contribution of Shear Displacement During Inelastic Cycles.

| Section | $M_p$ (k-in.) ($\sigma_y = 36 ksi$) | $M_p$ (k-in.) ($\sigma_y = 48 ksi$) | $M_p$ (k-in.) ($\sigma_y = 48 ksi$) |
|---|---|---|---|
| W18x40 | 2820 | 3760 | 2630 |
| W18x60 | 4430 | 5900 | 4420 |

Table 5.3 Plastic Moment Capacities of the Sections Used in This Investigation.

| Specimen | Free End | | Fixed End | |
|---|---|---|---|---|
| | $M_{max}$ (k-in) | $M_{min}$ (k-in) | $M_{max}$ (k-in) | $M_{min}$ (k-in) |
| 16 | 4820 | 4520 | 5040 | 4960 |
| 17 | 3030 | 3320 | 3520 | 3290 |
| 18 | 4270 | 4390 | 4600 | 4750 |
| 20 | 3220 | 3220 | 3460 | 3550 |
| 21 | 3300 | 3240 | 3460 | 3550 |
| 20 | 3520 | 2570 | 3400 | 3430 |
| 23 | 3270 | 3300 | 3430 | 3440 |
| 24 | 3450 | 3460 | 3820 | 3190 |
| 25 | 3060 | 3390 | 3300 | 3410 |
| 26 | 3530 | 3550 | 3900 | 4020 |
| 27 | 3940 | 3960 | 3940 | 4140 |
| 28 | 3620 | 3580 | 3280 | 3520 |

Table 5.4 Maximum End Moments Resisted by the Specimens.

| Specimen 16 | |
|---|---|
| Gage No. | Maximum Strain ( *in./in.* ) |
| 1 | 26100 |
| 2 | 20300 |
| 3 | 14600 |
| 4 | 27900 |
| 5 | 13200 |
| 6 | 11700 |
| 7 | 26800 |
| 8 | 17900 |
| 9 | 13200 |
| 10 | 22300 |
| 11 | 6400 |
| 12 | 6900 |

Table 5.5 Maximum Strains for Each Flange Gage of Specimen 16.

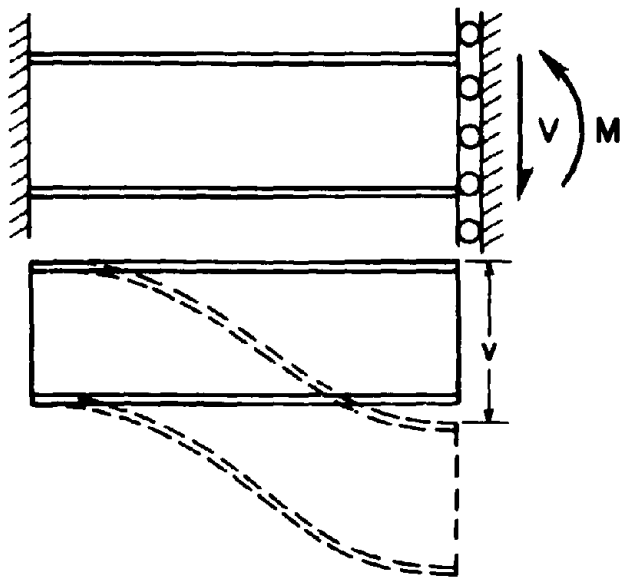


Fig. 5.1 Simple Analytical Model of the Experiments.

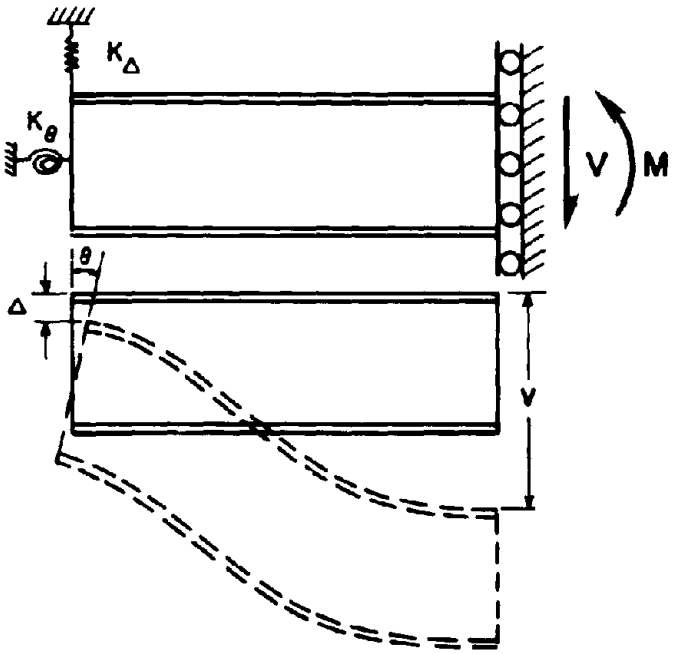


Fig. 5.2 Refined Analytical Model of the Experiments.

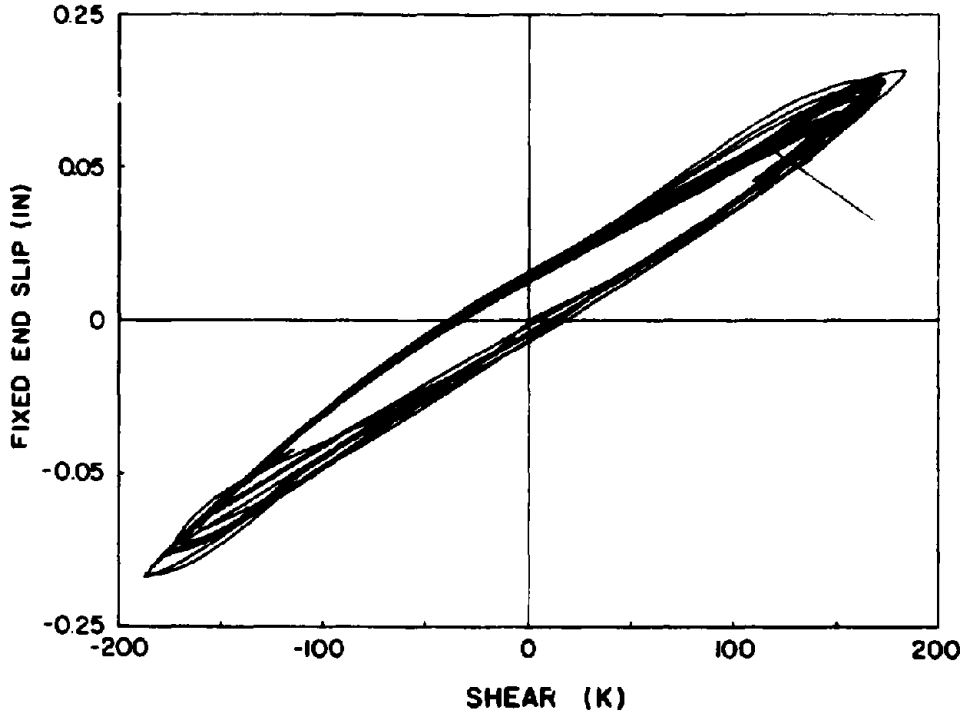


Fig. 5.3 Plot of Fixed End Slip vs. Shear Used to Determine the Lateral Support Displacement Stiffness, $K_\Delta$.

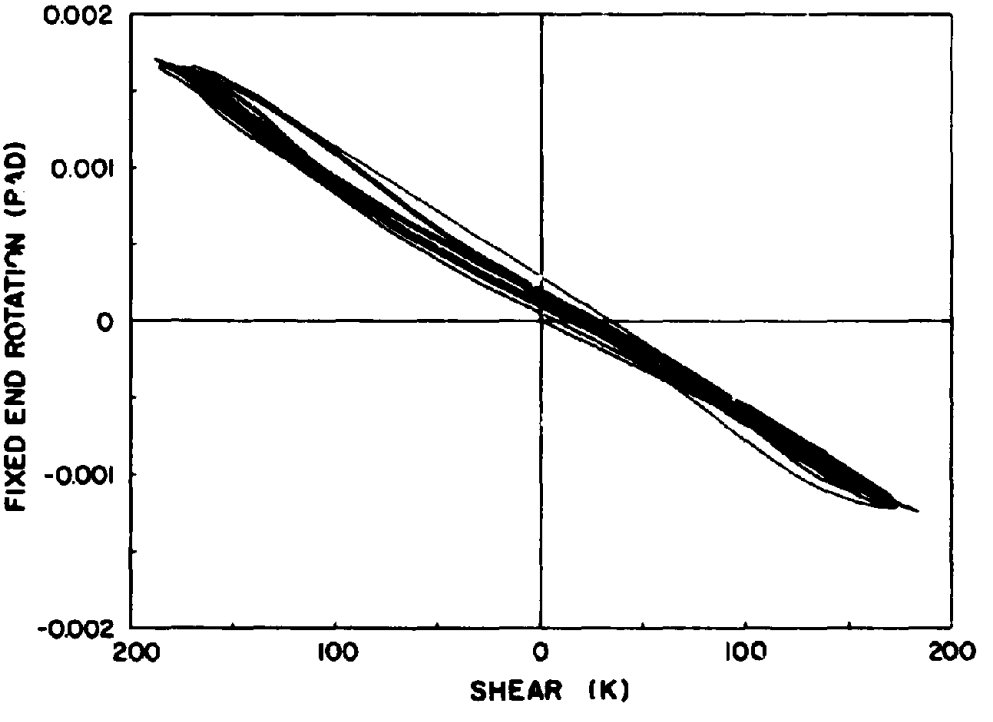


Fig. 5.4 Plot of Fixed End Rotation vs. Shear Used to Determine the Rotational Support Stiffness, $K_\theta$.

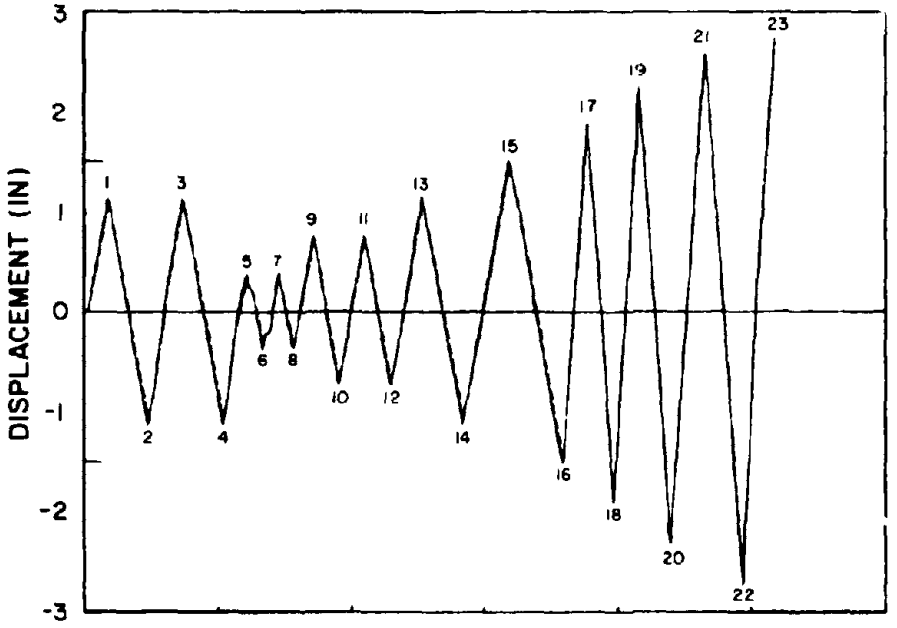


Fig. 5.5 Plot Comparing the Recorded (Solid Line) and Adjusted (Dotted Line) Displacements of Specimen 20.

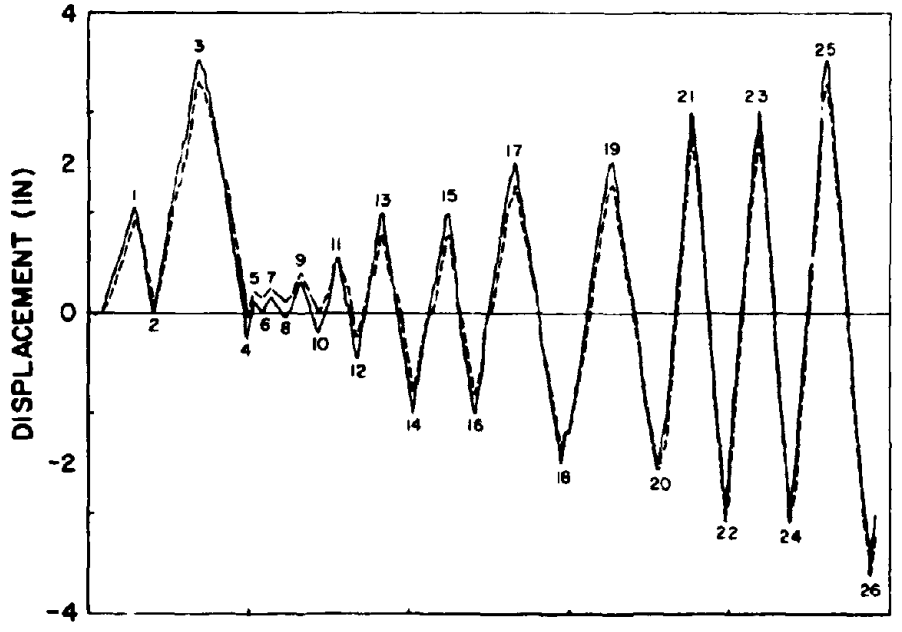


Fig. 5.6 Plot Comparing the Recorded (Solid Line) and Adjusted (Dotted Line) Displacements of Specimen 16.

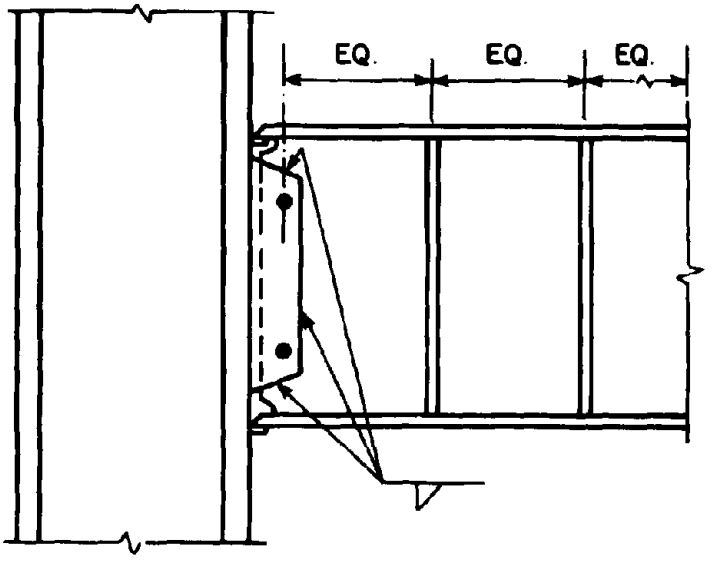


Fig. 5.7 Suggested Stiffener Spacing for Shear Links with the Web Fillet Welded to a Shear Tab.

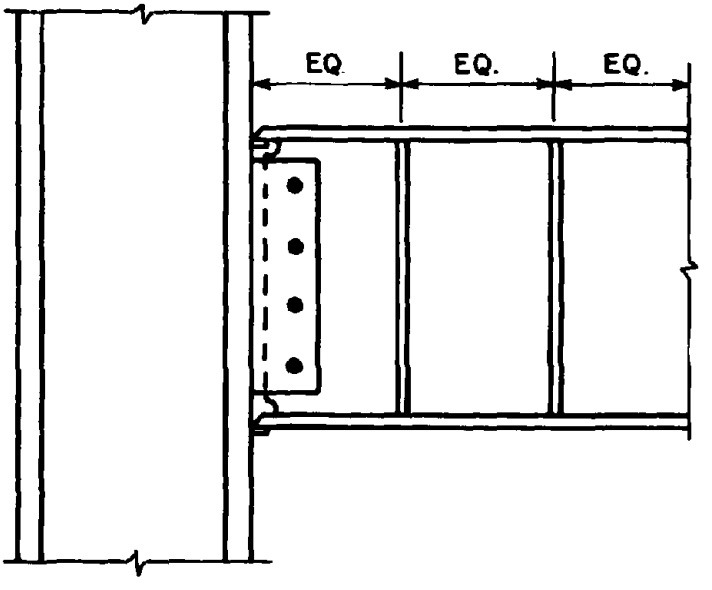


Fig. 5.8 Suggested Stiffener Spacing for Shear Links with the Web Bolted to a Shear Tab.

# CHAPTER 6 - EVALUATION OF LINK PERFORMANCE

From a structural standpoint, shear links can be designed to absorb a tremendous amount of energy and exhibit a ductile failure. But, since many links are required for typical applications, the cost of such a link becomes important. It is essential, therefore, to reach a balance between the structural response characteristics and cost. Only through such a process can rational design recommendations be made.

## 6.1 Energy Dissipation as a Measure of Structural Performance

The concept of eccentrically braced frames for seismic applications strongly depends on the ability of the active links to dissipate large amounts of energy during inelastic response. Energy dissipation capacity therefore becomes the primary basis for quantitative link comparison.

The load vs. displacement curves presented in Chapter 4 depicted the response characteristics of the tested specimens. The functionally important energy dissipated by the active link is the area enclosed by the hysteretic loops of these curves. Formally, the energy dissipated, $E_D$, can be expressed as:

$$E = \int P(\delta) d\delta \tag{6.1}$$

In this equation, $\delta$ is the relative specimen end displacement, and $P(\delta)$ is the shear force in the specimen.

To make meaningful conclusions regarding energy dissipation, it was necessary to make comparisons which accounted for different material properties and member sizes. This was done by normalizing the energy dissipated by the link with the energy which would have been dissipated by an ideal elasto-perfectly plastic link with the same yield load and displacement as the

actual specimen. For the specimens with different loading programs, the normalized energy, $\lambda$, is plotted against cumulative ductility, $\sum\mu$, in Fig. 6.1. For the eight specimens which were subjected to the same loading sequence, the normalized energy is plotted against ductility, $\mu$, in Figs. 6.2 and 6.3. These normalized energy dissipation values are defined as:

$$\lambda = \frac{\textit{energy dissipated by test specimen}}{\textit{energy dissipated by equivalent elasto-plastic system}} \tag{6.1}$$

$$\mu = \frac{v_{max}}{v_y} \tag{6.2}$$

$$\Sigma\mu = \textit{summation of } \mu\textit{'s for all cycles} \tag{6.3}$$

Table 6.1 is also presented to provide comparison of these eight similar specimens. The energy dissipation measures in this table are: $E_{tot}$, the total energy dissipated before the failure cycle, $E^*_\Sigma$, the total energy dissipated before the first buckling cycle, $E_{tot}-E^*_\Sigma$, the total energy dissipated after buckling, and $\lambda_{max}$, the maximum value of normalized energy dissipation obtained by each specimen. This table also includes the maximum displacement ductility, $\mu_{max}$, and the cumulative ductility, $\sum\mu$.

Examination of these tables and figures leads to the following conclusions:

1. *For the type of loading used in these experiments, properly designed shear links can dissipate large amounts of energy regardless of the loading history.*

2. *Large initial displacements which cause web buckling tend to cause more rapid decreases in energy dissipative capacity than incrementally increasing loadings or low level inelastic repeated cycling. The ductility supply is not greatly affected by early web buckling.*

3. *Shear links can resist monotonic displacements, up to 20 percent of their length without significant loss of capacity.* Since the Pacoima Dam Record of the 1971 San Fernando Earthquake showed that long pulses can occur during a major earthquake, the shear links may be required to withstand large monotonic displacements. The results of Specimen 24 indicate that the links can meet such a large ductility demand.

4. *From a structural standpoint, properly designed one-sided stiffeners are equivalent to two-sided stiffeners. Both the pre-buckled and post-buckled responses were virtually identical for the one-sided and two-sided specimens with otherwise identical details. In either case, the stiffeners must be provided with sufficient axial strength and bending rigidity to fully develop the link energy dissipation capacity.* A method for sizing shear link web stiffeners is given in Chapter 7.

5. *Stiffeners not welded to both beam flanges do not change a link's energy dissipation before buckling, although the postbuckled capacity is reduced. The overall ductility capacity is not greatly affected by using such a detail. The post-buckled energy dissipation capacity is further reduced if the stiffeners are not connected to either flange.*

6. *All-welded link-column connections exhibit excellent performance. Properly designed and fabricated all-welded end connections develop the full capacity of shear links.*

7. *Bolted web, welded flange connections may be satisfactory in terms of energy dissipation capacity for some applications. The pre-buckled and moderate displacement response of the bolted web connection is comparable to that of the all-welded connection. However, fully stiffened webs may be required to develop large shear forces which, can cause bolt slip. This bolt slip transfers a portion of the applied shear to the flanges, which may cause sudden, premature failure of the link-column connection.*

8. *Excessively close stiffener spacing can lead to abrupt failures before the initiation of web buckling. Large amounts of inelastic displacement causes strain hardening which can overstress welds and lead to sudden weld failures.*

9. *Based on one experiment, it appears that the connection of a link to the column web does not significantly alter the performance of the link. Due to the reduced stiffness of this configuration, the energy dissipation capacity is only slightly reduced during the loading history. The dissipative capacity reduces more rapidly during post-buckled response. However, the total dissipated energy and the ductility are not significantly lower than connections of links to column flanges.*

It must be emphasized that all of the links tested were attached to essentially rigid elements at both ends. Caution must therefore be exercised in extrapolating the conclusions listed

above to situations where column panel zones exhibit flexibility or inelastic action.

### 6.2 Design Recommendations

Based on the conclusions listed in the previous section, and appropriate consideration of cost factors, the following design recommendations for shear links in eccentrically braced frames can be presented:

1. *One-sided stiffeners can be employed to delay web buckling in shear links of moderate depth, such as those used in these experiments.* Since the structural performance of one-sided and two-sided stiffeners were found to be almost identical, cost considerations suggest the use of one-sided stiffeners, although as shown in Chapter 7, one-sided stiffeners require more material than the two-sided ones.

2. *The minimum stiffener spacing in shear links should be* $20t_w$. *Spacing stiffeners less than* $20t_w$ *can precipitate sudden connection failures.*

3. *Web stiffeners may be welded to only one flange of the link.* For the specimens tested, one-sided stiffeners welded to only one flange performed quite adequately, although they are slightly less effective than the fully welded detail. To provide stability against flange buckling, the stiffeners should be welded to the bottom flange. The top flange is somewhat restrained from buckling by the floor system, though this resistance may be diminished by cracking of a concrete slab during large displacement cycles.

4. *An all-welded link-column connection should be used for links with large ductility demands.* The all-welded connection appears to be more reliable, since the bolted web connection has a greater propensity for sudden failures during large displacement cycles. All-welded link-column connections are therefore preferable for links which are likely to experience large inelastic deformations.

5. *For links with low or moderate ductility demands, bolted web, welded flange connections may be employed.* Bolted web connections appear to exhibit satisfactory performance unless large inelastic deformations are imposed.

6. *Shear links may be connected to the column web. This connection should be detailed according to the recommendations for typical moment resisting frames.* The large shear to moment ratio present in the links does not cause the large moments which can result in flange weld failures. The problem studied by the investigators at Lehigh University [6] may therefore be more critical for typical moment-resisting connections than it is for shear links. All-welded link-column web connections are recommended for links with large ductility demand.

| Specimen Number | $E_{TOT}$ (k-in.) | $E_{\Sigma}^{+}$ (k-in.) | $E_{TOT}-E_{\Sigma}^{+}$ (k-in.) | $\lambda_{max}$ | $\mu_{max}$ | $\Sigma\mu$ |
|---|---|---|---|---|---|---|
| 17 | 6870 | 2910 | 3960 | 0.993 | 46.1 | 525 |
| 21 | 8590 | 4010 | 4580 | 0.991 | 58.5 | 751 |
| 22 | 7040 | 4150 | 2890 | 0.977 | 51.0 | 576 |
| 23 | 7070 | 4100 | 2465 | 0.991 | 46.1 | 525 |
| 25 | 7890 | 2980 | 4920 | 0.934 | 58.5 | 693 |
| 26 | 10800 | 7300 | 3500 | 1.115 | 66.0 | 700 |
| 27 | 7520 | 7520 | 0 | 1.140 | 46.1 | 525 |
| 28 | 2550 | 2550 | 0 | .910 | 31.9 | 237 |

Table 6.1 Energy Dissipation of the Test Specimens.

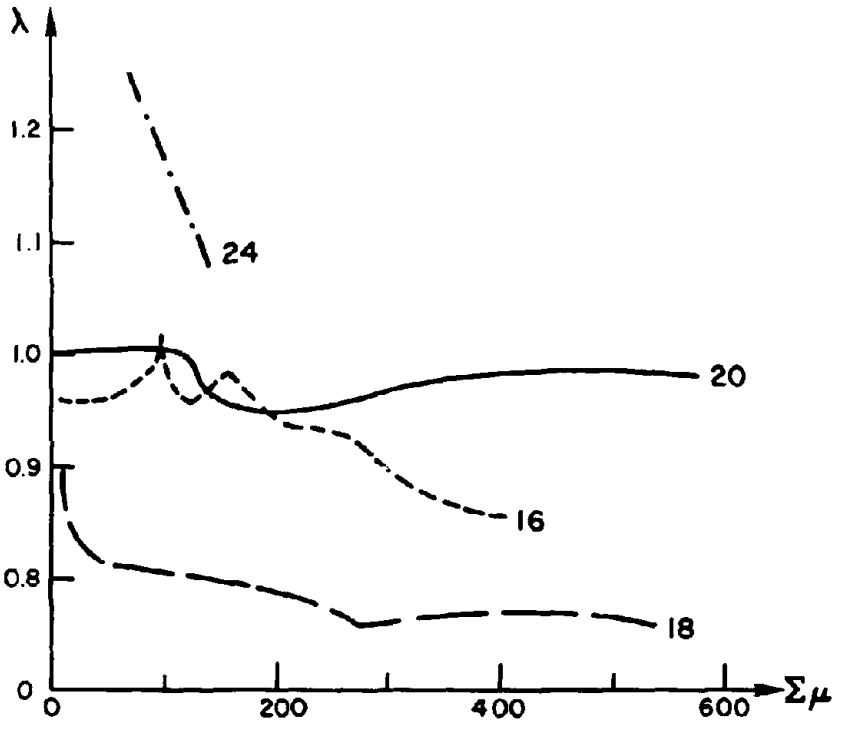


Fig. 6.1 Plot of Normalized Energy Dissipation, λ, vs. Cumulative Ductility, $\Sigma\mu$, for Specimens With Different Loading Conditions.

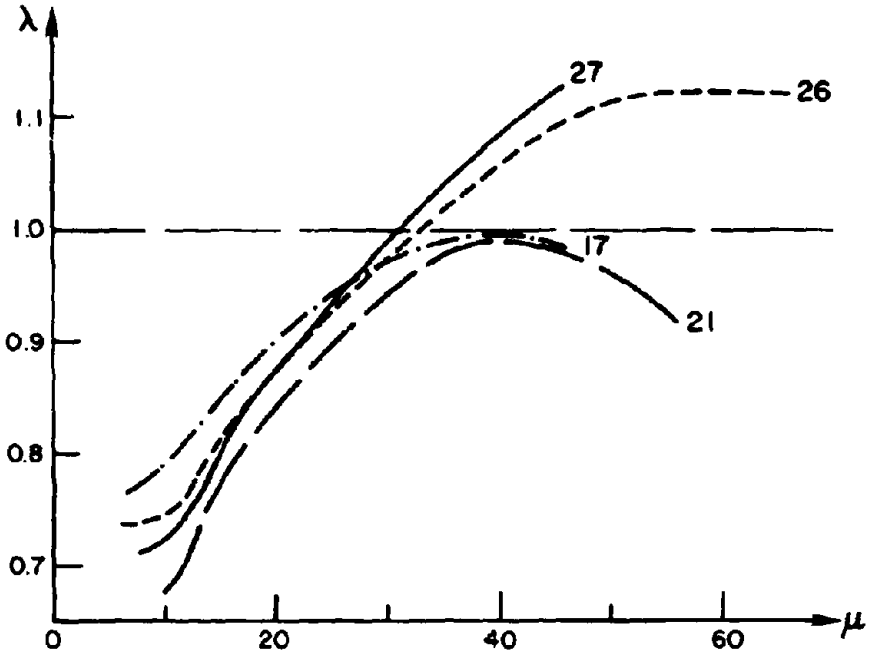


Fig. 6.2 Plot of Normalized Energy Dissipation, λ, vs. Ductility, μ, for Specimens With Different Stiffener Details and/or Spacing.

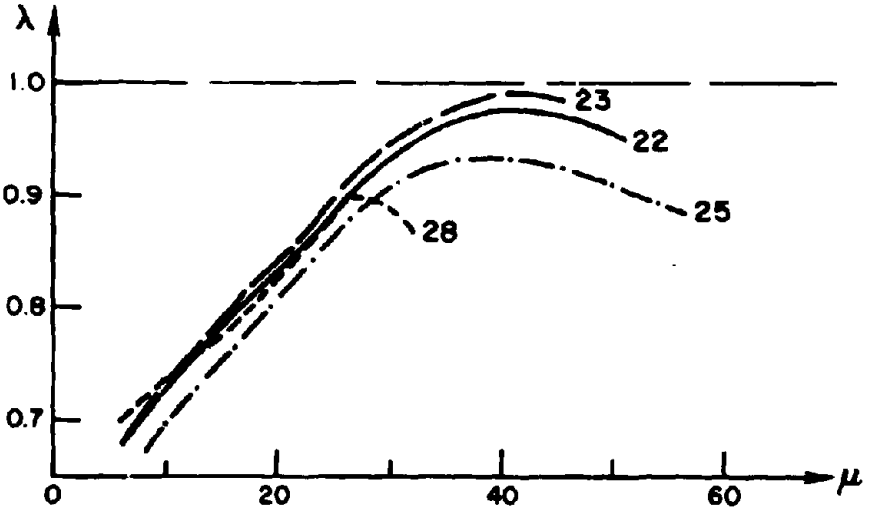


Fig. 6.3 Plot of Normalized Energy Dissipation, λ, vs. Ductility, μ, for Specimens With Different Connection Details.

# CHAPTER 7 - WEB STIFFENERS IN SHEAR LINKS

The benefits derived from stiffening the webs of shear links have been demonstrated by experimental results of twenty-eight specimens. Delayed buckling and increased energy dissipation capacity directly result from web stiffening. The extent to which these benefits are realized depends on the integrity of the stiffeners.

In all previous research and early applications of the eccentrically braced system, stiffener design has been accomplished without benefit of a rational method. Even though these previously designed stiffeners have performed quite adequately, a more rational practical stiffener design method is necessary to ensure proper performance of future applications.

## 7.1 Experimental Results

In the tests presented in this report the stiffeners were sized using the results of previous investigations as a guide. In an effort to analyze their requirements in shear links, stiffener strains were monitored during the tests. From these results axial strains were plotted and compared. A representative plot is presented in Fig. 7.1.

Comparison of the stiffener strain plots for the different tests resulted in the following conclusions:

1. *The stiffeners were virtually unstressed prior to shear yielding.*
2. *Before buckling, the average axial strain in the stiffeners was independent of the panel size and stiffener detail. The average axial compressive stress was well below yield during this stage of loading.*
3. *Once buckling occurred the stiffeners often yielded due to the combination of axial and bending stresses.*

4. *The most highly stressed stiffeners were those adjacent to the buckled panel.*

Also, it should be noted that the largest stiffener strains occurred in Specimen 20, which exhibited excellent post-buckling behavior. It seems then that some yielding of the stiffeners does not seriously detract from the post-buckling behavior of the links.

### 7.2 The Design of Shear Link Stiffeners

The delay and control of web buckling and the resulting increased shear link energy dissipation capacity can be achieved by the addition of web stiffeners. The design of these stiffeners can be separated into three stages: spacing, sizing, and detailing.

**7.2.1 Spacing of Web Stiffeners-** The relationship between energy dissipation capacity and web stiffener spacing was studied by Hjelmstad and Popov [12]. Based on fifteen test specimens, they proposed the following empirical relationships:

$$\frac{a}{t_w} = 90 - 9 \ln \frac{E_\Sigma^*}{E_e} \tag{7.1}$$

$$\frac{a}{t_w} = 94 - 14 \ln \frac{E^*}{E_e} \tag{7.2}$$

The smallest panel dimension, $a$, and the web thickness, $t_w$, are the topological parameters in these equations. The energy dissipation parameters are $E_\Sigma^*$, the total energy dissipated prior to buckling, $E_e$, the elastic energy stored by the link at yield, and $E^*$, the energy absorbed during the largest prebuckling cycle of an experiment.

Eq. 7.2 is intended to estimate the required stiffener spacing for monotonic loading histories. The results of the monotonic test (Specimen 24) presented in this report provide some corroboration for this relationship. Since the test specimens used to generate Eq. 7.2 were loaded cyclically with incrementally increasing displacements, the monotonic buckling energy, $E^*$, was probably overestimated. It is likely, therefore, that Eq. 7.2 is conservative, and is subject to future revision.

Without the results of a series of inelastic dynamic analyses, the shear link energy dissipation requirements must be approximated by estimating the ductility demand. With the ductility, $\mu$, defined in Eq. 6.2, and $\mu_i$, defined as the ductility demanded in the $i-$ th cycle of a loading history, the following relationships result for an elasto-perfectly plastic material undergoing predominately shear deformations [12]:

$$\frac{E_\Sigma^*}{E_e} = 2\Sigma_i(\mu_i - 1) \tag{7.3}$$

$$\frac{E^*}{E_e} = 2\mu - 1 \tag{7.4}$$

The $a/t_w$ ratio chosen should be the smaller of the values given by Eqs. 7.1 and 7.2. If the resulting $a/t_w$ ratio is less than 20, the energy dissipation demands on the shear links may be unattainable [12], thereby requiring revision of the beam section. Stiffener spacing based on these equations should delay web buckling and therefore allow the links to meet their energy dissipation requirements.

**7.2.2 Sizing Shear Link Web Stiffeners-** Once the stiffener spacing has been determined, they must be sized to meet two structural requirements. First, the stiffeners must have sufficient axial strength to develop the link web tension field action. Second, the stiffeners must be rigid enough to prevent buckling of the whole link web as a single panel.

The AISC Specifications [1] provide design equations for web stiffeners in plate girders. While shear link web stiffeners must satisfy requirements resulting from similar considerations of statics, these equations cannot be used here since they are based on elastic solutions. The inelastic nature of shear link web buckling makes an exact solution for the sizing of the stiffeners extremely complex and impractical for design applications. An approximate method must therefore be devised for the sizing of shear link web stiffeners.

*7.2.2.1 Axial Forces in Web Stiffeners-* The AISC design equations for the required axial strength of plate girders are based on the work of Basler [3]. These equations were derived

from tension field theory, as depicted in Fig. 7.2. Tension field action is analogous to a Pratt Truss in which principal tensile stresses act as the diagonal member, the beam flanges act as the upper and lower chords, and the stiffeners act as the vertical struts. As illustrated in Fig. 7.3, the stiffeners develop compressive stresses. The AISC equations based on this theory apply for the elastic case, where the ratio of the girder depth to the web thickness is large (eg. $d/t_w = 150$ ). Since the rolled sections used in eccentrically braced frame applications have low $d/t_w$ ratios which can lead to inelastic web buckling, the tension field theory must be modified for shear link stiffener design.

The approach followed here is similar to the formulation presented by Adams, Krentz, and Kulak [2]. For the system depicted in Fig. 7.2, $V_t$, the shear due to tension field action, is:

$$V_t = \sigma_t t_w (h\cos\Theta - a\sin\Theta)\sin\Theta \tag{7.5}$$

where $\sigma_t$ is the diagonal tension stress, $h$ and $a$ are the height and width of the web panel, respectively, and $\Theta$ is the angle between the diagonal tension and horizontal. Since the tension field will orient itself in the most efficient manner, the maximum $V_t$ can be found by differentiating Eq. 7.5 with respect to $\Theta$, and setting the derivative equal to zero. This procedure yields the following equation:

$$\sin\Theta = \left[ \frac{1}{2} - \frac{\frac{a}{2h}}{\sqrt{1+(\frac{a}{h})^2}} \right]^{1/2} \tag{7.6}$$

Considering vertical equilibrium of the free body depicted in Fig. 7.3, the maximum axial force in each stiffener becomes:

$$F_s = \sigma_t t_w a \sin^2\Theta \tag{7.7}$$

Because of the extensive strain hardening exhibited by well stiffened experimental shear links, $\sigma_t$ can be reasonably assumed to be approximately equal to $\sigma_u$, the ultimate tensile stress

of the steel. Using this conservative assumption in combination with Eqs. 7.6 and 7.7 results in the following expression for the axial force in shear link web stiffeners:

$$F_s = \sigma_u t_w \frac{a}{2}\left[1 - \frac{\frac{a}{h}}{\sqrt{1 + (\frac{a}{h})^2}}\right] \tag{7.8}$$

Experimental shear links indicated that local stiffener buckling generally does not occur, and that stiffener yielding does not reduce their energy dissipation capacity (See Section 7.1). Therefore, yielding of the stiffeners will be allowed and local stability considerations will be ignored in the determination of the required stiffener area. Assuming a web participation equal to half the flange width, as shown in Fig. 7.3, the area required of a pair of two-sided stiffeners, $A_{st}$, becomes:

$$A_{st} = \frac{F_s}{\sigma_y} - b_f \frac{t_w}{2} \tag{7.9}$$

For one-sided stiffeners, Fig. 7.4 approximates the stresses necessary to maintain static equilibrium assuming a fully yielded condition [3]. In this case, the required area of one-sided stiffeners, $A'_{st}$, is approximately:

$$A'_{st} = 2.4\left[\frac{F_s}{\sigma_y} - b_f \frac{t_w}{2}\right] \tag{7.10}$$

In Eqs. 7.9 and 7.10, $F_s$ is the stiffener axial force given by Eq. 7.8, $\sigma_y$ is the yield stress of the stiffener material, $b_f$ is the flange width, and $t_w$ is the web thickness. Even though over twice as much stiffener area may be required, one-sided web stiffening may be more economical than the two-sided detail because of reduced welding costs.

Web stiffeners are usually detailed so that they do not protrude outside the longitudinal edge of the beam flanges. For stiffeners which just reach the edge of the flanges, the required thickness of two-sided stiffeners, $t_{st}$, is:

$$t_{st} = \frac{A_{st}}{b_f - t_w} \tag{7.11}$$

For stiffeners provided on only one side of the web, the required thickness, $t'_{st}$, becomes:

$$t'_{st} = 2\frac{A'_{st}}{b_f - t_w} \tag{7.12}$$

In either case, the stiffener thickness should not be less than $t_w$, the thickness of the web.

*7.2.2.2 Rigidity Requirements of Shear Link Web Stiffeners-* For a simply supported plate of width "a" and height "b", with one transverse stiffener, Timoshenko [30] stated the rigidity requirement of web stiffeners this way:

> *If the rigidity of the stiffener is not sufficient, the inclined waves of the buckled plate run across the stiffener, and buckling of the plate is accompanied by bending of the rib. By subsequent increase of the rigidity of the rib we may finally arrive at a condition in which each half of the plate will buckle as a rectangular plate with simply supported edges of dimensions a/2 and b and the rib will remain straight.*

The web stiffeners must therefore form nodal lines for the web plate. If the stiffeners are not rigid enough to form these nodal lines, the effective panel size increases, causing significant reduction of the link energy dissipation capacity. The stiffeners must therefore be rigid enough so that the whole link web does not buckle as a single panel. In the late phases of the experiment, Specimen 26 exhibited a tendency for this type of response, as may be discerned from the photograph in Fig. 4.11.

The required stiffener rigidity in the elastic buckling case has been studied extensively since the 1930s. Through an energy method, Timoshenko first developed a theory for the case of one or two stiffeners [30]. Wang [32] extended Timoshenko's theory, giving diagrams for three and four stiffeners, and infinitely long plates. In 1949, Stein and Fralich concluded that the results obtained by Timoshenko and Wang were unconservative [28]. For the infinitely long, simply supported plate problem, they developed a solution by minimizing the systems' potential energy using the Lagrangian multiplier method. Based on this approach, they presented charts for the required stiffness as a function of the critical stress for different panel aspect ratios. In the early 1960s, Rockey and Cook extended the theory of Stein and Fralich

for the case of clamped longitudinal edges [23].

All of the elastic solutions for the required rigidity of web stiffeners [23, 28, 30, 32] relate the critical shear buckling stress to the non-dimensional parameter, $\bar{\gamma}$, as a function of the plate aspect ratio, $\bar{\beta}$. This stiffener rigidity parameter is defined as:

$$\bar{\gamma} = \frac{EI}{aD} \tag{7.13}$$

In this equation, $E$ is the elastic modulus, $I$ is the stiffener moment of inertia, $a$ is the smallest panel dimension, and $D$ is the plate stiffness factor. This factor is defined as:

$$D = E\frac{t_w^3}{12\,(1-\nu^2)} \tag{7.14}$$

The $\nu$ term in this equation is Poisson's ratio.

Bleich [5] used the results of Stein and Fralich to determine the minimum stiffener rigidity required to obtain the largest critical shear stress as a function of the panel aspect ratio, $\bar{\beta}$. With $\bar{\beta}$ defined as the ratio of the larger to smaller panel dimension, the required rigidity, $\bar{\gamma}_{req}$, was postulated to be:

$$\bar{\gamma}_{req} = 2\bar{\beta}^2 - 20 \tag{7.15}$$

This relationship results from a solution which assumes that the longitudinal edges of the plate are simply supported and therefore free to rotate. Rockey and Cook [23] developed an analogous solution for the case in which the longitudinal edges are assumed to be fixed against rotation. Using a procedure similar to that employed by Bleich, the following relationship can be proposed for this case:

$$\bar{\gamma}_{req} = 16\bar{\beta}^2 - 8 \tag{7.16}$$

The derivation of this relationship is given in Appendix A.1. Note that Eqs. 7.15 and 7.16 apply for $1 < \bar{\beta} < 5$.

These relationships all pertain to the problem of elastic shear buckling. The complex nature of inelastic plate buckling problems makes theoretical solutions for the required bending rigidity of shear link stiffeners impractical for design purposes. An approximate method will therefore be presented which modifies the elastic solution to account for inelastic effects.

Massonnet and Maquoi [19] attempted to account for the inelastic effects by conservatively recommending that the stiffener rigidity required to keep the stiffeners straight in the postbuckled range be obtained by multiplying the required rigidity for the elastic case by a factor of 4 to 5. This recommendation has received some justification from both analytical [7] and experimental [22] research on plate girders loaded to collapse. While this research did not consider the cyclic loadings which shear links are designed to resist, it is believed that this recommendation is sufficiently conservative for design applications.

Since shear links are relatively short and laterally braced at both ends, the flanges of the usual rolled sections would appear to provide significant restraint along the longitudinal edges of the web. Eq. 7.16 rather than Eq. 7.15 is therefore adopted for the design of shear link web stiffeners. Moreover, since in seismic design some damage to the links can be tolerated at extreme overloads, the lower Massonnet and Maquoi multiplier of 4 is taken. The resulting required rigidity of shear link web stiffeners therefore becomes:

$$\bar{\gamma}_{req} = 64\bar{\beta}^2 - 32 \tag{7.17}$$

Combination of Eqs. 7.13, 7.14, and 7.17 produces the following equation for the required stiffener moment of inertia:

$$I_{req} = at_w^3 \frac{\bar{\gamma}_{req}}{12(1-\nu^2)} \tag{7.18}$$

Following the usual practice [1], $I_{req}$ can be taken about an axis in the plane of the web for both one-sided and two-sided stiffeners. This practice implicitly assumes some participation by the beam web in the rigidity of one-sided stiffeners.

If the stiffeners are again assumed to just reach the longitudinal edge of the flanges, the required thickness of two-sided stiffeners, $t_s$, becomes:

$$t_s = 12\frac{I_{req}}{b_f^3} = \frac{t_w^3}{b_f^3}\bar{\gamma}_{req}\frac{a}{(1-\nu^2)} \tag{7.19}$$

The required thickness for one-sided stiffeners, $t_s'$, is:

$$t_s' = 24\frac{I_{req}}{b_f^3} = 2\frac{t_w^3}{b_f^3}\bar{\gamma}_{req}\frac{a}{(1-\nu^2)} \tag{7.20}$$

As remarked earlier, it is not recommended to use a stiffener thickness less than the beam web thickness.

An example of the shear link stiffener design method presented above is given in Appendix A.2.

**7.2.3 Detailing Shear Link Web Stiffeners-** The final step in shear link web stiffener design is the specification of proper details. In past research and design applications, the web stiffeners have been fitted to allow fillet welding to both flanges as well as to the web, as shown in Fig. 7.5(a). The experimental results indicated, however, that only a small reduction of energy dissipation capacity occurs for links with stiffeners which are not fully welded. It therefore appears possible to relax the requirements of fitted stiffeners. If this simpler detail is utilized, the stiffeners should terminate a distance "k" (as defined in the AISC Manual [1] ) below the top beam flange, as shown in Fig. 7.5(b). In such cases it appears reasonable to weld the stiffener to the bottom flange, and depend on the concrete floor to adequately restrain the top flange from buckling. This assumption may not be justified in some applications, since the possible cracking of the floor slab during a major seismic event may reduce this restraint. Under such circumstances, fitted stiffeners (Fig. 7.5(a)) may become advisable.

Fitted stiffeners may again be avoided when two-sided stiffeners are employed. In this case equal restraint for the top and bottom beam flanges can be provided by welding the stiffeners on opposite sides of the web to different flanges, as shown in Fig. 7.5(c).

In all cases, the stiffener fillet welds should be continuous, full length welds on both sides of the stiffeners, meeting AISC Specifications for minimum and maximum size.

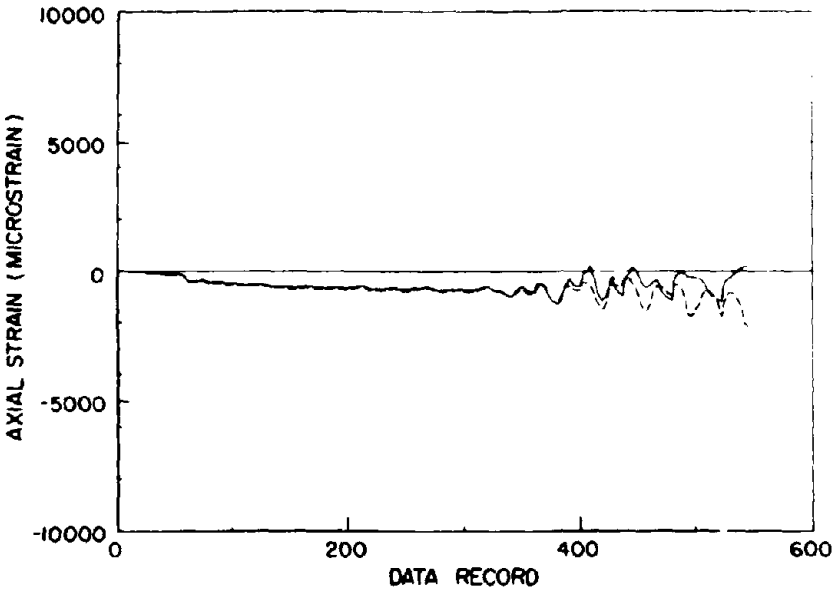


Fig. 7.1 Plot of the Average Axial Strain in Each of the Stiffeners Employed in Specimen 20.

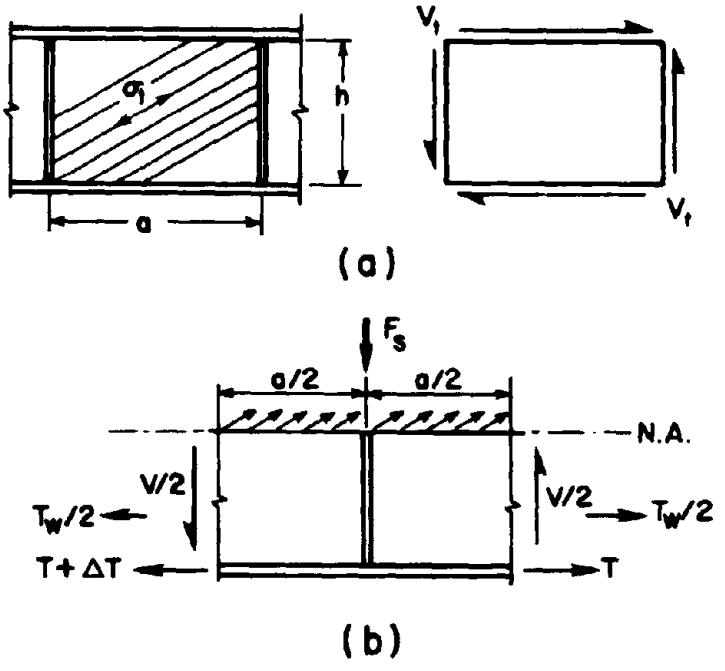


Fig. 7.2 Free Body Diagram For Determining Stiffener Forces Using Tension Field Theory.

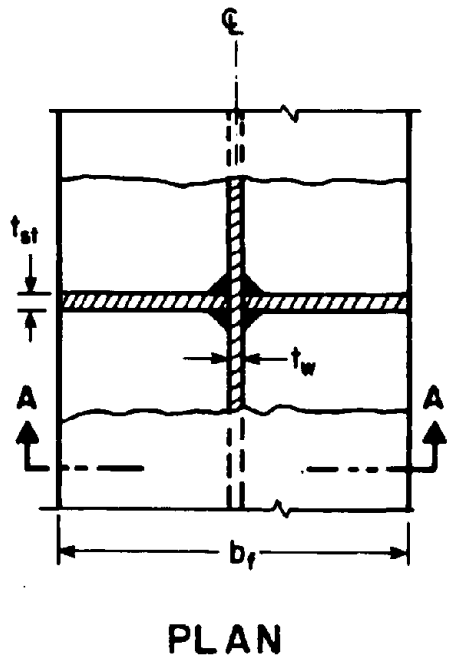


Fig. 7.3 Assumed Distribution of Axial Stresses for Two-Sided Stiffeners.

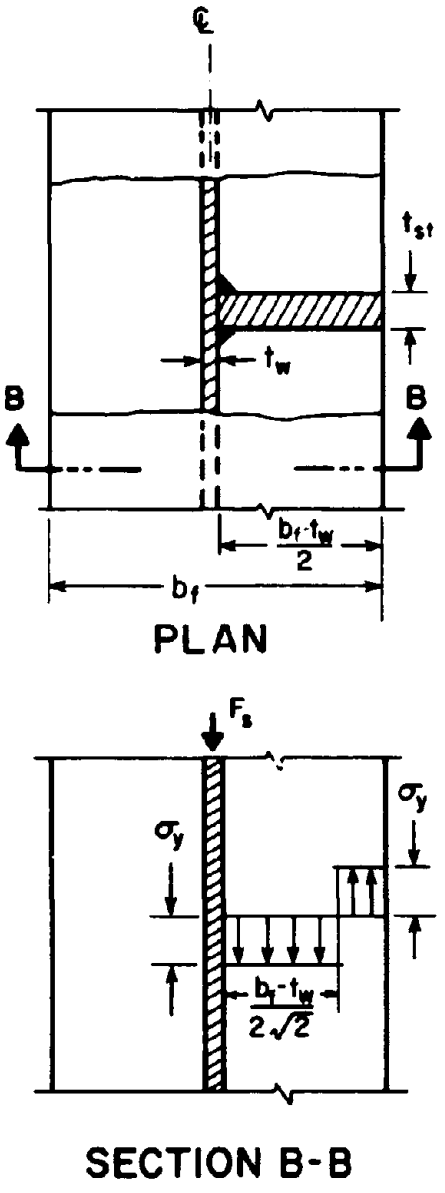


Fig. 7.4 Assumed Distribution of Axial Stresses for One-Sided Stiffeners.

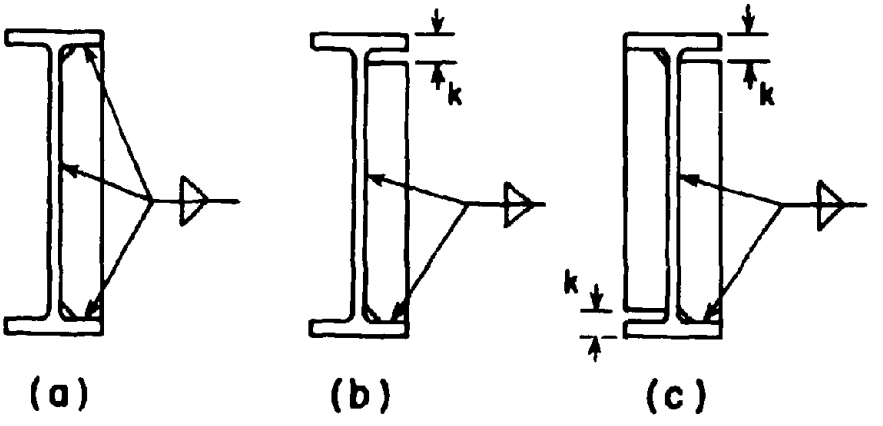


Fig. 7.5 Three Possible Details for Connection of Stiffeners to Shear Links.

# CHAPTER 8 - A DESIGN PROCEDURE FOR SHEAR LINKS IN ECCENTRICALLY BRACED FRAMES

The experimental work reported here and in earlier investigations has demonstrated that properly designed shear links can dissipate a great deal of energy and undergo large displacement ductilities. The results of this research on eccentrically braced steel frames together with common design practice leads to a procedure for the design of shear links. The basic procedure includes the following steps: 1.) Determination of structural configuration, 2.) Determination of member sizes, 3.) Design of link connections, and 4.) Design and detailing of web stiffeners.

## 8.1 Determination of Structural Configuration

Once the eccentrically braced framing system has been selected, the engineer must first choose an appropriate structural configuration. The flexibility of brace location inherent to this system allows the designer to choose from a number of arrangements to meet both architectural and structural requirements. This flexibility can result in fewer obstructions to the functional requirements of a building than would occur with concentric bracing. Fig. 8.1 [11] shows the location of possible architectural openings for four alternative framing schemes.

It is advantageous to locate the active links such that they are not required to axially transfer the large lateral forces to the braces. Judicious location of the links, as shown in Fig. 8.2, or the use of parallel gathering beams, can minimize this problem. The effect of axial forces on shear link behavior has not yet been fully investigated, and is the subject of current research.

After the brace configuration has been selected, the appropriate eccentricities must be chosen. This is a critical step in the efficient design of an eccentrically braced frame since the amount of eccentricity provided determines both the elastic stiffness of the frame and the

ductility demand on the active links. It is at this point in the design process that the engineer can satisfy both the drift and ductility requirements of seismic design.

Drift control requirements are satisfied by providing the structure with sufficient elastic stiffness. As the length of the active links increase, the elastic stiffness of the frame of the frame decreases, in the limiting case reaching the stiffness of a moment resisting frame. An earlier investigation [11] demonstrated that for a simple structural configuration, as in Fig. 8.3, there is little increase in elastic stiffness when the ratio of $e/L>0.5$. As the $e/L$ ratio approaches zero, the frame stiffness increases toward that of a concentrically braced frame. This work also showed that neglecting the effects of shear deformations in the links leads to an overestimate of the elastic frame stiffness for $e/L < 0.5$. Conventional elastic analysis procedures which include the effects of shear deformation in the links are sufficiently accurate for design applications.

Structural ductility requirements of seismic design dictate that the structural configuration limit member ductility demands below the available supply. Earlier research using rigid-plastic analysis methods [11] demonstrated that the active link ductility demands in eccentrically braced framing systems are reduced as the eccentricity of the braces is increased. The collapse mechanism for a simple eccentrically braced frame shown in Fig. 8.3(b), illustrates this point. The collapse mechanism of this system leads to an approximate geometrical relationship between the structure and active link deformations:

$$\theta L=\gamma e \tag{8.1}$$

The structure deformation measure, $\theta$, can be interpreted as an ultimate story drift index. The angular deformation requirement of the active link, $\gamma$, measures the average shear strain for shear links, while for bending links $\gamma$ is the plastic hinge rotations.

Since the eccentricity, $e$, is usually much smaller than $L$ in eccentrically braced frames, the links must undergo large displacements to meet the story drift. These localized regions are therefore required to dissipate large amounts of energy during inelastic response, making their

performance critical to the proper functioning of an eccentrically braced frame during a major seismic event. It is apparent that in a moment resisting frame, where $e=L$, the ductility demands on the beams are much smaller.

Minimum $\theta$ values of 0.015 to 0.020 have been recommended by ATC 03-06 [29] for highly seismic regions. Smaller $\theta$ values are required in regions of lower seismicity. Since seismic loadings can produce complete load reversals, recommended $\gamma$ values should be determined from cyclic experiments. The results of previous experiments and those described in this report indicate that properly designed shear links can attain $\gamma$ values of up to $\pm 0.10$ for cyclic loading and 0.20 for monotonic loading. Once the values of $L$, $\theta$, and $\gamma$, have been specified, the minimum eccentricity, $e$, can be estimated using Eq. 8.1. Relationships similar to that of Eq. 8.1 can be derived for other eccentrically braced configurations.

Determination of the maximum eccentricity necessary to meet elastic stiffness (drift) requirements, and the minimum eccentricity needed to limit active link inelastic demand form bounds for the length of the shear links. A suitable eccentricity within these bounds must then be selected.

### 8.2 Determination of Member Sizes

Because of the importance of providing the desired energy dissipation mechanism during extreme overloads, preliminary member sizing should be performed using plastic analysis techniques. The system of lateral forces employed in this initial sizing can be determined by applying a load factor to the equivalent static lateral forces specified in a building code [29,31]. Several procedures have been suggested for determining the member forces and moments for the desired collapse mechanism [15,18,24].

Roeder [25,26] used the moment balancing technique [9,14] to determine preliminary member forces. This procedure is based on the concept that if a structure is designed for any moment diagram which satisfies statics, the assumed loadings will be a lower bound for the strength of the structure. If the design also exhibits the desired collapse mechanism, the upper

bound solution will also be satisfied.

Roeder's approach makes an assumption of the proportion of the story lateral shear resisted by the brace and then solves for the forces and moments in the beams, such that the plastic hinges form in the desired locations. The remaining story shear is then distributed to the columns and the column moments are determined. The resulting unbalanced column end moments are then adjusted by moment balancing methods until all the nodes of the frame are in equilibrium, satisfying statics and thereby achieving a lower bound solution.

Manheim's method [18] is an upper bound approach to satisfy the desired collapse mechanism. This method equates the internal and external work based on an assumed distribution of shear link strength. Once the required strength of the links has been determined, the remaining member forces can be determined from statics.

Kasai [15] noted that both of these preliminary member sizing methods may encounter difficulties in obtaining acceptable column design moments. Roeder and Popov [26] observed that the columns may be in single curvature over multiple stories, resulting in large column sizes. Also, unless the initial assumptions are quite accurate, these two approaches may require a number of iterations to obtain an acceptable solution.

A third preliminary design method was developed to provide more acceptable column design moments without requiring any assumptions concerning the distribution of story shears or beam strength. Kasai [15] obtained a statically and kinematically admissible solution based on the desired collapse mechanism. In this method the location of column inflection points are assumed to ensure that the columns are in double curvature under any fixed loading condition. The resulting force and moment distribution forms both an upper and lower bound solution to the plastic design problem, and inelastic activity is confined to the appropriate locations.

Once a satisfactory set of design forces and moments in all the frame members has been determined, the preliminary sizes can be chosen using the recommendations of Part 2 of the AISC Specification [1]. In choosing appropriate beam sections it should be noted that energy dissipation data from previous tests indicated that shear hinge behavior is preferred over

moment hinge action [12,13]. A shear-moment interaction diagram for a wide flange beam [2,12,18], as shown in Fig 8.4, can be combined with consideration of static equilibrium to ensure shear rather than moment link behavior. The $M_p^*$, $V_p^*$, and $M_p$ terms for this figure are given by the following equations [12,13]:

$$M_p^* = \sigma_y (d - t_f)(b_f - t_w) t_f \tag{8.2}$$

$$V_p^* = \tau_y (d - t_f) t_w \tag{8.3}$$

$$M_p = \sigma_y Z \tag{8.4}$$

In these equations, the section properties, $d$, $t_f$, $t_w$, $b_f$, and $Z$ are the beam depth, flange thickness, web thickness, flange width, and plastic section modulus, respectively, such as given in the AISC Manual [1]. The terms $\sigma_y$ and $\tau_y$ are the yield stresses in pure tension and pure shear, respectively. Using the von Mises yield criterion, $\tau_y = \sigma_y/\sqrt{3}$.

Satisfying statics of the assumed link model (See Section 2.1) results in the following relationship:

$$e = \frac{2M}{V} \tag{8.5}$$

The existence of a rapid change in slope in the shear-moment interaction diagram at ($M_p^*$, $V_p^*$) is characteristic of wide flange sections. The balance point locates where the entire web yields in shear while the flanges yield simultaneously in uniaxial tension or compression. Using this point of the shear-moment interaction diagram, the balanced length for a section, $b^*$, can be defined as:

$$b^* = 2\frac{M_p^*}{V_p^*} \approx 2\sqrt{3} b_f \frac{t_f}{t_w} \tag{8.6}$$

Active links should therefore act as shear links if $e < b^*$. The test results to date indicate that shear link action continues to predominate for lengths up to approximately $e = 1.15 b^*$.

Combining this experimental observation with Eq. 8.6 results in the following simplified expression for the maximum length of a shear link:

$$b^*_{max} \approx 4 b_f \frac{t_f}{t_w} \tag{8.7}$$

To attain the desired shear link inelastic response characteristics the beam sizes chosen should therefore have a $b^*_{max}$ greater than $e$, the eccentricity provided.

It should be noted that Eq. 8.7 was developed from experimental data which simulated links with reverse curvature and equal end moments, such as shown in Fig. 2.1(c). For the links illustrated in Figs. 8.1 (b), (c), and (d), in the elastic range of behavior larger link moments tend to develop at the column ends than at the brace ends. Whether these moments equalize under severe cyclic loading has not yet been fully established. This topic is the subject of a current experimental investigation. If an elastic analysis indicates that $M^*_p$ will be reached at the column face before the initiation of shear yielding, either the eccentricity should be reduced, or an alternative section should be selected.

The preliminary design of columns and beams in eccentrically braced frames should follow the basic provisions of Part 2 of the AISC Specifications [1], with the following modification. Since significant strain hardening of shear links has been observed in experiments, an additional safety factor should be used in the design of braces to preclude the occurrence of brace buckling. The previously recommended safety factor of 1.5 appears to be reasonable [24]. A comparable factor should also be considered in the design of the columns.

Since current building codes [31] are based on elastic analysis techniques, the plastically designed frame should be checked at working force levels. Satisfaction of both elastic drift and member size requirements should be ensured. If the elastic design requirements result in increased member sizes, the plastic design procedure given above should be rechecked to ensure that the desired inelastic behavior will occur.

**8.3 Design of Link Connections**

**8.3.1 Link-Column Connections-** The structural configuration of eccentrically braced frames frequently are such that the active links are located in the portion of the beam adjacent to the supporting column. In this instance the integrity of the beam-column connection becomes critical for developing the dissipation capacity of the active links. The designer must therefore understand the nature of the inelastic response of the frame to adequately detail the link connections. Without sufficiently ductile connection details the active links may not be able to withstand the large displacement requirements which they could be subjected to during extreme seismic events.

Eq. 8.1 demonstrated that the ductility demand on active links can become quite large as their length decreases. Since these shorter links yield in shear, the link-column connection must be able to develop the full yield shear capacity of the links. The increased shear capacity of well stiffened links, up to 75 per cent above the initial yield level, must be recognized in the connection design.

The test results described earlier showed that all-welded link-column connections can provide the required shear capacity and ductility. As Specimen 28 showed, in bolted web, welded flange connections the large shear forces can cause bolt slippage which can lead to premature brittle flange failures. To avoid such failures, all-welded shear link connections, which can achieve large energy dissipation and ductility, should be employed. A detail such as that shown in Fig. 8.5 was found to sustain a large number of load reversals in the inelastic range. A satisfactory alternative detail which provides for a more direct transfer of shear forces is shown in Fig. 8.6. If an analysis shows that the ductility and energy dissipation demands on an active link are moderate, the bolted web, welded flange connection shown in Fig. 8.7 can be expected to perform adequately.

Since shear links must resist large end moments (See Section 5.2.2), the link flanges must be connected to the columns with full penetration welds in all cases. In fabricating any one of these connections in order to minimize residual stresses, the flange welds must be made before

final attachment of the beam webs.

Similar details can be used for the connection of active links to column webs. But, previous research showed such connections to be less ductile than those to column flanges [20]. Lehigh University investigators [6] recommend extending the connecting plates beyond the column flanges to decrease the possibility of weld failure, as shown in Fig. 8.8 for links with large ductility demands. For links with moderate ductility demands a detail with a bolted web similar to that shown in Fig. 8.7 should be satisfactory.

**8.3.2 Link-Brace Connections-** The link-brace connections must be designed to develop the full yield capacity of the shear links, including the anticipated strain hardening of the material.

The link-brace connections shown in Figs. 8.5 through 8.8 illustrate a typical detail for braces composed of a pair of angles. A similar detail can be adopted for tubular braces. The gusset plate detail consists of two plates welded into a T section in order to stiffen the connection and to provide better alignment of the weld centroid. Another detail, in which the braces are welded directly to the link flanges, has also been used in design applications.

Since active links are susceptible to lateral torsional buckling, the link ends at the eccentric braces must be laterally supported. A link-brace connection which is T-shaped in plan, as shown in Figs. 8.5 through 8.8 tends to reduce the load induced to the lateral bracing beam [18].

## 8.4 Design of Shear Link Stiffeners

The design of shear link stiffeners should follow the recommendations given in Section 7.2 of this report.

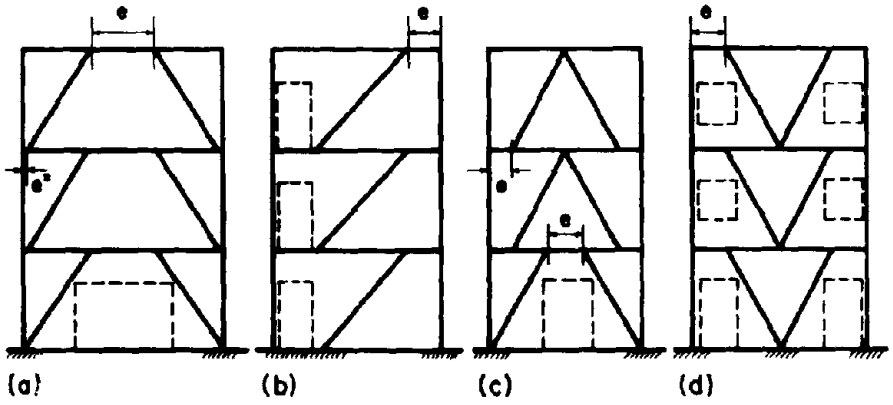


Fig. 8.1 Alternative Arrangements for Eccentric Bracing Showing Possible Location of Architectural Openings [11].

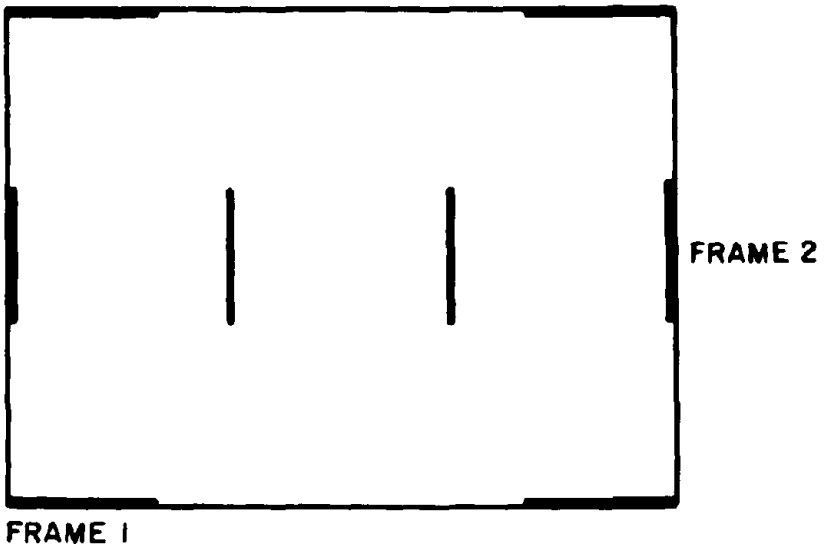


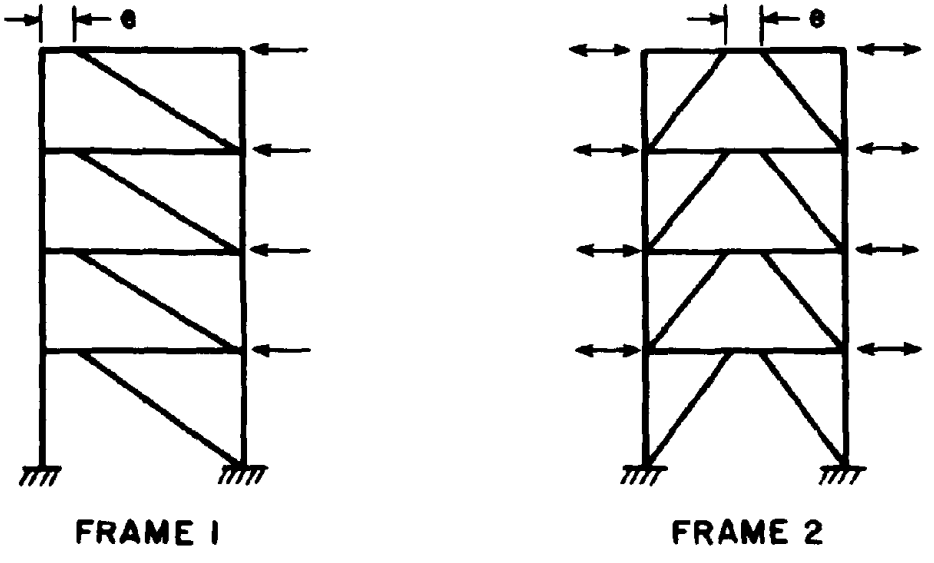


Fig. 8.2 Proper Configuration of Framing to Limit the Axial Forces Introduced Into the Active Links.

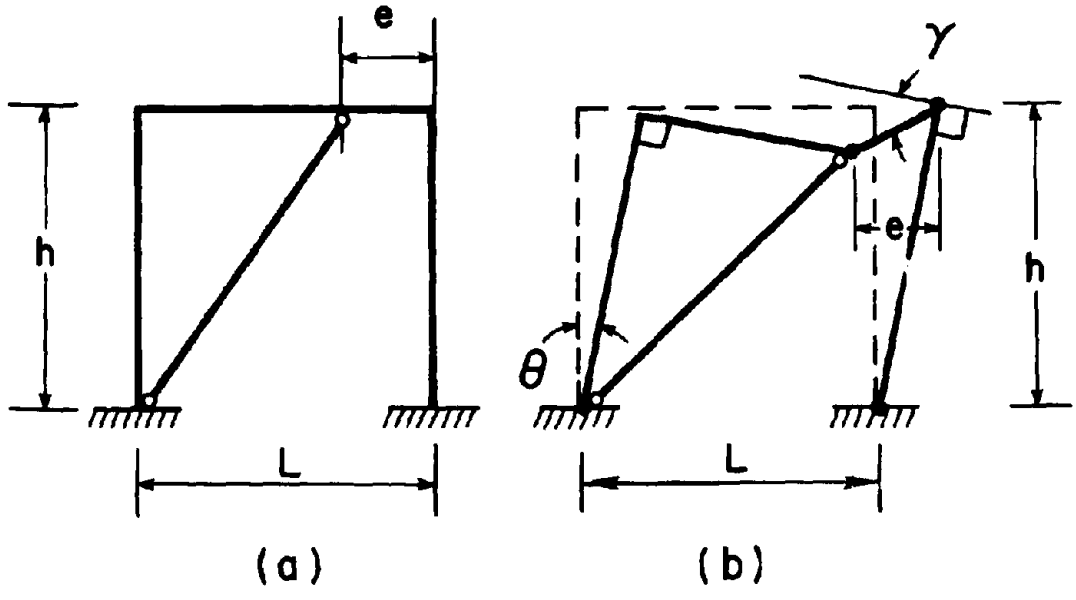


Fig. 8.3 A Simple Eccentrically Braced Frame and Its Collapse Mechanism [11].

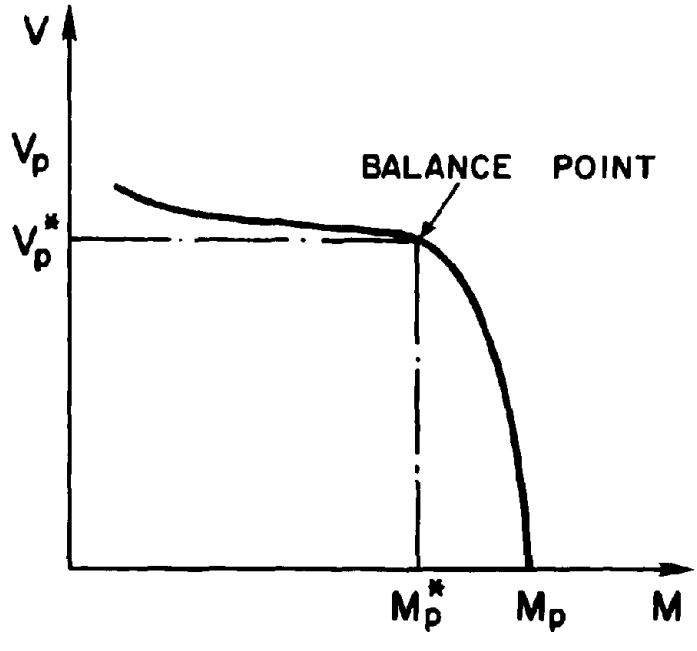


Fig. 8.4 Typical Moment-Shear Interaction Diagram for Wide Flange Sections.

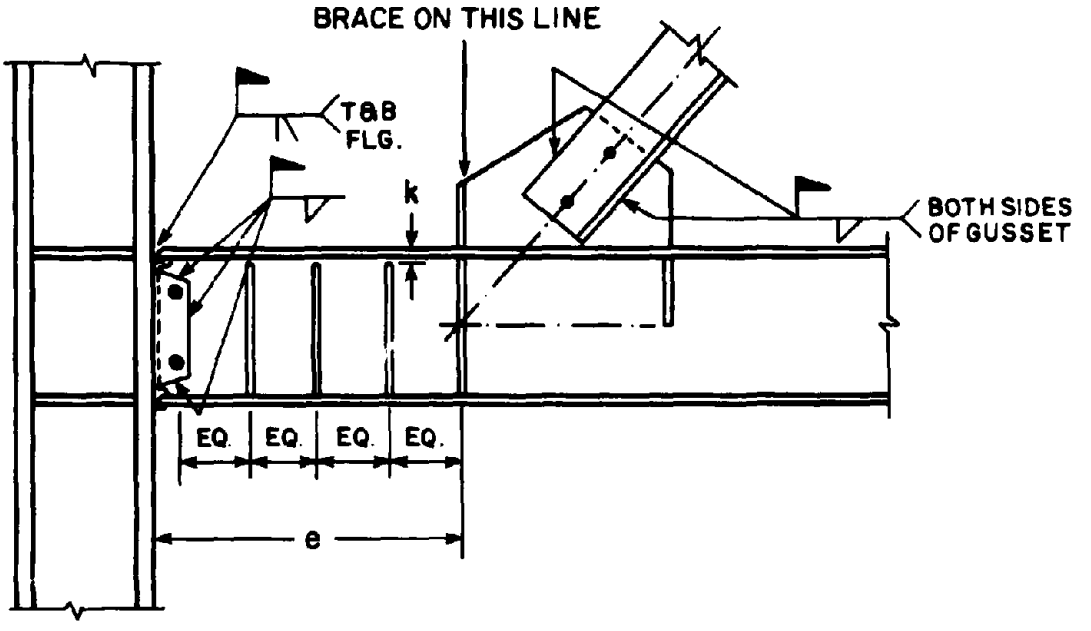


Fig. 8.5 All-Welded Link-Column Flange Connection with Fillet Welded Web Showing Suggested Stiffener Spacing.

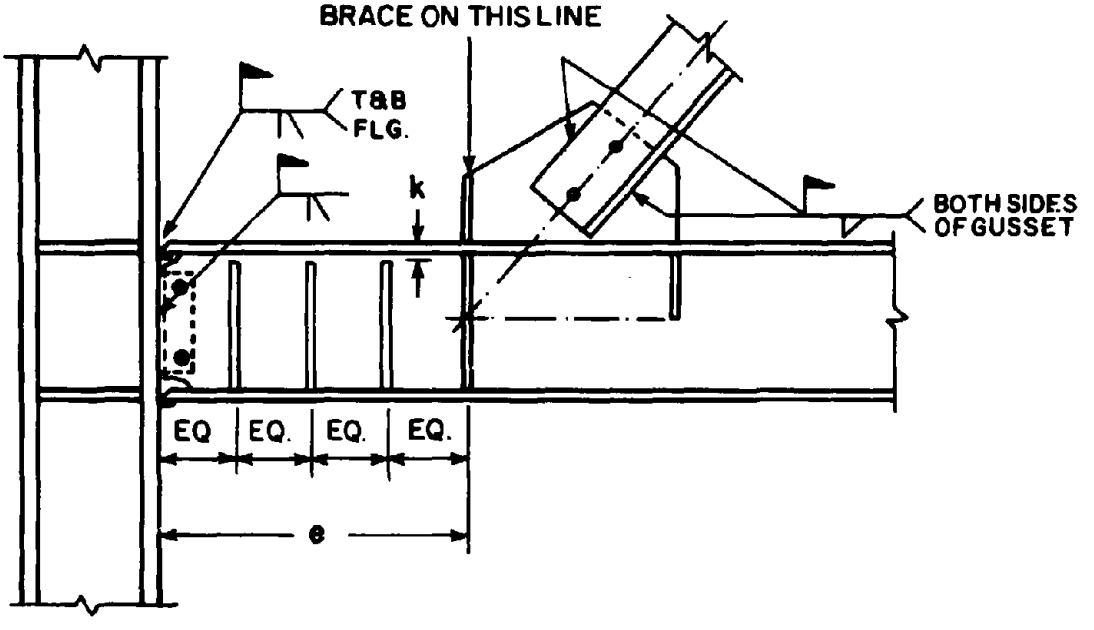


Fig. 8.6 All-Welded Link-Column Flange Connection with Full Penetration Web Weld Showing Suggested Stiffener Spacing.

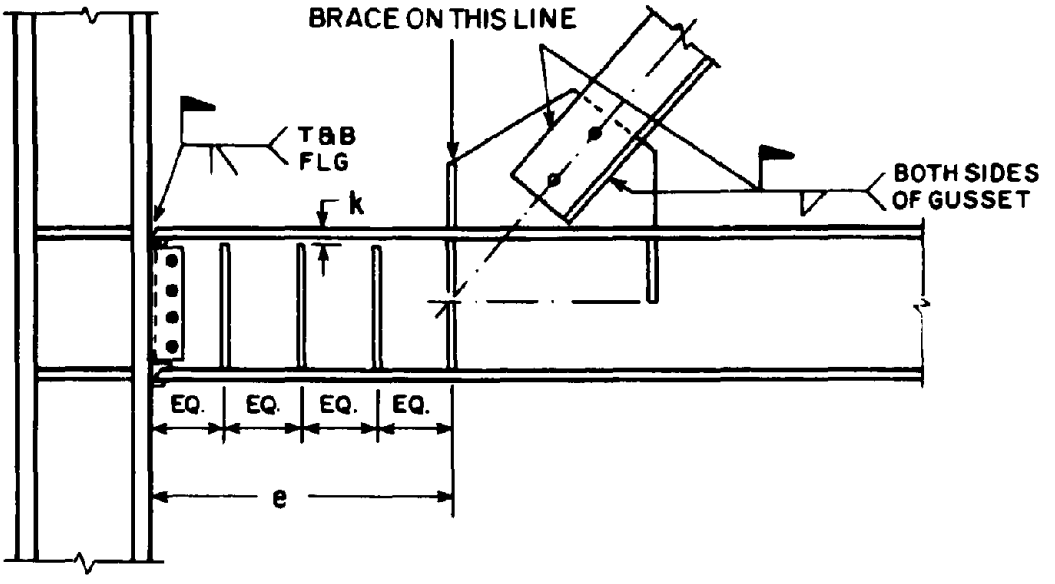


Fig. 8.7 Bolted Web, Welded Flange Link-Column Flange Connection Showing Suggested Stiffener Spacing.

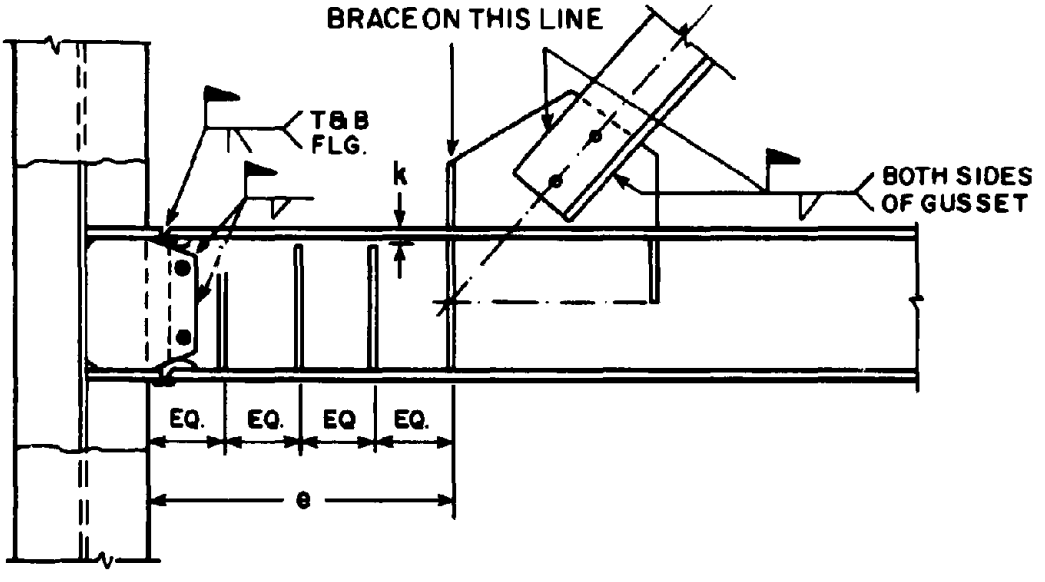


Fig. 8.8 Suggested All-Welded Link-Column Web Connection Showing Suggested Stiffener Spacing.

# CHAPTER 9 - SUMMARY AND CONCLUSIONS

## 9.1 Summary

Eccentrically braced framing can exhibit both excellent elastic stiffness and large energy dissipation capacity. These characteristics make eccentrically braced frames a viable alternative to the more conventional structural steel framing systems in seismic regions. Previous studies [18, 24] demonstrated the overall behavior of frames with different bracing systems. A recent study [13] analyzed the local behavior of the crucial active link elements.

The results of these previous investigations provided a good deal of information on the cyclic behavior of active links. However, some aspects concerning the practical design of an eccentrically braced framing system had not been addressed, including the sensitivity of link behavior to the imposed loading history, the link-column connection detail, and the web stiffener details. The purpose of this investigation was to examine these aspects of the design problem.

To investigate these aspects, a series of twelve full-size specimens were designed and tested. These tests again demonstrated the excellent energy dissipative capacity of shear links. Analysis of the test results provided the information necessary to make design recommendations considering both economic and performance characteristics. A method for stiffener sizing was developed and a procedure for shear link design was presented.

## 9.2 Conclusions

The major conclusions of this investigation are:

1. *Timoshenko Shear Beam Theory closely approximates the linear elastic behavior of shear links. Shear displacement effects should be considered in elastic analyses of eccentrically braced frames employing shear links.*

2. *For the type of loading used in these experiments, properly designed and detailed shear links can dissipate large amounts of energy regardless of the loading history.*

3. *Monotonic relative end displacements of up to 20 per cent of the link length can be resisted without significant loss of capacity. This conclusion demonstrates that shear links can meet the large ductility demand which may result from long pulse seismic disturbances similar to that recorded during the 1971 San Fernando Earthquake.*

4. *Properly designed one-sided web stiffening sufficiently delays and restrains web buckling. The use of one-sided web stiffeners can provide significant cost economies due to reduced welding requirements.*

5. *Web stiffeners need not be connected to both link flanges; the stiffeners can be terminated a distance k (see AISC Manual [1]) from the top of the upper flange. The concrete floor supported by the beam may be counted upon to provide the necessary restraint against flange buckling. However, this restraint is not entirely reliable, since it may be reduced by cracking of the slab during a seismic event. The stiffeners should be welded to the lower flange to provide buckling restraint.*

6. *Stiffeners should be designed for axial forces and bending stiffness. The use of tension field theory provides a method for the axial force design. Bending stiffness requirements can be estimated by modifying previously available elastic buckling solutions to account for the inelastic nature of shear link web buckling.*

7. *From energy dissipation and failure mode considerations, the minimum spacing for stiffeners in shear links should be $20t_w$. Equal spacing of stiffeners should be used with a modified panel zone size for panels adjacent to the beam-column connection. For a web which is fillet welded to a shear tab, spacing of the stiffeners should begin from the erection bolt line. For bolted and full penetration welded connections, the stiffeners should be spaced from the face of the column.*

8. *All welded connections develop the full capacity of shear links. This detail is recommended for links with large ductility demands to provide assurance against abrupt connection failures.*

9. *Under cyclic loading, well stiffened webs develop a great deal of strain hardening which increases the shear capacity of the link significantly. For welded flange, bolted web connections, bolt slippage transfers a large portion of this increased shear to the flanges, tending to cause of premature flange failures. This type of failure mode makes this connection undesirable for links with large ductility demands. The bolted web detail should perform adequately for shear links with moderate ductility demands.*

10. *Based on one experiment, it appears that shear links connected to the column web can dissipate a large amount of energy. The shear link web yielding reduces flange forces in the member, diminishing the possibility of weld failures.*

## BIBLIOGRAPHY


(1) AISC, Specification for the Design, Fabrication and Erection of Structural Steel Buildings, with Commentary, Manual of Steel Construction, American Institute of Steel Construction, Chicago, 1980.

(2) Adams, P.F., Krentz, H.A., and Kulak, G.L., Limit State Design in Structural Steel, *Canadian Institute of Steel Construction*, 1979.

(3) Basler, K., "Strength of Plate Girders in Shear", *Journal of the Structural Division*, ASCE, October, 1961, pp. 151-180.

(4) Black, R.G., Wenger, W.A., and Popov, E.P., "Inelastic Buckling of Steel Struts Under Cyclic Load Reversal", *EERC Report 80-40*, University of California, Berkeley, October, 1980.

(5) Bleich, F., Buckling Strength of Metal Structures, McGraw-Hill, New York, 1952, pp. 409-418.

(6) Driscoll, G.C., and Beedle, L.S., "Suggestions for Avoiding Beam-to-Column Web Connection Failure", *AISC Engineering Journal*, Vol. 19, No. 1, 1982, pp. 16-19.

(7) E.C.C.S. - I.A.B.S.E.: Liege Colloquium on Stability of Steel Structures, April 1977, pp. 273-278.

(8) Fujimoto, M., Aoyagi, T., Ukai, K., Wada, A., and Saito, K., "Structural Characteristics of Eccentric K-Braced Frames", *Trans AIJ*, No. 195, May, 1972.

(9) Gaylord, E.H., "Plastic Design by Moment Balancing", Steel Structures Symposium, Univ. of Illinois, Urbana, October, 1966.

(10) Hisatoku, T., et. al., "Experimental Study on the Static Behavior of the Y-Typed Bracings", Report of Takenaka Technical Institute, No. 12, August, 197[illegible]

(11) Hjelmstad, K.D., and Popov, E.P., "Some Characteristics of Eccentrically Braced Frames", *Journal of Structural Engineering*, ASCE, in press.

(12) Hjelmstad, K.D., and Popov, E.P., "Cyclic Behavior and Design of Link Beams", *Journal of Structural Engineering*, ASCE, in press.

(13) Hjelmstad, K.D., "Seismic Behavior of Active Beam Links in Eccentrically Braced Frames", Ph.D. Thesis, University of California, Berkeley, June, 1983.

(14) Horne, M.R., "A Moment Distribution Method for the Analysis and Design of Structures by the Plastic Theory", *Proceedings*, Institute of Civil Engineers 3, No. 1, April, 1954.

(15) Kasai, K., "A Plastic Design Method for Eccentrically Braced Frames," Dept. of Civil Engineering, University of California, Berkeley, CE 299 Report, 1983.

(16) Krawinkler, H., Bertero, V.V., and Popov, E.P., "Inelastic Behavior of Steel Beam-to-Column Subassemblages", *EERC Report 71-7*, University of California, Berkeley, 1971.

(17) Maison, B.F., and Popov, E.P., "Cyclic Response Prediction for Braced Steel Frames", *Journal of the Structural Division*, ASCE, 106, No. ST7, Proc. Paper 15534, July, 1980, pp. 1401-1416.

(18) Manheim, D.N., "On the Design of Eccentrically Braced Frames", D. Eng. Thesis, Department of Civil Engineering, University of California, Berkeley, February, 1982.

(19) Massonnet, Ch., and Maquoi, R., "Recent Progress in the Field of Structural Stability of Steel Structures", *I.A.B.S.E. Surveys*, S-5/78, May, 1978, pp.13-16.

(20) Popov, E.P., and Pinkney, R.B., "Cyclic Yield Reversal in Steel Building Connections", *Journal of the Structural Division*, ASCE, Vol. 95, No. ST3, Proc. Paper 6441, March, 1969, pp. 327-352.

(21) Popov, E.P., and Stephen, R.M., "Cyclic Loading of Full-Size Steel Connections", *Steel Research for Construction,* Bulletin No. 21, American Iron and Steel Institute, New York, N.Y., Feb., 1972.

(22) Regional Colloquium on Stability of Steel Structures, Budapest, Hungary, October, 1977, pp. 219-229.

(23) Rockey, K.C., and Cook, I.T., "Shear Buckling of Clamped Infinitely Long Plates - Influence of Torsional Rigidity of Transverse Stiffeners", *Aeronautical Quarterly,* Vol. XVI, February, 1965, pp. 92-95.

(24) Roeder, C.W., and Popov, E.P., "Inelastic Behavior of Eccentrically Braced Steel Frames Under Cyclic Loadings", *EERC Report 77-18,* University of California, Berkeley, August, 1977.

(25) Roeder, C.W., and Popov, E.P., "Eccentrically Braced Steel Frames for Earthquakes", *Journal of the Structural Division,* ASCE, Vol. 104, No. ST3, March, 1978, pp. 391-411.

(26) Roeder, C.W., and Popov, E.P., "Design of an Eccentrically Braced Steel Frame", *AISC Engineering Journal,* 3rd Quarter, 1978.

(27) Spurr, H.V., Wind Bracing, McGraw-Hill, New York, 1930.

(28) Stein, M., and Fralich, R.W., "Critical Shear Stress of an Infinitely Long Simply Supported Plate with Transverse Stiffeners", N.A.C.A Technical Note 1851 (1949).

(29) "Tentative Provisions for the Development of Seismic Regulations for Buildings", *Report No. ATC 03-06,* Applied Technology Council, Palo Alto, Calif., 1978.

(30) Timoshenko, S.P., Theory of Elastic Stability, McGraw-Hill, New York, 1930.

(31) *Uniform Building Code, 1982 Edition,* International Conference of Building Officials, Whittier, Calif.

(32) Wang, T.K., "Buckling of Transverse Stiffened Plates Under Shear", *Journal of Applied Mechanics,* (ASME), Vol. 3, No. 4, 1947.

# APPENDIX A.1 DERIVATION OF THE REQUIRED STIFFENER RIGIDITY RELATIONSHIP

Bleich [5] used the results obtained by Stein and Fralich [28] to postulate a relationship between the required stiffener rigidity, $\bar{\gamma}_{req}$, and $\bar{\beta}$, the panel aspect ratio (See Eq. 7.15). The solution presented by Stein and Fralich assumed that the longitudinal edges of the web plate are simply supported. Since shear links are relatively short and laterally braced at both ends, the flanges of the rolled sections used in eccentrically braced frames appear to provide significant restraint along the longitudinal edges. A relationship similar to that given by Bleich should therefore be developed for the required stiffener rigidity when the longitudinal edges of the web plate are fixed against rotation, corresponding to the above case.

Rockey and Cook [23] obtained an analytical solution for the critical elastic buckling stress factor, $K$, as a function of the stiffener rigidity, $\gamma_T$, when the longitudinal edges are fixed against rotation. The results of this solution were presented in a series of graphs for different aspect ratios, some of which are shown in Figs. A.1 through A.4. The $C_T/B_T$ term shown in these figures is the ratio of the torsional to bending rigidity of the stiffeners [23]. The maximum value of 0.769 is for a thin walled circular tube stiffener. For the single plate stiffeners used in eccentrically braced frame applications the $C_T/B_T$ ratio is near zero.

In the derivation of Eq. 7.5, Bleich used the results of Stein and Fralich [28] to determine the minimum value of $\gamma_T$ which would develop the maximum critical buckling stress, for different panel aspect ratios. He then developed a relationship between these values of $\gamma_T$ and the corresponding aspect ratios.

A similar approach is followed in the derivation of Eq. 7.16. For six panel aspect ratios, including those given in Figs. A.1 through A.4, the table presented with Fig. A.5 lists the minimum value of $\gamma_T$ which allows the web to develop its maximum elastic critical shear stress

for a $C_T/B_T$ ratio of zero. This figure plots these values of $\gamma_T$ against $\bar{\beta}^2$. From this graph, the following equation relating the stiffener bending rigidity to the panel aspect ratio is obtained:

$$\bar{\gamma}_{req} = 16\bar{\beta}^2 - 8 \tag{A.1}$$

This equation, also plotted in Fig. A.5, is given as Eq. 7.16 in the derivation of the required shear link stiffener rigidity. Note that Eq. A.1 applies for elastic shear buckling of the web plate when $1 < \beta < 5$. The recommendations of Massonnet and Maquoi [19] can be used to account for the inelastic nature of shear link web buckling.

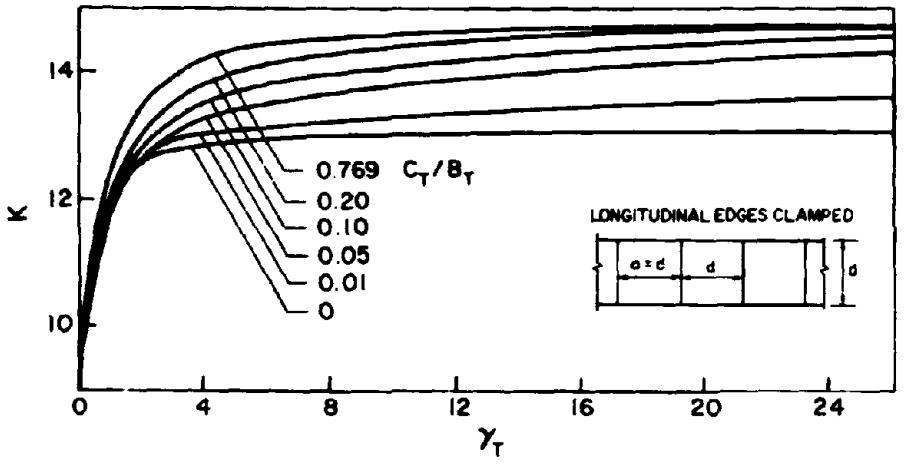


Fig. A.1 Critical Buckling Stress Factor vs. Stiffener Rigidity for $\bar{\beta} = 1.0$ [23].

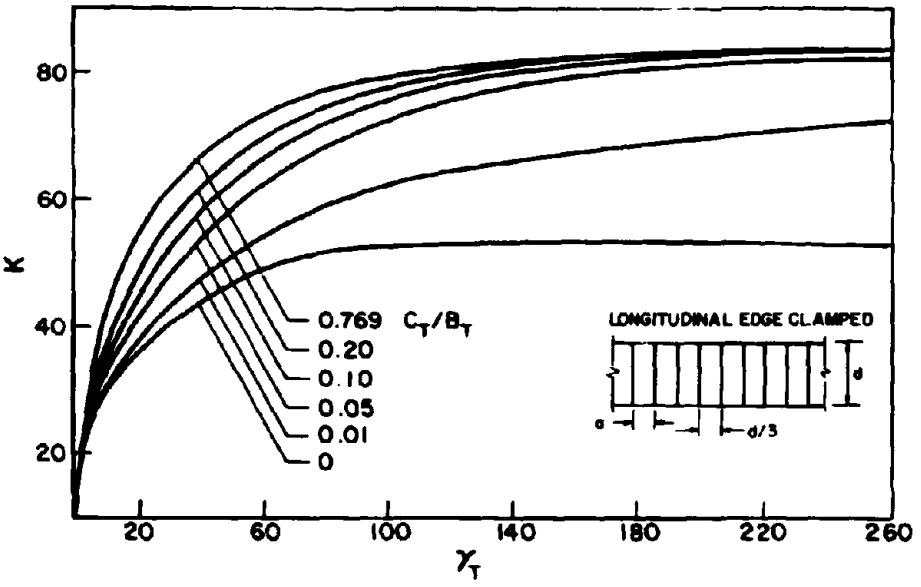


Fig. A.2 Critical Buckling Stress Factor vs. Stiffener Rigidity for $\bar{\beta} = 3.0$ [23].

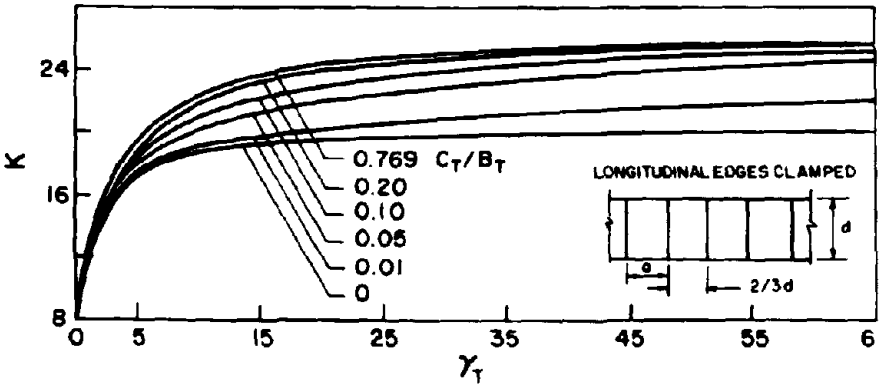


Fig. A.3 Critical Buckling Stress Factor vs. Stiffener Rigidity for $\bar{\beta} = 1.5$ [23].

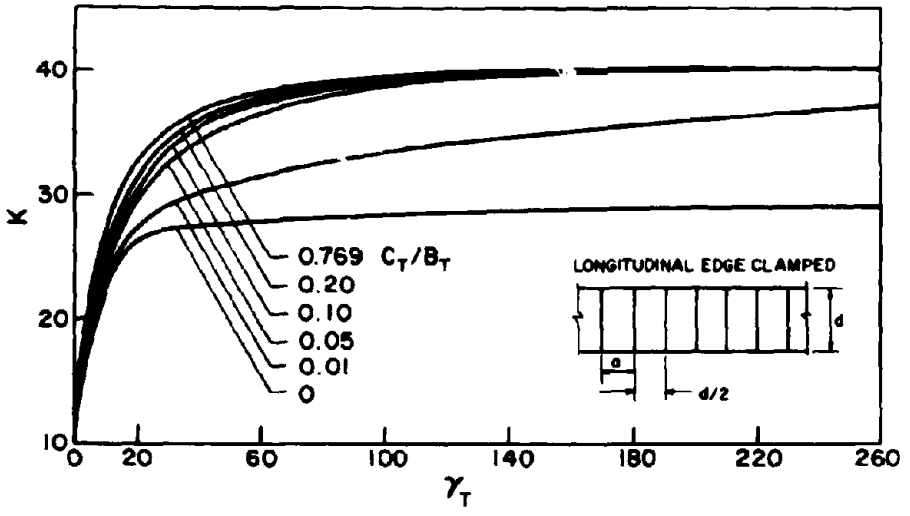


Fig. A.4 Critical Buckling Stress Factor vs. Stiffener Rigidity for $\bar{\beta} = 2.0$ [23].

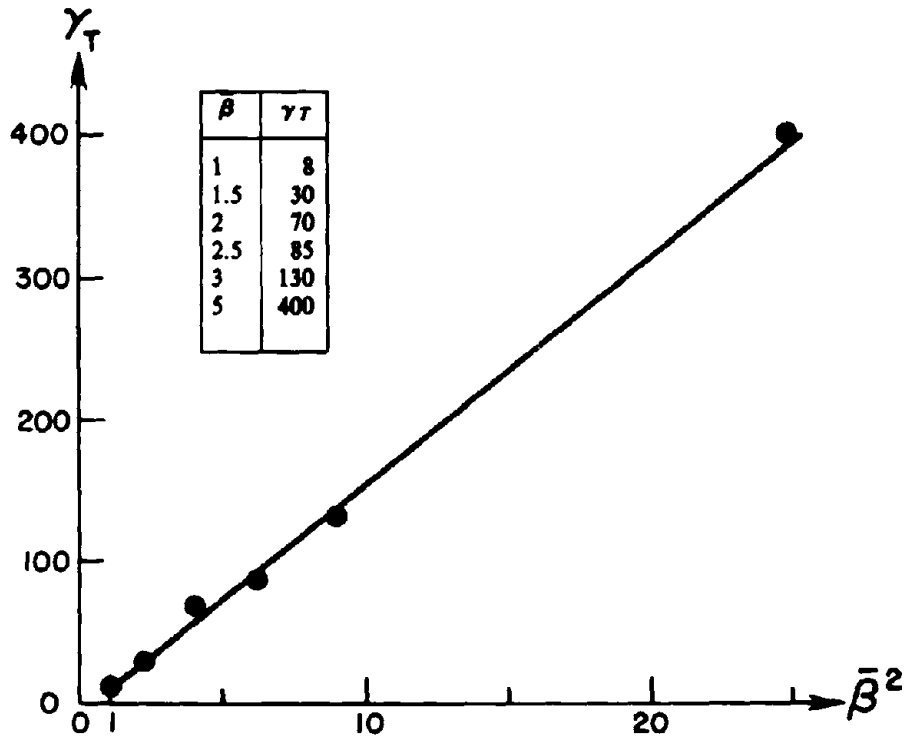


Fig. A.5 Plot of Minimum Required Stiffener Rigidity $\gamma_T$ Which Develops the Maximum Elastic Critical Stress ( $K$ ) for Different Values of Panel Aspect Ratio ( $\bar{\beta}$).

# APPENDIX A.2 AN EXAMPLE OF SHEAR LINK WEB STIFFENER DESIGN

This example is given to illustrate the procedure for shear link web stiffener design presented in Section 7.2.

Given: A W18x50 section of A36 steel shear link. Assume that the stiffener spacing has been determined from an inelastic dynamic analysis, or an estimated ductility demand, as $a/t_w = 25$.

The following section properties of a W 18x50 section are required for shear link stiffener design [1]:

$$t_w = 0.355 \ in.$$

$$d = 17.99 \ in.$$

$$b_f = 7.495 \ in.$$

$$t_f = 0.570 \ in.$$

$$h = d - 2t_f = 16.85 \ in.$$

The required stiffener spacing is therefore:

$$a = 25t_w = 25\ (0.355) = 8.875 \ in.$$

The following material properties have been assumed:

$$\sigma_y = 36 \ ksi$$

$$\sigma_u = 60 \ ksi$$

$$\nu = 0.30$$

**Design for Axial Forces (See Section 7.2.2.1)**

Using the values assumed above, by Eq. 7.6, the maximum panel shear, $V_l$, is developed when:

$$\sin\Theta = \left[\frac{1}{2} - \frac{(8.875)/(2)(16.85)}{\sqrt{1 + ((8.875)/(16.85))^2}}\right]^{1/2}$$

$$\sin\Theta = 0.517$$

For an ultimate tensile stress, $\sigma_u$, of 60 ksi, by Eq. 7.7, the force in the stiffener, $F_s$, is:

$$F_s = 60(0.355)(8.875)(0.517)^2$$

$$F_s = 50.5 \ kips$$

The area required for two-sided stiffeners, $A_w$, becomes:

$$A_w = \frac{50.5}{36} - \frac{(7.495)(0.355)}{2} = 0.0724 \ in.^2$$

and the thickness, $t_w$, is therefore:

$$t_{st} = \frac{0.0724}{7.495 - 0.355} = 0.01 \text{ in.} < t_w$$

The thickness required of two-sided stiffeners for axial forces will therefore be controlled by the thickness of the link web.

For one-sided stiffeners, the required area, $A_{st}$, is:

$$A_{st} = 2.4\left[(50.5)/(36) - (7.495)(0.355)/2\right] = 0.174 \text{ in.}^2$$

and the thickness of one-sided stiffeners, $t_{st}$ becomes:

$$t_{st} = 2\frac{(0.174)}{7.495 - 0.355} = 0.049 \text{ in.} < t_w$$

The thickness required of one-sided stiffeners for axial forces is also controlled by the thickness of the web.

**Design of Shear Link Stiffeners for Bending Rigidity (See Section 7.2.2.2)**

The panel aspect ratio, $\bar{\beta}$, is:

$$\bar{\beta} = h/a = (16.85)/(8.875) = 1.90$$

By Eq. 7.17, the required stiffener rigidity, $\bar{\gamma}_{req}$, is:

$$\bar{\gamma}_{req} = 64(1.90)^2 - 32 = 199$$

The stiffener moment of inertia, $I_{req}$, is given by Eq. 7.18, as:

$$I_{req} = \frac{(8.875)(0.355)^3(199)}{12(1 - 0.3^2)} = 7.22 \text{ in.}^4$$

The thickness of two-sided stiffeners, $t_{st}$, is therefore:

$$t_{st} = (12)(7.22)/(7.495)^3 = 0.206 \text{ in.} < t_w$$

Since the thickness of two-sided stiffeners required for bending rigidity is also less than $t_w$, the stiffeners sizing is controlled by the web thickness. Two-sided stiffeners should therefore be 3/8 *in.* thick.

For one-sided stiffeners, the required thickness, $t_{st}$, is:

$$t_{st} = (24)(7.22)/(7.495)^3 = 0.412 \text{ in.}$$

The size of one-sided stiffeners is therefore controlled by the bending rigidity design, and 1/2 *in.* thick stiffeners should be chosen.

EARTHQUAKE ENGINEERING RESEARCH CENTER REPORTS

NOTE: Numbers in parentheses are Accession Numbers assigned by the National Technical Information Service; these are followed by a price code. Copies of the reports may be ordered from the National Technical Information Service, 5285 Port Royal Road, Springfield, Virginia, 22161. Accession Numbers should be quoted on orders for reports (PB --- ---) and remittance must accompany each order. Reports without this information were not available at time of printing. The complete list of EERC reports (from EERC 67-1) is available upon request from the Earthquake Engineering Research Center, University of California, Berkeley, 47th Street and Hoffman Boulevard, Richmond, California 94804.

UCB/EERC-77/01 "PLUSH - A Computer Program for Probabilistic Finite Element Analysis of Seismic Soil-Structure Interaction," by M.P. Romo Organista, J. Lysmer and H.B. Seed - 1977 (PB81 177 651)A05

UCB/EERC-77/02 "Soil-Structure Interaction Effects at the Humboldt Bay Power Plant in the Ferndale Earthquake of June 7, 1975," by J.E. Valera, H.B. Seed, C.F. Tsai and J. Lysmer - 1977 (PB 265 795)A04

UCB/EERC-77/03 "Influence of Sample Disturbance on Sand Response to Cyclic Loading," by K. Mori, H.B. Seed and C.K. Chan - 1977 (PB 267 352)A04

UCB/EERC-77/04 "Seismological Studies of Strong Motion Records," by J. Shoja-Taheri - 1977 (PB 269 655)A10

UCB/EERC-77/05 Unassigned

UCB/EERC-77/06 "Developing Methodologies for Evaluating the Earthquake Safety of Existing Buildings," by No. 1 - B. Bresler; No. 2 - B. Bresler, T. Okada and D. Zisling; No. 3 - T. Okada and B. Bresler; No. 4 - V.V. Bertero and B. Bresler - 1977 (PB 267 354)A08

UCB/EERC-77/07 "A Literature Survey - Transverse Strength of Masonry Walls," by Y. Omote, R.L. Mayes, S.W. Chen and R.W. Clough - 1977 (PB 277 933)A07

UCB/EERC-77/08 "DRAIN-TABS: A Computer Program for Inelastic Earthquake Response of Three Dimensional Buildings," by R. Guendelman-Israel and G.H. Powell - 1977 (PB 270 693)A07

UCB/EERC-77/09 "SUBWALL: A Special Purpose Finite Element Computer Program for Practical Elastic Analysis and Design of Structural Walls with Substructure Option," by D.Q. Le, H. Peterson and E.P. Popov - 1977 (PB 270 567)A05

UCB/EERC-77/10 "Experimental Evaluation of Seismic Design Methods for Broad Cylindrical Tanks," by D.P. Clough (PB 272 280)A13

UCB/EERC-77/11 "Earthquake Engineering Research at Berkeley - 1976," - 1977 (PB 273 507)A09

UCB/EERC-77/12 "Automated Design of Earthquake Resistant Multistory Steel Building Frames," by N.D. Walker, Jr. - 1977 (PB 276 526)A09

UCB/EERC-77/13 "Concrete Confined by Rectangular Hoops Subjected to Axial Loads," by J. Vallenas, V.V. Bertero and E.P. Popov - 1977 (PB 275 165)A06

UCB/EERC-77/14 "Seismic Strain Induced in the Ground During Earthquakes," by Y. Sugimura - 1977 (PB 284 201)A04

UCB/EERC-77/15 Unassigned

UCB/EERC-77/16 "Computer Aided Optimum Design of Ductile Reinforced Concrete Moment Resisting Frames," by S.W. Zagajeski and V.V. Bertero - 1977 (PB 280 137)A07

UCB/EERC-77/17 "Earthquake Simulation Testing of a Stepping Frame with Energy-Absorbing Devices," by J.M. Kelly and D.F. Tsztoo - 1977 (PB 273 506)A04

UCB/EERC-77/18 "Inelastic Behavior of Eccentrically Braced Steel Frames under Cyclic Loadings," by C.W. Roeder and E.P. Popov - 1977 (PB 275 526)A15

UCB/EERC-77/19 "A Simplified Procedure for Estimating Earthquake-Induced Deformations in Dams and Embankments," by F.I. Makdisi and H.B. Seed - 1977 (PB 276 820)A04

UCB/EERC-77/20 "The Performance of Earth Dams during Earthquakes," by H.B. Seed, F.I. Makdisi and P. de Alba - 1977 (PB 276 821)A04

UCB/EERC-77/21 "Dynamic Plastic Analysis Using Stress Resultant Finite Element Formulation," by P. Lukkunapvasit and J.M. Kelly - 1977 (PB 275 453)A04

UCB/EERC-77/22 "Preliminary Experimental Study of Seismic Uplift of a Steel Frame," by R.W. Clough and A.A. Huckelbridge 1977 (PB 278 769)A08

UCB/EERC-77/23 "Earthquake Simulator Tests of a Nine-Story Steel Frame with Columns Allowed to Uplift," by A.A. Huckelbridge - 1977 (PB 277 944)A09

UCB/EERC-77/24 "Nonlinear Soil-Structure Interaction of Skew Highway Bridges," by M.-C. Chen and J. Penzien - 1977 (PB 276 176)A07

UCB/EERC-77/25 "Seismic Analysis of an Offshore Structure Supported on Pile Foundations," by D.D.-N. Liou and J. Penzien 1977 (PB 283 180)A06

UCB/EERC-77/26 "Dynamic Stiffness Matrices for Homogeneous Viscoelastic Half-Planes," by G. Dasgupta and A.K. Chopra - 1977 (PB 279 654)A06

UCB/EERC-77/27 "A Practical Soft Story Earthquake Isolation System," by J.M. Kelly, J.M. Eidinger and C.J. Derham - 1977 (PB 276 814)A07

UCB/EERC-77/28 "Seismic Safety of Existing Buildings and Incentives for Hazard Mitigation in San Francisco: An Exploratory Study," by A.J. Meltsner - 1977 (PB 281 970)A05

UCB/EERC-77/29 "Dynamic Analysis of Electrohydraulic Shaking Tables," by D. Rea, S. Abedi-Hayati and Y. Takahashi 1977 (PB 282 569)A04

UCB/EERC-77/30 "An Approach for Improving Seismic - Resistant Behavior of Reinforced Concrete Interior Joints," by B. Galunic, V.V. Bertero and E.P. Popov - 1977 (PB 290 870)A06

UCB/EERC-78/01 "The Development of Energy-Absorbing Devices for Aseismic Base Isolation Systems," by J.M. Kelly and D.F. Tsztoo - 1978 (PB 284 978)A04

UCB/EERC-78/02 "Effect of Tensile Prestrain on the Cyclic Response of Structural Steel Connections," by J.G. Bouwkamp and A. Mukhopadhyay - 1978

UCB/EERC-78/03 "Experimental Results of an Earthquake Isolation System using Natural Rubber Bearings," by J.M. Eidinger and J.M. Kelly - 1978 (PB 281 686)A04

UCB/EERC-78/04 "Seismic Behavior of Tall Liquid Storage Tanks," by A. Niwa - 1978 (PB 284 017)A14

UCB/EERC-78/05 "Hysteretic Behavior of Reinforced Concrete Columns Subjected to High Axial and Cyclic Shear Forces," by S.W. Zagajeski, V.V. Bertero and J.G. Bouwkamp - 1978 (PB 283 858)A13

UCB/EERC-78/06 "Three Dimensional Inelastic Frame Elements for the ANSR-I Program," by A. Riahi, D.G. Row and G.H. Powell - 1978 (PB 295 755)A04

UCB/EERC-78/07 "Studies of Structural Response to Earthquake Ground Motion," by O.A. Lopez and A.K. Chopra - 1978 (PB 282 790)A05

UCB/EERC-78/08 "A Laboratory Study of the Fluid-Structure Interaction of Submerged Tanks and Caissons in Earthquakes," by R.C. Byrd - 1978 (PB 284 957)A08

UCB/EERC-78/09 Unassigned

UCB/EERC-78/10 "Seismic Performance of Nonstructural and Secondary Structural Elements," by I. Sakamoto - 1978 (PB81 154 593)A05

UCB/EERC-78/11 "Mathematical Modelling of Hysteresis Loops for Reinforced Concrete Columns," by S. Nakata, T. Sproul and J. Penzien - 1978 (PB 298 274)A05

UCB/EERC-78/12 "Damageability in Existing Buildings," by T. Blejwas and B. Bresler - 1978 (PB 80 166 978)A05

UCB/EERC-78/13 "Dynamic Behavior of a Pedestal Base Multistory Building," by R.M. Stephen, E.L. Wilson, J.G. Bouwkamp and M. Button - 1978 (PB 286 650)A08

UCB/EERC-78/14 "Seismic Response of Bridges - Case Studies," by R.A. Imbsen, V. Nutt and J. Penzien - 1978 (PB 286 503)A10

UCB/EERC-78/15 "A Substructure Technique for Nonlinear Static and Dynamic Analysis," by D.G. Row and G.H. Powell - 1978 (PB 288 077)A10

UCB/EERC-78/16 "Seismic Risk Studies for San Francisco and for the Greater San Francisco Bay Area," by C.S. Oliveira - 1978 (PB 81 120 115)A07

UCB/EERC-78/17 "Strength of Timber Roof Connections Subjected to Cyclic Loads," by P. Gülkan, R.L. Mayes and R.W. Clough - 1978 (HUD-000 1491)A07

UCB/EERC-78/18 "Response of K-Braced Steel Frame Models to Lateral Loads," by J.G. Bouwkamp, R.M. Stephen and E.P. Popov - 1978

UCB/EERC-78/19 "Rational Design Methods for Light Equipment in Structures Subjected to Ground Motion," by J.L. Sackman and J.M. Kelly - 1978 (PB 292 357)A04

UCB/EERC-78/20 "Testing of a Wind Restraint for Aseismic Base Isolation," by J.M. Kelly and D.E. Chitty - 1978 (PB 292 833)A03

UCB/EERC-78/21 "APOLLO - A Computer Program for the Analysis of Pore Pressure Generation and Dissipation in Horizontal Sand Layers During Cyclic or Earthquake Loading," by P.P. Martin and H.B. Seed - 1978 (PB 292 835)A04

UCB/EERC-78/22 "Optimal Design of an Earthquake Isolation System," by M.A. Bhatti, K.S. Pister and E. Polak - 1978 (PB 294 735)A06

UCB/EERC-78/23 "MASH - A Computer Program for the Non-Linear Analysis of Vertically Propagating Shear Waves in Horizontally Layered Deposits," by P.P. Martin and H.B. Seed - 1978 (PB 293 101)A05

UCB/EERC-78/24 "Investigation of the Elastic Characteristics of a Three Story Steel Frame Using System Identification by I. Kaya and H.D. McNiven - 1978 (PB 296 225)A06

UCB/EERC-78/25 "Investigation of the Nonlinear Characteristics of a Three-Story Steel Frame Using System Identification," by I. Kaya and H.D. McNiven - 1978 (PB 301 363)A05

UCB/EERC-78/26 "Studies of Strong Ground Motion in Taiwan," by Y.M. Hsiung, B.A. Bolt and J. Penzien - 1978 (PB 298 436)A06

UCB/EERC-78/27 "Cyclic Loading Tests of Masonry Single Piers: Volume 1 - Height to Width Ratio of 2," by P.A. Hidalgo, R.L. Mayes, H.D. McNiven and R.W. Clough - 1978 (PB 296 211)A07

UCB/EERC-78/28 "Cyclic Loading Tests of Masonry Single Piers: Volume 2 - Height to Width Ratio of 1," by S.-W.J. Chen, P.A. Hidalgo, R.L. Mayes, R.W. Clough and H.D. McNiven - 1978 (PB 296 212)A09

UCB/EERC-78/29 "Analytical Procedures in Soil Dynamics," by J. Lysmer - 1978 (PB 298 445)A06

UCB/EERC-79/01 "Hysteretic Behavior of Lightweight Reinforced Concrete Beam-Column Subassemblages," by B. Forzani, E.P. Popov and V.V. Bertero - April 1979(PB 298 267)A06

UCB/EERC-79/02 "The Development of a Mathematical Model to Predict the Flexural Response of Reinforced Concrete Beams to Cyclic Loads, Using System Identification," by J. Stanton & H. McNiven - Jan. 1979(PB 295 875)A10

UCB/EERC-79/03 "Linear and Nonlinear Earthquake Response of Simple Torsionally Coupled Systems," by C.L. Kan and A.K. Chopra - Feb. 1979(PB 298 262)A06

UCB/EERC-79/04 "A Mathematical Model of Masonry for Predicting its Linear Seismic Response Characteristics," by Y. Mengi and H.D. McNiven - Feb. 1979(PB 298 266)A06

UCB/EERC-79/05 "Mechanical Behavior of Lightweight Concrete Confined by Different Types of Lateral Reinforcement," by M.A. Manrique, V.V. Bertero and E.P. Popov - May 1979(PB 301 114)A06

UCB/EERC-79/06 "Static Tilt Tests of a Tall Cylindrical Liquid Storage Tank," by R.W. Clough and A. Niwa - Feb. 1979 (PB 301 167)A06

UCB/EERC-79/07 "The Design of Steel Energy Absorbing Restrainers and Their Incorporation into Nuclear Power Plants for Enhanced Safety: Volume 1 - Summary Report," by P.N. Spencer, V.F. Zackay, and E.R. Parker - Feb. 1979(UCB/EERC-79/07)A09

UCB/EERC-79/08 "The Design of Steel Energy Absorbing Restrainers and Their Incorporation into Nuclear Power Plants for Enhanced Safety: Volume 2 - The Development of Analyses for Reactor System Piping,""Simple Systems" by M.C. Lee, J. Penzien, A.K. Chopra and K. Suzuki "Complex Systems" by G.H. Powell, E.L. Wilson, R.W. Clough and D.G. Row - Feb. 1979(UCB/EERC-79/08)A10

UCB/EERC-79/09 "The Design of Steel Energy Absorbing Restrainers and Their Incorporation into Nuclear Power Plants for Enhanced Safety: Volume 3 - Evaluation of Commercial Steels," by W.S. Owen, R.M.N. Pelloux, R.O. Ritchie, M. Faral, T. Ohhashi, J. Toplosky, S.J. Hartman, V.F. Zackay and E.R. Parker - Feb. 1979(UCB/EERC-79/09)A04

UCB/EERC-79/10 "The Design of Steel Energy Absorbing Restrainers and Their Incorporation into Nuclear Power Plants for Enhanced Safety: Volume 4 - A Review of Energy-Absorbing Devices," by J.M. Kelly and M.S. Skinner - Feb. 1979(UCB/EERC-79/10)A04

UCB/EERC-79/11 "Conservatism In Summation Rules for Closely Spaced Modes," by J.M. Kelly and J.L. Sackman - May 1979(PB 301 328)A03

UCB/EERC-79/12 "Cyclic Loading Tests of Masonry Single Piers; Volume 3 - Height to Width Ratio of 0.5," by P.A. Hidalgo, R.L. Mayes, H.D. McNiven and R.W. Clough - May 1979(PB 301 321)A08

UCB/EERC-79/13 "Cyclic Behavior of Dense Course-Grained Materials in Relation to the Seismic Stability of Dams," by N.G. Banerjee, H.B. Seed and C.K. Chan - June 1979(PB 301 373)A13

UCB/EERC-79/14 "Seismic Behavior of Reinforced Concrete Interior Beam-Column Subassemblages," by S. Viwathanatepa, E.P. Popov and V.V. Bertero - June 1979(PB 301 326)A10

UCB/EERC-79/15 "Optimal Design of Localized Nonlinear Systems with Dual Performance Criteria Under Earthquake Excitations," by M.A. Bhatti - July 1979(PB 80 167 109)A06

UCB/EERC-79/16 "OPTDYN - A General Purpose Optimization Program for Problems with or without Dynamic Constraints," by M.A. Bhatti, E. Polak and K.S. Pister - July 1979(PB 80 167 091)A05

UCB/EERC-79/17 "ANSR-II, Analysis of Nonlinear Structural Response, Users Manual," by D.P. Mondkar and G.H. Powell July 1979(PB 80 113 301)A05

UCB/EERC-79/18 "Soil Structure Interaction in Different Seismic Environments," A. Gomez-Masso, J. Lysmer, J.-C. Chen and H.B. Seed - August 1979(PB 80 101 520)A04

UCB/EERC-79/19 "ARMA Models for Earthquake Ground Motions," by M.K. Chang, J.W. Kwiatkowski, R.F. Nau, R.M. Oliver and K.S. Pister - July 1979(PB 301 166)A05

UCB/EERC-79/20 "Hysteretic Behavior of Reinforced Concrete Structural Walls," by J.M. Vallenas, V.V. Bertero and E.P. Popov - August 1979(PB 80 165 905)A12

UCB/EERC-79/21 "Studies on High-Frequency Vibrations of Buildings - 1: The Column Effect," by J. Lubliner - August 1979 (PB 80 158 553)A03

UCB/EERC-79/22 "Effects of Generalized Loadings on Bond Reinforcing Bars Embedded in Confined Concrete Blocks," by S. Viwathanatepa, E.P. Popov and V.V. Bertero - August 1979(PB 81 124 018)A14

UCB/EERC-79/23 "Shaking Table Study of Single-Story Masonry Houses, Volume 1: Test Structures 1 and 2," by P. Gülkan, R.L. Mayes and R.W. Clough - Sept. 1979 (HUD-000 1763)A12

UCB/EERC-79/24 "Shaking Table Study of Single-Story Masonry Houses, Volume 2: Test Structures 3 and 4," by P. Gülkan, R.L. Mayes and R.W. Clough - Sept. 1979 (HUD-000 1836)A12

UCB/EERC-79/25 "Shaking Table Study of Single-Story Masonry Houses, Volume 3: Summary, Conclusions and Recommendations," by R.W. Clough, R.L. Mayes and P. Gülkan - Sept. 1979 (HUD-000 1837)A06

UCB/EERC-79/26 "Recommendations for a U.S.-Japan Cooperative Research Program Utilizing Large-Scale Testing Facilities," by U.S.-Japan Planning Group - Sept. 1979(PB 301 407)A06

UCB/EERC-79/27 "Earthquake-Induced Liquefaction Near Lake Amatitlan, Guatemala," by H.B. Seed, I. Arango, C.K. Chan, A. Gomez-Masso and R. Grant de Ascoli - Sept. 1979(NUREG-CR1341)A03

UCB/EERC-79/28 "Infill Panels: Their Influence on Seismic Response of Buildings," by J.W. Axley and V.V. Bertero Sept. 1979(PB 80 163 371)A10

UCB/EERC-79/29 "3D Truss Bar Element (Type 1) for the ANSR-II Program," by D.P. Mondkar and G.H. Powell - Nov. 1979 (PB 80 169 709)A02

UCB/EERC-79/30 "2D Beam-Column Element (Type 5 - Parallel Element Theory) for the ANSR-II Program," by D.G. Row, G.H. Powell and D.P. Mondkar - Dec. 1979(PB 80 167 224)A03

UCB/EERC-79/31 "3D Beam-Column Element (Type 2 - Parallel Element Theory) for the ANSR-II Program," by A. Riahi, G.H. Powell and D.P. Mondkar - Dec. 1979(PB 80 167 216)A03

UCB/EERC-79/32 "On Response of Structures to Stationary Excitation," by A. Der Kiureghian - Dec. 1979(PB 80166 929)A03

UCB/EERC-79/33 "Undisturbed Sampling and Cyclic Load Testing of Sands," by S. Singh, H.B. Seed and C.K. Chan Dec. 1979(ADA 087 298)A07

UCB/EERC-79/34 "Interaction Effects of Simultaneous Torsional and Compressional Cyclic Loading of Sand," by P.M. Griffin and W.N. Houston - Dec. 1979(ADA 092 352)A15

UCB/EERC-80/01 "Earthquake Response of Concrete Gravity Dams Including Hydrodynamic and Foundation Interaction Effects," by A.K. Chopra, P. Chakrabarti and S. Gupta - Jan. 1980(AD-A087297)A10

UCB/EERC-80/02 "Rocking Response of Rigid Blocks to Earthquakes," by C.S. Yim, A.K. Chopra and J. Penzien - Jan. 1980 (PB80 166 002)A04

UCB/EERC-80/03 "Optimum Inelastic Design of Seismic-Resistant Reinforced Concrete Frame Structures," by S.W. Zagajeski and V.V. Bertero - Jan. 1980(PB80 164 635)A06

UCB/EERC-80/04 "Effects of Amount and Arrangement of Wall-Panel Reinforcement on Hysteretic Behavior of Reinforced Concrete Walls," by R. Iliya and V.V. Bertero - Feb. 1980(PB81 122 525)A09

UCB/EERC-80/05 "Shaking Table Research on Concrete Dam Models," by A. Niwa and R.W. Clough - Sept. 1980(PB81 122 368)A06

UCB/EERC-80/06 "The Design of Steel Energy-Absorbing Restrainers and their Incorporation into Nuclear Power Plants for Enhanced Safety (Vol 1A): Piping with Energy Absorbing Restrainers: Parameter Study on Small Systems," by G.H. Powell, C. Oughourlian and J. Simons - June 1980

UCB/EERC-80/07 "Inelastic Torsional Response of Structures Subjected to Earthquake Ground Motions," by Y. Yamazaki April 1980(PB81 122 327)A08

UCB/EERC-80/08 "Study of X-Braced Steel Frame Structures Under Earthquake Simulation," by Y. Ghanaat - April 1980 (PB81 122 335)A11

UCB/EERC-80/09 "Hybrid Modelling of Soil-Structure Interaction," by S. Gupta, T.W. Lin, J. Penzien and C.S. Yeh May 1980(PB81 122 319)A07

UCB/EERC-80/10 "General Applicability of a Nonlinear Model of a One Story Steel Frame," by B.I. Sveinsson and H.D. McNiven - May 1980(PB81 124 877)A06

UCB/EERC-80/11 "A Green-Function Method for Wave Interaction with a Submerged Body," by W. Kioka - April 1980 (PB81 122 269)A07

UCB/EERC-80/12 "Hydrodynamic Pressure and Added Mass for Axisymmetric Bodies," by F. Nilrat - May 1980(PB81 122 343)A08

UCB/EERC-80/13 "Treatment of Non-Linear Drag Forces Acting on Offshore Platforms," by B.V. Dao and J. Penzien May 1980(PB81 153 413)A07

UCB/EERC-80/14 "2D Plane/Axisymmetric Solid Element (Type 3 - Elastic or Elastic-Perfectly Plastic) for the ANSR-II Program," by D.P. Mondkar and G.H. Powell - July 1980(PB81 122 350)A03

UCB/EERC-80/15 "A Response Spectrum Method for Random Vibrations," by A. Der Kiureghian - June 1980(PB81 122 301)A03

UCB/EERC-80/16 "Cyclic Inelastic Buckling of Tubular Steel Braces," by V.A. Zayas, E.P. Popov and S.A. Mahin June 1980(PB81 124 885)A10

UCB/EERC-80/17 "Dynamic Response of Simple Arch Dams Including Hydrodynamic Interaction," by C.S. Porter and A.K. Chopra - July 1980(PB81 124 000)A13

UCB/EERC-80/18 "Experimental Testing of a Friction Damped Aseismic Base Isolation System with Fail-Safe Characteristics," by J.M. Kelly, K.E. Beucke and M.S. Skinner - July 1980(PB81 148 595)A04

UCB/EERC-80/19 "The Design of Steel Energy-Absorbing Restrainers and their Incorporation into Nuclear Power Plants for Enhanced Safety (Vol 1B): Stochastic Seismic Analyses of Nuclear Power Plant Structures and Piping Systems Subjected to Multiple Support Excitations," by M.C. Lee and J. Penzien - June 1980

UCB/EERC-80/20 "The Design of Steel Energy-Absorbing Restrainers and their Incorporation into Nuclear Power Plants for Enhanced Safety (Vol 1C): Numerical Method for Dynamic Substructure Analysis," by J.M. Dickens and E.L. Wilson - June 1980

UCB/EERC-80/21 "The Design of Steel Energy-Absorbing Restrainers and their Incorporation into Nuclear Power Plants for Enhanced Safety (Vol 2): Development and Testing of Restraints for Nuclear Piping Systems," by J.M. Kelly and M.S. Skinner - June 1980

UCB/EERC-80/22 "3D Solid Element (Type 4-Elastic or Elastic-Perfectly-Plastic) for the ANSR-II Program," by D.P. Mondkar and G.H. Powell - July 1980(PB81 123 242)A03

UCB/EERC-80/23 "Gap-Friction Element (Type 5) for the ANSR-II Program," by D.P. Mondkar and G.H. Powell - July 1980 (PB81 122 285)A03

UCB/EERC-80/24 "U-Bar Restraint Element (Type 11) for the ANSR-II Program," by C. Oughourlian and G.H. Powell July 1980(PB81 122 293)A03

UCB/EERC-80/25 "Testing of a Natural Rubber Base Isolation System by an Explosively Simulated Earthquake," by J.M. Kelly - August 1980(PB81 201 360)A04

UCB/EERC-80/26 "Input Identification from Structural Vibrational Response," by Y. Hu - August 1980(PB81 152 308)A05

UCB/EERC-80/27 "Cyclic Inelastic Behavior of Steel Offshore Structures," by V.A. Zayas, S.A. Mahin and E.P. Popov August 1980(PB81 196 180)A15

UCB/EERC-80/28 "Shaking Table Testing of a Reinforced Concrete Frame with Biaxial Response," by M.G. Oliva October 1980(PB81 154 304)A10

UCB/EERC-80/29 "Dynamic Properties of a Twelve-Story Prefabricated Panel Building," by J.G. Bouwkamp, J.P. Kollegger and R.M. Stephen - October 1980(PB82 117 128)A06

UCB/EERC-80/30 "Dynamic Properties of an Eight-Story Prefabricated Panel Building," by J.G. Bouwkamp, J.P. Kollegger and R.M. Stephen - October 1980(PB81 200 313)A05

UCB/EERC-80/31 "Predictive Dynamic Response of Panel Type Structures Under Earthquakes," by J.P. Kollegger and J.G. Bouwkamp - October 1980(PB81 152 316)A04

UCB/EERC-80/32 "The Design of Steel Energy-Absorbing Restrainers and their Incorporation into Nuclear Power Plants for Enhanced Safety (Vol 3): Testing of Commercial Steels in Low-Cycle Torsional Fatigue," by P. Spencer, E.R. Parker, E. Jongewaard and M. Drory

UCB/EERC-80/33 "The Design of Steel Energy-Absorbing Restrainers and their Incorporation into Nuclear Power Plants for Enhanced Safety (Vol 4): Shaking Table Tests of Piping Systems with Energy-Absorbing Restrainers," by S.F. Stiemer and W.G. Godden - Sept. 1980

UCB/EERC-80/34 "The Design of Steel Energy-Absorbing Restrainers and their Incorporation into Nuclear Power Plants for Enhanced Safety (Vol 5): Summary Report," by P. Spencer

UCB/EERC-80/35 "Experimental Testing of an Energy-Absorbing Base Isolation System," by J.M. Kelly, M.S. Skinner and K.E. Beucke - October 1980(PB81 154 072)A04

UCB/EERC-80/36 "Simulating and Analyzing Artificial Non-Stationary Earthquake Ground Motions," by R.F. Nau, R.M. Oliver and K.S. Pister - October 1980(PB81 153 397)A04

UCB/EERC-80/37 "Earthquake Engineering at Berkeley - 1980," - Sept. 1980(PB81 205 674)A09

UCB/EERC-80/38 "Inelastic Seismic Analysis of Large Panel Buildings," by V. Schricker and G.H. Powell - Sept. 1980 (PB81 154 338)A13

UCB/EERC-80/39 "Dynamic Response of Embankment, Concrete-Gravity and Arch Dams Including Hydrodynamic Interaction," by J.F. Hall and A.K. Chopra - October 1980(PB81 152 324)A11

UCB/EERC-80/40 "Inelastic Buckling of Steel Struts Under Cyclic Load Reversal," by R.G. Black, W.A. Wenger and E.P. Popov - October 1980(PB81 154 312)A08

UCB/EERC-80/41 "Influence of Site Characteristics on Building Damage During the October 3, 1974 Lima Earthquake," by P. Repetto, I. Arango and H.B. Seed - Sept. 1980(PB81 161 739)A05

UCB/EERC-80/42 "Evaluation of a Shaking Table Test Program on Response Behavior of a Two Story Reinforced Concrete Frame," by J.M. Blondet, R.W. Clough and S.A. Mahin

UCB/EERC-80/43 "Modelling of Soil-Structure Interaction by Finite and Infinite Elements," by F. Medina - December 1980(PB81 229 270)A04

UCB/EERC-81/01 **"Control of Seismic Response of Piping Systems and Other Structures by Base Isolation," edited by J.M. Kelly - January 1981 (PB81 200 735)A05**

UCB/EERC-81/02 **"OPTNSR - An Interactive Software System for Optimal Design of Statically and Dynamically Loaded Structures with Nonlinear Response," by M.A. Bhatti, V. Ciampi and K.S. Pister - January 1981 (PB81 218 851)A09**

UCB/EERC-81/03 **"Analysis of Local Variations in Free Field Seismic Ground Motions," by J.-C. Chen, J. Lysmer and H.B. Seed - January 1981 (AD-A099508)A13**

UCB/EERC-81/04 **"Inelastic Structural Modeling of Braced Offshore Platforms for Seismic Loading," by V.A. Zayas, P.-S.B. Shing, S.A. Mahin and E.P. Popov - January 1981(PB82 138 777)A07**

UCB/EERC-81/05 **"Dynamic Response of Light Equipment in Structures," by A. Der Kiureghian, J.L. Sackman and B. Nour-Omid - April 1981 (PB81 218 497)A04**

UCB/EERC-81/06 **"Preliminary Experimental Investigation of a Broad Base Liquid Storage Tank," by J.G. Bouwkamp, J.P. Kollegger and R.M. Stephen - May 1981(PB82 140 385)A03**

UCB/EERC-81/07 **"The Seismic Resistant Design of Reinforced Concrete Coupled Structural Walls," by A.E. Aktan and V.V. Bertero - June 1981(PB82 113 358)A11**

UCB/EERC-81/08 **"The Undrained Shearing Resistance of Cohesive Soils at Large Deformations," by M.R. Pyles and H.B. Seed - August 1981**

UCB/EERC-81/09 **"Experimental Behavior of a Spatial Piping System with Steel Energy Absorbers Subjected to a Simulated Differential Seismic Input," by S.F. Stiemer, W.G. Godden and J.M. Kelly - July 1981**

UCB/EERC-81/10 "Evaluation of Seismic Design Provisions for Masonry in the United States," by B.I. Sveinsson, R.L. Mayes and H.D. McNiven - August 1981 (PB82 166 075)A08

UCB/EERC-81/11 "Two-Dimensional Hybrid Modelling of Soil-Structure Interaction," by T.-J. Tzong, S. Gupta and J. Penzien - August 1981(PB82 142 118)A04

UCB/EERC-81/12 "Studies on Effects of Infills in Seismic Resistant R/C Construction," by S. Brokken and V.V. Bertero - September 1981 (PB82 166 190)A09

UCB/EERC-81/13 "Linear Models to Predict the Nonlinear Seismic Behavior of a One-Story Steel Frame," by H. Valdimarsson, A.H. Shah and H.D. McNiven - September 1981(PB82 138 793)A07

UCB/EERC-81/14 "TLUSH: A Computer Program for the Three-Dimensional Dynamic Analysis of Earth Dams," by T. Kagawa, L.H. Mejia, H.B. Seed and J. Lysmer - September 1981(PB82 139 940)A06

UCB/EERC-81/15 "Three Dimensional Dynamic Response Analysis of Earth Dams," by L.H. Mejia and H.B. Seed - September 1981 (PB82 137 274)A12

UCB/EERC-81/16 "Experimental Study of Lead and Elastomeric Dampers for Base Isolation Systems," by J.M. Kelly and S.B. Hodder - October 1981 (PB82 166 182)A05

UCB/EERC-81/17 "The Influence of Base Isolation on the Seismic Response of Light Secondary Equipment," by J.M. Kelly - April 1981 (PB82 255 266)A04

UCB/EERC-81/18 "Studies on Evaluation of Shaking Table Response Analysis Procedures," by J. Marcial Blondet - November 1981 (PB82 197 278)A10

UCB/EERC-81/19 "DELIGHT.STRUCT: A Computer-Aided Design Environment for Structural Engineering," by R.J. Balling, K.S. Pister and E. Polak - December 1981 (PB82 218 496)A07

UCB/EERC-81/20 "Optimal Design of Seismic-Resistant Planar Steel Frames," by R.J. Balling, V. Ciampi, K.S. Pister and E. Polak - December 1981 (PB82 220 179)A07

UCB/EERC-82/01 "Dynamic Behavior of Ground for Seismic Analysis of Lifeline Systems," by T. Sato and A. Der Kiureghian - January 1982 (PB82 218 926)A05

UCB/EERC-82/02 "Shaking Table Tests of a Tubular Steel Frame Model," by Y. Ghanaat and R. W. Clough - January 1982 (PB82 220 161)A07

UCB/EERC-82/03 "Behavior of a Piping System under Seismic Excitation: Experimental Investigations of a Spatial Piping System supported by Mechanical Shock Arrestors and Steel Energy Absorbing Devices under Seismic Excitation," by S. Schneider, H.-M. Lee and W. G. Godden - May 1982 (PB83 172 544)A09

UCB/EERC-82/04 "New Approaches for the Dynamic Analysis of Large Structural Systems," by E. L. Wilson - June 1982 (PB83 148 080)A05

UCB/EERC-82/05 "Model Study of Effects of Damage on the Vibration Properties of Steel Offshore Platforms," by F. Shahrivar and J. G. Bouwkamp - June 1982 (PB83 148 742)A10

UCB/EERC-82/06 "States of the Art and Practice in the Optimum Seismic Design and Analytical Response Prediction of R/C Frame-Wall Structures," by A. E. Aktan and V. V. Bertero - July 1982 (PB83 147 736)A05

UCB/EERC-82/07 "Further Study of the Earthquake Response of a Broad Cylindrical Liquid-Storage Tank Model," by G. C. Manos and R. W. Clough - July 1982 (PB83 147 744)A11

UCB/EERC-82/08 "An Evaluation of the Design and Analytical Seismic Response of a Seven Story Reinforced Concrete Frame - Wall Structure," by F. A. Charney and V. V. Bertero - July 1982(PB83 157 628)A09

UCB/EERC-82/09 "Fluid-Structure Interactions: Added Mass Computations for Incompressible Fluid," by J. S.-H. Kuo - August 1982 (PB83 156 281)A07

UCB/EERC-82/10 "Joint-Opening Nonlinear Mechanism: Interface Smeared Crack Model," by J. S.-H. Kuo - August 1982 (PB83 149 195)A05

UCB/EERC-82/11 "Dynamic Response Analysis of Techi Dam," by R. W. Clough, R. M. Stephen and J. S.-H. Kuo - August 1982 (PB83 147 496)A06

UCB/EERC-82/12 "Prediction of the Seismic Responses of R/C Frame-Coupled Wall Structures," by A. E. Aktan, V. V. Bertero and M. Piazza - August 1982 (PB83 149 203)A09

UCB/EERC-82/13 "Preliminary Report on the SMART 1 Strong Motion Array in Taiwan," by B. A. Bolt, C. H. Loh, J. Penzien, Y. B. Tsai and Y. T. Yeh - August 1982 (PB83 159 400)A10

UCB/EERC-82/14 "Shaking-Table Studies of an Eccentrically X-Braced Steel Structure," by M. S. Yang - September 1982

UCB/EERC-82/15 "The Performance of Stairways in Earthquakes," by C. Roha, J. W. Axley and V. V. Bertero - September 1982 (PB83 157 693)A07

UCB/EERC-82/16 "The Behavior of Submerged Multiple Bodies in Earthquakes," by W.-G. Liao - Sept. 1982 (PB83 158 709)A07

UCB/EERC-82/17 "Effects of Concrete Types and Loading Conditions on Local Bond-Slip Relationships," by A. D. Cowell, E. P. Popov and V. V. Bertero - September 1982 (PB83 153 577)A04

UCB/EERC-82/18 "Mechanical Behavior of Shear Wall Vertical Boundary Members: An Experimental Investigation," by M. T. Wagner and V. V. Bertero - October 1982 (PB83 159 764)A05

UCB/EERC-82/19 "Experimental Studies of Multi-support Seismic Loading on Piping Systems," by J. M. Kelly and A. D. Cowell - November 1982

UCB/EERC-82/20 "Generalized Plastic Hinge Concepts for 3D Beam-Column Elements," by P. F.-S. Chen and G. H. Powell - November 1982

UCB/EERC-82/21 "ANSR-III: General Purpose Computer Program for Nonlinear Structural Analysis," by C. V. Oughourlian and G. H. Powell - November 1982

UCB/EERC-82/22 "Solution Strategies for Statically Loaded Nonlinear Structures," by J. W. Simons and G. H. Powell - November 1982

UCB/EERC-82/23 "Analytical Model of Deformed Bar Anchorages under Generalized Excitations," by V. Ciampi, R. Eligehausen, V. V. Bertero and E. P. Popov - November 1982 (PB83 169 532)A06

UCB/EERC-82/24 "A Mathematical Model for the Response of Masonry Walls to Dynamic Excitations," by H. Sucuoğlu, Y. Mengi and H. D. McNiven - November 1982 (PB83 169 011)A07

UCB/EERC-82/25 "Earthquake Response Considerations of Broad Liquid Storage Tanks," by F. J. Cambra - November 1982

UCB/EERC-82/26 "Computational Models for Cyclic Plasticity, Rate Dependence and Creep," by B. Mosaddad and G. H. Powell - November 1982

UCB/EERC-82/27 "Inelastic Analysis of Piping and Tubular Structures," by K. Mahasuverachai and G. H. Powell - November 1982

UCB/EERC-83/01 "The Economic Feasibility of Seismic Rehabilitation of Buildings by Base Isolation," by J. M. Kelly - January 1983

UCB/EERC-83/02 "Seismic Moment Connections for Moment-Resisting Steel Frames," by E. P. Popov - January 1983

UCB/EERC-83/03 "Design of Links and Beam-to-Column Connections for Eccentrically Braced Steel Frames," by E. P. Popov and J. O. Malley - January 1983

UCB/EERC-83/04 "Numerical Techniques for the Evaluation of Soil-Structure Interaction Effects in the Time Domain," by E. Bayo and E. L. Wilson - February 1983

UCB/EERC-83/05 "A Transducer for Measuring the Internal Forces in the Columns of a Frame-Wall Reinforced Concrete Structure," by R. Sause and V. V. Bertero - May 1983

UCB/EERC-83/06 "Dynamic Interactions between Floating Ice and Offshore Structures," by P. Croteau - May 1983

UCB/EERC-83/07 "Dynamic Analysis of Multiply Tuned and Arbitrarily Supported Secondary Systems," by T. Igusa and A. Der Kiureghian - June 1983

UCB/EERC-83/08 "A Laboratory Study of Submerged Multi-body Systems in Earthquakes," by G. R. Ansari - June 1983

UCB/EERC-83/09 "Effects of Transient Foundation Uplift on Earthquake Response of Structures," by C.-S. Yim and A. K. Chopra - June 1983

UCB/EERC-83/10 "Optimal Design of Friction-Braced Frames under Seismic Loading," by M. A. Austin and K. S. Pister - June 1983

UCB/EERC-83/11 "Shaking Table Study of Single-Story Masonry Houses: Dynamic Performance under Three Component Seismic Input and Recommendations," by G. C. Manos, R. W. Clough and R. L. Mayes - June 1983

UCB/EERC-83/12 "Experimental Error Propagation in Pseudodynamic Testing," by P. B. Shing and S. A. Mahin - June 1983

UCB/EERC-83/13 "Experimental and Analytical Predictions of the Mechanical Characteristics of a 1/5-scale Model of a 7-story R/C Frame-Wall Building Structure," by A. E. Aktan, V. V. Bertero, A. A. Chowdhury and T. Nagashima - August 1983

UCB/EERC-83/14 "Shaking Table Tests of Large-Panel Precast Concrete Building System Assemblages," by M. G. Oliva and R. W. Clough - August 1983

UCB/EERC-83/15 "Seismic Behavior of Active Beam Links in Eccentrically Braced Frames," by K. D. Hjelmstad and E. P. Popov - July 1983

UCB/EERC-83/16 "System Identification of Structures with Joint Rotation," by J. S. Dimsdale and H. D. McNiven - July 1983

UCB/EERC-83/17 "Construction of Inelastic Response Spectra for Single-Degree-of-Freedom Systems," by S. Mahin and J. Lin - July 1983

UCB/EERC-83/18 "Interactive Computer Analysis Methods for Predicting the Inelastic Cyclic Behavior of Sections," by S. Kaba and S. Mahin - July 1983

UCB/EERC-83/19 "Effects of Bond Deterioration on Hysteretic Behavior of Reinforced Concrete Joints," by F. C. Filippo E. P. Popov and V. V. Bertero - August 1983

UCB/EERC-83/20 "Analytical and Experimental Correlation of Large-Panel Precast Building System Performance," by M. G. Oliva, R. W. Clough, M. Velkov, P. Gavrilovic and J. Petrovski - November 1983

UCB/EERC-83/21 "Mechanical Characteristics of the Materials Used in the 1/5 Scale and Full Scale Models of the 7-Stor Reinforced Concrete Test Structure," by V. V. Bertero, A. E. Aktan and A. A. Chowdhury - September 19E

UCB/EERC-83/22 "Hybrid Modelling of Soil-Structure Interaction in Layered Media," by T.-J. Tzong and J. Penzien - October 1983

UCB/EERC-83/23 "Local Bond Stress-Slip Relationships of Deformed Bars under Generalized Excitations," by R. Eligehausen, E. P. Popov and V. V. Bertero - October 198

UCB/EERC-83/24 "Design Considerations for Shear Links in Eccentrically Braced Frames," by J. O. Malley and E. P. Popov - November 1983